

Behaviour of Clayey Soils under Slow Repeated Loading
and
Laboratory Estimation of K_0 for Overconsolidated Sands

by

Hadj Abdi

A Thesis

Submitted under the supervision of

Dr. Vinod K. Garga

Professor

in partial fulfillment
of the requirements of the degree of
Master of Applied Science

Department of Civil Engineering

Faculty of Engineering

University of Ottawa

Ottawa, Canada

January 3, 1994

The Master of Science Program in Civil Engineering is a joint program between the University of Ottawa and the Carleton University, which is administered by the Ottawa-Carleton Institute for Civil Engineering.



Hadj Abdi, Ottawa, Canada, 1994



National Library
of Canada

Acquisitions and
Bibliographic Services Branch

395 Wellington Street
Ottawa, Ontario
K1A 0N4

Bibliothèque nationale
du Canada

Direction des acquisitions et
des services bibliographiques

395, rue Wellington
Ottawa (Ontario)
K1A 0N4

Your file *Votre référence*

Our file *Notre référence*

The author has granted an irrevocable non-exclusive licence allowing the National Library of Canada to reproduce, loan, distribute or sell copies of his/her thesis by any means and in any form or format, making this thesis available to interested persons.

L'auteur a accordé une licence irrévocable et non exclusive permettant à la Bibliothèque nationale du Canada de reproduire, prêter, distribuer ou vendre des copies de sa thèse de quelque manière et sous quelque forme que ce soit pour mettre des exemplaires de cette thèse à la disposition des personnes intéressées.

The author retains ownership of the copyright in his/her thesis. Neither the thesis nor substantial extracts from it may be printed or otherwise reproduced without his/her permission.

L'auteur conserve la propriété du droit d'auteur qui protège sa thèse. Ni la thèse ni des extraits substantiels de celle-ci ne doivent être imprimés ou autrement reproduits sans son autorisation.

ISBN 0-612-15692-3

Canada



UNIVERSITÉ D'OTTAWA
UNIVERSITY OF OTTAWA

Remerciements

Mes sincères remerciements á:

mon superviseur Dr. V.K. Garga pour son encouragement et son assistance constante et éclairée.

tous ceux qui ont aidé et entouré ce travail et son auteur, parmi lesquelles Mahbulul K.

le peuple algérien pour son support financier et sa lutte continue pour une vie juste et meilleure.

ABSTRACT

The existing software for controlling the apparatus used in experimental work presented in this thesis was changed from stress path control to cyclic load control. The main aim of this experimental work consists of two parts:

Part 1:

The repeated undrained load tests were carried out under the application of cyclic deviator stresses at a frequency that varies from 0.0001 Hz up to 0.001 Hz. For a specific amplitude of applied stress, a critical level of repeated loading (CLRL) was evaluated for both kaolinite and crust clays. This CLRL is approximately 70% of the original undrained static strength for kaolinitic clay and 60% for the clay crust. For these clays, the change in axial strain under cycling is quite similar. Cycling below CLRL causes a small increase in axial strain before equilibrium conditions is reached. If cycling is above CLRL, the rate of development of axial strain increases with cycling until failure. However, the change in pore pressure under repeated loading is dependent on the stress history of the soil. For normally consolidated kaolinitic clay, the change in pore pressure follows the same pattern as change axial strain as indicated above. For heavily overconsolidated clay crust, cycling below CLRL causes a development of more than 90% of the total pore pressure that can develop in the soil sample. The increase in number of cycles results in increasing higher pore pressures and higher values of (q/p') at failure. However, cycling above the CLRL generates the same pore pressure as would develop in a static test, identical value of (q/p') at failure for these samples is lower than the corresponding value for a static test.

The strength of the soil is affected by the frequency, cyclic fluctuation of water table, and the amount of axial strain developed during cycling. The decrease in postcyclic strength is strain-

dependent. It is further shown that cycling below the CLRL causes an increase in the overconsolidation of the clayey soils. The effect of cycling in behaviour of soils increases with increasing the OCR.

Part 2:

This part describes a method for the determination of in situ horizontal stresses of heavily overconsolidated sands using a stress-path triaxial apparatus. This method was proposed by Garga and Khan (1991) who applied it for overconsolidated clays. The proposed method is based on the concept that if the radial stress exceeds the in situ horizontal stress, while maintaining the axial stress constant and equal to the in situ vertical effective stress, only then will the sample experience significant axial strain. In this investigation, the above method is applied to the samples of known stress histories of overconsolidated sand. The effect of the complex stress history undergone by soils on the estimation of K_0 by the proposed method is investigated in laboratory. Simulation of that is done by subjecting soil samples to one and two cycles of loading at higher amplitudes of applied stresses. The rate of loading and unloading is slow enough to ensure full consolidation during the test. It is found that the proposed method replicated the imposed "in situ" horizontal stress exactly. Also this method is capable of estimating K_0 of an overconsolidated soil irrespective of the previously imposed stress history.

Table of Contents

Acknowledgements	i
Abstract	ii
Table of Contents	iv
List of Tables	vii
List of Figures	viii
Chapter 1: Introduction	1
1.1 Behaviour of Clayey Soils Under Repeated Loading	1
1.2 Evaluation of in Situ Horizontal stress for Overconsolidated Sand	4
1.3 Effect of the Complex Stress History Undergone by Soils on the Evaluation of K_0	5
1.4 Research Objectives	6
1.5 Outline of Thesis	7
Chapter 2: Literature Review	8
2.1 Behaviour of Clayey Soils Under Cyclic Loading	8
2.2 Determination of K_0 for Overconsolidated sand	16
Chapter 3: The Experimental Program	27
3.1 Introduction	27
3.2 Description of the Materials	28
3.2.1 Overconsolidated Clay Crust	28
3.2.2 Kaolinitic Clay	29
3.3 Equipment Used	29
3.4 Test Procedures	31
3.4.1 Specimen Preparation	31

3.4.2	Triaxial Cell Assembly	31
3.4.3	Saturation of the Specimen	32
3.4.4	Consolidation	32
3.5	Conventional Oedometer Tests	33
3.6	Monotonically and Cyclic Loading	33
Chapter 4: Behaviour of the Kaolinitic Clay Under Static and Repeated Loading		 38
4.1	Monotonic Tests	38
4.2	Repeated Loading Tests	39
4.2.1	Test Series S1 and S2	39
4.2.2	Test Results and discussion	40
4.2.3	Behaviour of Kaolinitic Clay Below CLRL	42
4.2.4	Behaviour of Kaolinitic Clay Above CLRL	47
4.2.5	Effect of the Step Increase in CSR	49
Chapter 5: Behaviour of the Clay Crust Under Static and Repeated Loading		 71
5.1	Monotonic Tests	71
5.2	Repeated Loading Tests	71
5.2.1	Test Series C1, C2, and C3	71
5.2.2	Test Results	73
5.2.3	Behaviour of Overconsolidated Clay Crust Below CLRL	78
5.2.4	Behaviour of Overconsolidated Crust Clay Above CLRL	78
5.2.5	Kaolinitic Clay Versus Clay Crust	79
Chapter 6: Further Consideration on the Effect of Cycling on Behaviour of Clayey Soils		 94
6.1	Variation of the CLRL with the Amplitude of Applied Stress	94
6.2	Effect of the Frequency on the Behaviour of Soils	96
6.3	Effect of the Fluctuation of Water Table on Strength of the Soil	98
6.4	Effect of Cycling on Overconsolidation of the Material	99

6.5 Effect of Cycling on Postcyclic Strength	101
Chapter 7: Laboratory Evaluation of K_0 for Overconsolidated sands	111
7.1 Introduction	111
7.2 Stress History of Overconsolidated sands	112
7.3 The Proposed Method	113
7.4 Material and Testing Procedure	113
7.5 Evaluation of K_0 by the Proposed Method Using Samples of Known Stress Histories	114
7.6 Effect of the Change in Geologic Conditions on the estimation of K_0 by the Proposed Method	116
7.6.1 One Cycle of Loading	118
7.6.2 Two Cycles of Loading	117
7.7 Conclusions	118
Chapter 8: Conclusions and Recommendations	133
8.1 Conclusions	133
8.2 Recommendations	136
References	137

List of Tables

Table 3.1. General properties of the crust and kaolinitic clays	34
Table 3.2. Complete program of testing on kaolinitic, crust, and lightly overconsolidated clays	35
Table 4.1. Summary of the testing conditions and test results of the test series K	51
Table 4.2. Summary of the testing conditions and test results of the test series S1 and S2	52
Table 5.1. Summary of the testing conditions and test results of the test series T	82
Table 5.2. Summary of the testing conditions and test results of the test series C1, C2, and C3	83
Table 7.1. Artificially prepared samples with simulated in situ stress state	121
Table 7.2. Estimation of the imposed in situ stress state for artificially prepared samples subjected to one cycle of loading	121
Table 7.3. Estimation of the imposed in situ stress state for artificially prepared samples subjected to two cycles of loading	122

List of Figures

Fig. 2.1. Typical stress-strain-pore pressure response under repeated loading (after Lefebvre et al. 1989): (a) For structured clay. (b) For normally consolidated clay 22
Fig. 2.2. Stress-path under repeated loading followed by monotonic loading after stabilization (after Lefebvre et al. 1989): (a) For structured clay. (b) For normally consolidated clay 23
Fig. 2.3. Loading data-time after the construction of grain elevator for a period of 5 years (after Deere and Davisson, 1956) 24
Fig. 2.4. Observed relationship between K_{o-nc} and $\sin\phi'$ for cohesive and cohesionless soils (after Mayne and Kulhawy, 1982) 25
Fig. 2.5. Simplified stress history of soil under K_0 conditions (after Mayne and Kulhawy, 1982) 26
Fig. 2.6. Measured and predicted response of Filter Sand during loading-unloading-reloading (after Mayne and Kulhawy, 1982) 26
Fig. 3.1. Hydrometer analysis for overconsolidated clay crust (depth, 3.30 m) 36
Fig. 3.2. Hydrometer analysis for kaolinitic clay 36
Fig. 3.3. Plot of pore pressure, back pressure, and cell pressure changes during saturation stage 37
Fig. 3.4. Representation of pore pressure dissipation 37
Fig. 4.1. Stress-strain, pore pressure-strain, and stress-path curves for CIUC under monotonic loading: Test K1 53
Fig. 4.2. Stress-strain, pore pressure-strain, and stress-path curves for CIUC under monotonic loading: Test K2 54
Fig. 4.3(a). Change in behaviour of kaolinitic clay during repeated loading at low levels of cyclic stress ratio 55

Fig. 4.3(b). Change in behaviour of kaolinitic clay during repeated loading at high levels of cyclic stress ratio	56
Fig. 4.4. Stress-strain, pore pressure-strain, and stress-path curves for CIUC under one-way repeated loading: CSR=0.5, Test S11	57
Fig. 4.5. Stress-strain, pore pressure-strain, and stress-path curves for CIUC under one-way repeated loading: CSR=0.63, Test S12	58
Fig. 4.6. Stress-strain, pore pressure-strain, and stress-path curves for CIUC under one-way repeated loading: CSR=0.7, Test S13	59
Fig. 4.7. Stress-strain, pore pressure-strain, and stress-path curves for CIUC under one-way repeated loading: CSR=0.78, Test S14	60
Fig. 4.8. Stress-strain, pore pressure-strain, and stress-path curves for CIUC under one-way repeated loading: CSR=0.85, Test S15	61
Fig. 4.9. Influence of the variation of the CSR on the peak strains and pore pressures: for test series S1	62
Fig. 4.10. Influence of the variation of the CSR on the peak strains and pore pressure for test series S1 in semi-log-plot	63
Fig. 4.11. CLRL (Results obtained from test series S1)	64
Fig. 4.12. Relationship between:	
(a) P' and the axial strains measured at peak of cycles of loading	
(b) P' and the pore pressure measured at peak of cycles of loading	65
Fig. 4.13. Relationship between: (a) Amplitude of applied stress and a maximum axial strain measured in tests S11, S12, and S13. (b) Amplitude of applied stress and a maximum pore pressure measured in tests S11, S12, and S13	66
Fig. 4.14. Variation of the coefficient a_i , b_i , c_i , and d_i with the amplitude of applied stress	67
Fig. 4.15. Variation of N_u and N_e with the amplitude of applied stress	68
Fig. 4.16. Boundaries for the tertiary cyclic loading stage	69
Fig. 4.17. Variation of: (a) axial strains measured at peak of cycles of loading with the number of cycles: Test S21. (b) pore pressure measured at peak of cycles of loading with the number of cycles. Test S21.	70

Fig. 5.1. Stress-strain, pore pressure-strain, and stress-path curves for CIUC under monotonic loading: Test T11	84
Fig. 5.2. Stress-strain, pore pressure-strain, and stress-path curves for CAUC under monotonic loading: Test T12	85
Fig. 5.3(a). Change in behaviour of clay crust during undrained repeated loading at low levels of CSR: Test C21, CSR=0.25	86
Fig. 5.3(b). Change in behaviour of clay crust during undrained repeated loading at high levels of CSR: Test C32, CSR=0.75	87
Fig. 5.4. Stress-strain, pore pressure-strain, and stress-path curves for CIUC under one-way repeated loading: Test C11, CSR=0.52	88
Fig. 5.5. Stress-strain, pore pressure-strain, and stress-path curves for CAUC under one-way repeated loading: Test C12, CSR=0.62	88
Fig. 5.6. Stress-strain, pore pressure-strain, and stress-path curves for CIUC under one-way repeated loading at different CSRs: Test C21	89
Fig. 5.7. Stress-strain, pore pressure-strain, and stress-path curves for CIUC under one-way repeated loading at different CSRs, Test C22	90
Fig. 5.8. Variation of both axial strains and pore pressure measured at peak of cycles with the number of cycles: Test C21	91
Fig. 5.9. Stress-strain, pore pressure-strain, and stress-path curves for CIUC under one-way repeated loading: Test C31, CSR=0.65	92
Fig. 5.10. Stress-strain, pore pressure-strain, and stress-path curves for CIUC under one-way repeated loading: Test C32, CSR=0.75	93
Fig. 6.1. Variation of the CLRL with the amplitude of applied stress	103
Fig. 6.2. Stress-strain, pore pressure-strain, and stress-path curves for CIUC tests under monotonic load: Tests K1 and S41	104
Fig. 6.3. Stress-strain curve for CIUC test under one-way repeated loading: Test S42	105
Fig. 6.4. Simplified stress history of soil subjected to fluctuation of water table	106
Fig. 6.5. A stress history applied to the sample S51	106

Fig. 6.6. Stress-strain, pore pressure-strain, and stress-path curves for CIUC tests under monotonic load: Tests K2 and S51	107
Fig. 6.7. Stress history imposed on samples C43 and C44	108
Fig. 6.8. Stress-strain, pore pressure-strain, and stress-path curves for CIUC tests under monotonic load: Tests C42 and C44	109
Fig. 6.9. Stress-strain curves for CIUC tests under one-way repeated loading: Tests S61, S62, and S63	110
Fig. 7.1. Simplified stress history of overconsolidated soils	121
Fig. 7.2. The concept of the proposed method	122
Fig. 7.3. Ideal and experimental ϵ_a - σ'_{H1} plot (after Garga and Khan 1991)	122
Fig. 7.4(a). K_c determination	123
Fig. 7.4(b) and (c). K_c determination	124
Fig. 7.4(d) and (e). K_c determination	125
Fig. 7.5. Representation of the stress history (loading and unloading)	126
Fig. 7.6. σ'_v - σ'_{H1} , σ'_v - ϵ_a , σ'_{H1} - ϵ_a plots for the test R1S01	127
Fig. 7.7. K_c determination after loading and unloading	128
Fig. 7.8(a) and (b). Representation of the stress history (two cycles of loading) for the test R2S01 and R2S02, respectively	129
Fig. 7.9. σ'_v - σ'_{H1} , σ'_v - ϵ_a , σ'_{H1} - ϵ_a plots for the test R2S01	130
Fig. 7.10. σ'_v - σ'_{H1} , σ'_v - ϵ_a , σ'_{H1} - ϵ_a plots for the test R2S02	131
Fig. 7.11. K_c determination after two cycles of loading	132

CHAPTER 1

Introduction

1.1 Behaviour of clayey soils under repeated loading

A problem of considerable importance in geotechnical engineering is that of understanding the behaviour of soils under slow repeated loading. While considerable research has been carried out on seismic response of soils, the problems of offshore technology have focused attention on slow repeated loading of soils. Highway engineers have also been interested in the response of subgrade soil and pavement materials to repeated loads of the type caused by moving vehicles, and testing of these materials under simulated loading conditions has been carried out in laboratories (Monismith et al. 1975). However, engineering problems of soils under repeated loading have to be considered not only in earthquake loading, wave action, and wheel traffic, but also in the case of structures subjected to slow repeated loading.

Storage of the materials such as grain, water, and oil, has led to the development of special structures like silos, reservoirs, and tanks. These structures are subject to many cycles of loading and unloading during their life. Loading and unloading causes a change in stress level, which has to be transmitted to and carried by the soil foundations. As a result, soil material beneath structure foundations experience cyclic stresses with different amplitudes and frequencies which will lead to cyclic deformations. These deformations will affect the structure and may cause damage. In addition, the change in stress-strain and soil strength during cyclic loading may have a significant influence on the stability of the structure. Therefore, the design of the foundation must ensure satisfactory performance both in terms of stability and

deformation. Prediction of these require an understanding of fundamental soil behaviour under loading and unloading conditions, which are typically of cyclic nature and involve slow shearing rates.

The behaviour of clay subjected to slow repeated loading is an important foundation design consideration for this type of structures. Up to present, only limited research has been done on the behaviour of clays under repeated loading, especially on their effective stress response under different amplitudes and slow frequencies.

In recent years, many experimental investigations were performed to study the behaviour of clays under cyclic loading. Although the conclusions of these examinations are not identical, several facts have emerged. The most important of these is that, under undrained loading, excess pore pressure and strains are generated and if cyclic loading is continued for a sufficiently long time a failure or a state of non-failure is reached. The limit separating failure and non-failure conditions is called the "Critical Level of Repeated Loading" (CLRL). A CLRL was first defined by Larew and Leonard (1962) as the maximum level of repeated stress that will not lead to failure. It was found also the CLRL depends on different parameters including plasticity of the soil (Lefebvre et al. 1989) and overconsolidation ratio (Conn and Hyde 1986).

An experimental investigation of the clay soil in a foundation would require the study of its behaviour under a wide range of loading conditions. The stress regime can be modeled approximately using a cyclic triaxial test. To simulate in the laboratory, the complex features of the cyclic loading history of a soil element beneath foundation of structure require a triaxial apparatus with the capability of applying vertical and radial stresses independently to simulate different amplitudes. Most experiments on repeated loading of soils have used the axi-symmetric triaxial test wherein the cell pressure is held constant and the deviatoric stress is pulsed. Therefore, the soil specimens is subjected to a pulsating axial load while the confining pressure is maintained constant. In reality, however, all principal stresses acting on a soil element subjected to repeated loads may vary in magnitude and direction simultaneously.

A major part of the investigation presented in this thesis concerns the examination of the undrained response of two clayey soils under various combinations of slow cyclic shear stresses. The first clay is an undisturbed overconsolidated clay crust obtained from Fraser Farm, 30 km Southwest of the University of Ottawa, while the second clay is the reconstituted kaolinitic clay commercially obtained from Alberta. These clayey soils have low plasticity and low coefficient of consolidation. Therefore, in most cases the stress changes will take place under undrained conditions. However, some dissipation of the excess pore pressure may occur during loading and unloading. The rate and magnitude of the pore pressure dissipation will be a function of the type and dimensions of the foundation of a structure and geotechnical characteristics of the soil profile. Thus, the dynamic response characteristics and stability are controlled by the effective stress regime in the soil. Because of the wide range of stresses used during testing, the results are expected to be useful in the analysis of many problems.

This study examines the following aspects:

- (1) The behaviour of both kaolinitic and clayey crust soils under different combinations of cyclic stresses.
- (2) Variation of the CLRL with the amplitude of applied stresses.
- (3) Effect of frequency.
- (4) Effect of the fluctuation of water table on strength of the soil.
- (5) Effect of cycling on the overconsolidation of normally consolidated clay and lightly and heavily overconsolidated soils.
- (6) Effect of cycling on postcyclic strength.

In the present experiments, repeated undrained load tests were carried out and involved the application of cyclic deviator stresses at a frequency of 0.0001 Hz for large amplitudes, and up to 0.001 Hz for small ones. To eliminate variation of the effect of the rate of repeated loading, the rate was kept constant in all tests equal to 1 kPa/min. This slow rate also permitted a reliable measurements of the pore pressure.

Triangular pulses were chosen for this investigation as they approximate the realistic case of loading and unloading conditions, although, in general, there is a short time that separates the end of loading and the beginning of unloading. Deere and Davisson (1956) observed and recorded data (load versus time) for a period of 5 years on a grain elevator; the load change with time was approximately triangular. Consequently, the effect of the shape of the pulse is not considered in this investigation.

1.2 Evaluation of in situ horizontal stress for overconsolidated sand:

The second and minor part of this thesis describes a method for the determination of in-situ horizontal stress of heavily overconsolidated sand using a stress-path triaxial apparatus. The evaluation of in situ stresses for sands is very important for variety of geotechnical problems including the problems related to deformation behaviour, foundations, excavations, and numerical analysis. The in situ vertical effective stress at any depth can be easily determined if the densities of the overlying materials, the thickness of the various layers, and the location of the ground water table are known. But the magnitude of the horizontal effective stress has remained speculative because the measurement of this stress is highly dependent on the geologic history of the soil and a reconstruction of this in laboratory is difficult. Practically, it is virtually impossible to install an earth pressure cell in-situ without causing a densification of the sand around the cell.

The method used for the evaluation of in situ horizontal stress is the one proposed by Garga and Khan (1991) who applied it for overconsolidated clay. They evaluated K_0 for overconsolidated

clay and demonstrated its validity by using samples of known stress histories. The proposed method is based on the concept that if an undisturbed soil sample is consolidated isotropically to a stress equivalent to the effective in situ vertical stress and subsequently the radial stress is increased while maintaining the in situ vertical stress constant, the sample will experience significant axial strain only when the radial stress exceeds the in situ horizontal stress.

Clean sand were used for this investigation and the sand samples were consolidated anisotropically without taking into account the likely field stress history. The specimen were consolidated arbitrarily to some anisotropic stress state such that $K_c > 1$. The consolidation stresses were applied simultaneously in vertical and horizontal directions, where the horizontal stress rate was greater than that of the vertical one to provide a value of K_c greater than unity. After full consolidation, both effective vertical and horizontal stresses were reduced to a low isotropic stress in drained conditions. By first consolidating the specimen isotropically to the imposed in situ effective vertical stress and, then, continuing the test, by increasing the radial stress (0.25 kPa/min) while keeping the effective vertical stress constant, it is found that the sample experienced significant axial strain only when the radial stress exceeded the imposed in situ horizontal stress.

1.3 Effect of the complex stress history undergone by soils on the evaluation of K_0 :

The coefficient of earth pressure at rest (K_0) is very sensitive to the geologic and engineering stress history, as well as to the densities of the overlying layers. Due to this, the effect of sedimentation and erosional process on the evaluation of K_0 by the proposed method was investigated. In past, the soil sample was subjected to a series of sedimentation and erosional processes during which the sand is normally consolidated and overconsolidated under K_0 conditions, respectively. Simulation of this in the laboratory was undertaken by subjecting sand samples to one and two cycles of loading at higher amplitudes of applied stresses and under a slow rate of loading of 0.05 kPa/min to ensure full consolidation during testing.

1.4 Research objectives:

The objectives of the study reported in this thesis are:

- (1) to achieve a better understanding of the behaviour of clayey soils under slow repeated loading at small and large amplitudes,
- (2) to study the effect of cycling on overconsolidation and strength of the clayey soils, as well as the effect of the frequency and fluctuation of water table on behaviour of clayey soils and the variation of the CLRL with the amplitude of applied stress,
- (3) to compare the behaviour of the normally consolidated clays under cycling to the one of overconsolidated clays,
- (4) to compare the general behaviour of clayey soils under slow repeated loading with the one under relatively fast cyclic loading reported in literature,
- (5) to evaluate the in situ horizontal stress for overconsolidated sand.

1.5 Outline of thesis:

The thesis consists of eight chapters as follows:

Chapter 2 : describes the previous studies on the behaviour of clayey soils under cyclic loading and on the determination of K_0 for overconsolidated sand.

Chapter 3 : describes the characteristics of the soil used for this investigation, equipment used, and test procedures.

Chapter 4 : describes the behaviour of kaolinitic clay under different combination of applied stresses.

Chapter 5 : describes the behaviour of the clay crust under different combination of applied stresses.

Chapter 6 : describes the variation of the CLRL with the amplitude of applied stresses, effect of the axial strain produced by repeated loading on postcyclic strength, effect of frequency, effect of cycling on the overconsolidation of the material, and the effect of the fluctuation of water table on behaviour of soils.

Chapter 7 : explores a new method for the evaluation of in situ horizontal stresses for overconsolidated sand. Also this chapter describes whether the sedimentation and erosional process as have an effect on the evaluation of in situ horizontal stress by this method.

Chapter 8 : presents conclusions and suggestions for future research.

CHAPTER 2

Literature Review

2.1 Behaviour of clayey soils under cyclic loading

The behaviour of clayey soils subjected to cyclic loading has been studied by a large number of researchers. Early investigations reported in literature and now classic experiments were performed by Bishop and Henkel (1953), who showed that, on removal of an applied shear stress under undrained conditions, some of the pore pressure generated during loading remained in the sample upon unloading. They named this remaining pore pressure as residual pore water pressure, which was found to be a function of the magnitude of the applied shear stress and the stress history of the soil.

Once a soil sample is subjected to repeated or cyclic loading, a change of residual pore water pressure may be associated with each cycle, so that the stress path followed by the sample may migrate in the effective stress space. Brown et al. (1975), applying fast, one-way repeated loading in triaxial tests in undrained conditions, on lightly and heavily overconsolidated samples of Keuper marl, showed that during a particular repeated load test, the maximum deviator stress remained constant, while the mean normal stress changed as the pore pressure changed. They also found that the direction of migration depended on the overconsolidation ratio (OCR). Positive values of pore pressure occurred for lightly overconsolidated samples, while negative values developed for heavily overconsolidated samples. Sangrey et al. (1969) found similar behaviour in their slow one-way repeated loading on Newfield clay, a small negative pore pressures developed in overconsolidated samples while the mean effective stresses was reduced in normally

consolidated samples.

A systematic study of the effect of applying slow undrained cycles of triaxial compression loading with constant amplitude (A) to samples of Newfield clay was reported by Sangrey, Henkel, and Esrig (1969). It was found that the development of pore pressure caused the effective stress cycles to migrate either to failure, or to equilibrium without failure. The limit separating failure and non-failure conditions was defined as the "Critical Level of Repeated Loading" (CLRL). This definition was first given by Larew and Leonard (1962), as the maximum level of repeated stress that will not lead to failure. Later Sangrey (1968), Sangrey et al. (1969), France and Sangrey (1977), and Sangrey et al. (1978) demonstrated the validity of this concept. Below this critical stress level, a state of non-failure equilibrium will be reached in which a stress-strain curve follows a closed hysteresis loop. Above the CLRL, each cycle of loading produces additional plastic deformation and an additional pore pressure which moves the effective stress path towards the dry side of the yield surface and eventual failure. It has also been found that, for any particular consolidation history, a CLRL always exists (Sangrey et al. 1969).

Non-failure conditions below a given level of repeated one-way loading have also been reported for other clay soils like sensitive Champlain Sea Clay (Mitchell and King 1977). Conn and Hyde (1986) found similar behaviour in their one-way and two-way cyclic triaxial tests on silty clay and identified a CLRL for all stress histories considered. They also reported that the CLRL decreased with increasing degree of overconsolidation, and the samples subjected to one-way loading in compression side appear to have a higher CLRL than those subjected to two-way loading.

Anderson et al. (1976) mentioned that below a certain critical shear stress level, cyclic loading has a negligible effect on the behaviour of Drammen Clay tested under two-way cyclic loading in the simple shear apparatus. Matsui et al. (1980), based on results of two-way cyclic loading triaxial tests on the Senry Clay, have also suggested the existence of a critical level of cyclic loading below which the rate of permanent pore water pressure generation would tend to zero. Ansal and Erken (1989), on cyclic simple shear tests on a kaolinite clay, showed that a critical

shear stress ratio exists for this soils and is approximately equal to 50% of the static shear strength at a frequency of 0.1 Hz. A critical shear stress ratio can also be defined as the CLRL.

In geotechnical earthquake engineering, it is useful to express the undrained resistance as a function of the number of cycles to failure. However, when the number of load cycles is very large and applied over a long period, it is better to express the cyclic undrained resistance as a threshold limit. The threshold limit theoretically corresponds to the maximum cyclic stress level at which the soil will not suffer failure regardless of the number of cycles (Lefebvre et al. 1989). Lefebvre et al. (1989) suggested the existence of threshold limit, approximately around 60-65% of the original undrained shear strength, measured at the same strain rate as that used in the cyclic tests. Their conclusion was based on results of repeated loading triaxial tests on a sensitive clay. A typical stress-strain and pore pressure-strain obtained from their tests on both structured Grande Baleine and normally consolidated clay, in which cycling was below a threshold limit, are shown in Fig. 2.1. They also found that undrained shear strength and the failure envelope remain essentially unchanged if the repeated preloading is kept below the threshold limit. Raymond et al. (1979) investigated the same concept, and indicated threshold values of about 0.5. Their results was based on triaxial drained tests on Leda Clay (PI=46). Different authors found that the threshold limit is a function of the plasticity index: the higher value of threshold limit were generally reported for high-plasticity soil and the lower values for low-plasticity soil; e.g. Anderson et al. (1980), Hicher (1980), Hyde and Ward (1985), Houston and Hermann (1980). Airey and Fahey (1991) conducted a cyclic tests (two-way) on calcareous soil, and showed the existence of a threshold limit for this soil.

A number of definitions for failure under undrained cyclic loading have been proposed which, because of the lack of continuous observations of effective stress changes, have not been linked to effective stress state. The most common criteria are the cyclic strain amplitude criteria, where failure is assumed when a given type of strain reaches a certain limiting value. Single or double amplitude cyclic repeated or shear strains have been randomly used. However, soil type, stress system, and consolidation or stress history affect the way in which deformation occurs so that such criteria cannot be used in general. Furthermore, as pointed out by Pande and Zeinkiewicz

(1982) in their recent review on laboratory investigation of the behaviour of soils under cyclic loading, differences between a steady build up of deformation and a sudden loss of strength cannot be distinguished.

In their tests on Newfield Clay, Sangrey, Henkel and Esrig (1969) found that failure under cyclic loading occurred at the failure envelope defined for the soil in slow monotonic loading tests.

The build up of pore pressure under cycling causes the effective stress space to migrate in stress space defined for the soil. Consequently, the soil generally weakens and loses stiffness. Cyclic strains build up and permanent strains may develop depending on the anisotropic characteristics of the material and of the test configuration (Anderson et al., 1977). A unique relationship between permanent axial strains and the residual pore water pressure has been shown to exist (Lo 1961). This relationship was based on one-way triaxial tests conducted on the normally consolidated Fomebu Clay. It has been also shown that the generation of permanent pore pressure is fundamentally a strain dependent process (Wilson and Greenwood, 1974; Lee and Focht, 1976). In contrast, the results of similar types of tests on the sensitive champlain clay obtained by Mitchell and King (1977) did not indicate any unique or any straightforward relation between strains and pore pressures.

Herrmann and Houston (1976, 1978) and Houston and Herrmann (1980) suggest that the rate of migration of effective stresses may strongly depend on the level of a bias static loading applied in undrained conditions prior to cyclic loading. The rate of deterioration (number of cycles to reach failure) under cyclic loading depends on the combination of the level of bias static loading and of the cyclic stress level. Their suggestion is based on results obtained from one-way and two-way triaxial tests on a number of clays at high frequency. They indicate that the higher the plasticity of the clay soil, the lower is the rate of deterioration under cyclic loading. They also suggest that higher sensitivity clays may offer higher resistance to cyclic loading because of the high bonding strengths which are generally associated with such soils. This view is supported by observations reported by Lee (1979) who reports above average resistance to cyclic loading in tests on sensitive clays.

The symmetric two-way cyclic loading does not always represent the worse loading conditions as observed by many authors such as Seed and Chan (1966), Seed and Lee (1969), Houston and Hermann (1980). In contrast, Hyde and Conn (1986) reported that stress reversal is more effective in inducing shear failure than cyclic loading without reversal.

The most dramatic effect of repeated loading on most saturated soils is a loss of strength or failure after some number of loading cycles. The potential for strength loss and failure increases as the level of cycled stress increases. Lower levels of undrained repeated loading do not produce failure even under a large number of stress cycles. During repeated loading, each cycle may be associated with an increase in the amount of strain. Below the CLRL, the amount of axial strain produced is negligible, the final soil behaviour is essentially elastic, and the level of static strength is still intact. Above the CLRL, each loading cycle leads to further non-recoverable deformations and the peak value of static strength decreases. Fig. 2.2 shows the stress-path obtained from repeated loading tests for both structured and normally consolidated clay in which cycling was imposed below a threshold limit (Lefebvre et al. 1989). This figure demonstrates that some excess of pore pressure developed in both soils, and the specimen failed on the original strength envelope in monotonic loading after cycling.

The decreases in strength has been generally related to the maximum cyclic or permanent strain (axial or shear strain) developed in the sample. The larger the strain, the greater is the decrease in strength. Thiers and Seed (1969) showed that the reduction in postcyclic strength is basically a function of the amount of cyclic straining a clay sample suffered before it is loaded monotonically to failure. A study by Anderson et al. (1980) on Drammen Clay has shown that a clay monotonically loaded to failure after having reached a $\pm 3\%$ axial strain under cyclic loading does not suffer a strength loss greater than 25%. Similar conclusions were reached by Lee (1979) from cyclic loading tests on two sensitive clays of Eastern Canada. The development of permanent axial strain in relatively slow cyclic triaxial compression tests on a lacustrine clay from Hamilton, Ontario, is reported by Wilson and Greenwood (1974). The amplitudes are expressed in terms of the peak deviator stress q as a proportion of the value of q required to

produce failure in monotonic loading. As might be expected, the larger the amplitude, the larger the resulting deformation, and, indeed, for the amplitudes greater or equal to 0.59, the test had to be halted when the continuing deformation of the sample could no longer be accommodated and failure was deemed to have occurred.

It was reported that the highly overconsolidated clay would exhibit larger strength loss than a normally consolidated material; Lee and Focht (1976). In contrast, however, the opposite behaviour was observed by Koutsoftas (1978). Moreover, Houston and Herrmann (1980) and Herrmann and Houston (1978) suggest that an increase in strength may result from a previous cyclic loading history.

The reduction in effective stress during cyclic loading in undrained condition results in a corresponding overconsolidation of the normally consolidated material. Lefebvre et al. (1989) suggest that the effect of migration of effective stress state is to make the clay behave as an overconsolidated soil. Their conclusion was based on results obtained from one-way repeated tests in compression side on sensitive clay. The stress path followed by the specimen after cycling in monotonic loading is similar to that occurring in a static test of an overconsolidated specimen. Wroth and Loudon (1967), based on results from one-way repeated tests on kaolin clay, reported that loading and unloading leaves a residual pore pressure in the sample, which makes the clay behave as an overconsolidated soil. This view is shared by other authors such as Taylor and Bacchus (1969), Koutsoftas (1978), and Anderson et al. (1980).

The soil response under cyclic loading is a function of frequency of loading. However, the published results are inconclusive. Anderson (1975) concluded, from his cyclic stress controlled simple shear tests on Drammen Clay ($PI=26$), that changing the frequency of loading from 0.05 up to 0.1 Hz has no significant effect on the number of cycles required to reach a cyclic strain of $\pm 3\%$. Similar conclusion was reached by Brown et al. (1975). They also stated that varying the frequency in the range 0.01 up to 10 Hz has no significant effect, for cyclic triaxial tests on Keuper marl ($PI=14$). However, Lefebvre et al. (1989), in their triaxial tests on sensitive clay ($PI=12$), reported that increasing the frequency from 0.01 up to 2.0 Hz increased the absolute

stability threshold by about 33 %. Brewer (1972) showed that for cyclic triaxial tests on Kaolinite (PI=35) in the frequency range 0.01 to 4 Hz, the lower the frequency, the higher in general is the strain. On the behaviour of saturated clay under seismic loading, Thiers and Seed (1969) showed that doubling the frequency from 1 Hz to 2 Hz considerably increases the number of cycles to failure for cyclic simple shear tests on San Francisco Bay mud (PI=45). However, the number of cycles to failure is not a very good parameter for giving a feel for the behaviour of the soil as it is bound to be heavily influenced by imperfections of apparatus and sample. The same conclusion was reported by Farmer (1983). Sherif and Wu (1971) showed that in general increasing the frequency from 1 Hz to 2 Hz has little effect on the permanent and cyclic strains and pore pressure, for a given cyclic stress level, for cyclic triaxial tests on clay (PI=26). Ansal and Erken (1989) reported that the response of normally consolidated clays obtained under different frequencies indicate that the decrease in the rate of loading leads to an increase in the accumulated pore pressures with respect to the number of cycles. This was also observed by Matsui et al. (1980). On the other hand, data obtained from cyclic triaxial tests on calcareous soil ($f= 0.1$ to 10 Hz) by Airey and Fahey (1991), showed that the stiffness during cycling appear to be unaffected by the loading rate, whereas, the measured pore pressure amplitude is significantly greater at the faster testing rate. However, Takahashi et al. (1980) suggested (on fast cyclic loading) that the pore pressure measured at the ends of the samples may be unrepresentative of the sample as a whole.

It seems likely that the effect of frequency is greater for more plastic clays, and intuitively it seems reasonable that slower cycles give the clay, as a viscous material, more time to follow the applied load and are likely to produce greater pore pressures.

The shape of the pulse has an effect on the determination of soil behaviour under cyclic loading. Rectangular, trapezoidal, sinusoidal and triangular shapes have been used by different investigators in their cyclic tests. The relative effect of different pulse shapes can be expected to depend on the proportion of time that the soil spends at the higher loads. Seed and Chan (1966) (on clay strength under earthquake loading conditions) showed that the rectangular stress pulses have a much more serious effect than triangular pulses. On the other hand, Anderson

(1975) (on repeated loading on clay) reported that, in terms of the number of cycles to reach a cyclic strain amplitude of $\pm 3\%$ in stress controlled simple shear tests on Drammen Clay, rectangular and trapezoidal pulses produced the same results for normally consolidated samples, whereas the rectangular pulses were slightly more damaging for samples with an overconsolidation ratio equal to 4. Deere and Davisson (1956) reported loading data for a period of five years after the construction of grain elevator, the load change with time was approximately triangular in form, as shown in Fig. 2.3. Also the cyclic tests considered in this thesis are done at slow rate of loading and the test results are expected to be applicable for the foundation of grain elevator, tanks, reservoirs and even for rail track pavement. In most of these cases the shape of the pulse is close to triangular shape. Consequently, the shape of the pulse chosen in this research is of a triangular form and the shape effect of the pulse has not been examined.

Finally, it is important to notice that the vast majority of the data available in the literature indicate that the peak cyclic stress necessary to cause failure under a finite number of stress applications is lower than the reference strength obtained in monotonic tests.

2.2 Determination of K_0 for overconsolidated sand:

The coefficient of lateral earth pressure under conditions of no lateral deformation, K_0 , has been of interest to soil engineers for over 100 years. This coefficient is defined as the ratio of in situ effective horizontal stress to the in situ effective vertical stress. For any soil, the in situ effective vertical stress can be easily estimated. However, the estimation of the in situ effective horizontal stress for overconsolidated sand is a complicated problem. This is because natural soil deposits have undergone a complex stress history and reconstruction of that in laboratory is difficult (Hanna and Carr 1971).

For an overconsolidated sand, the measurement of in situ stresses by field testing has been limited and the degree of accuracy has been questionable (Brooker and Ireland 1965, Duncan and Seed 1986). It is virtually impossible to install an earth pressure cell in situ, for example, without causing some disturbance and densification of the sand around the cell, and this changes the stress field at the very point of measurement. Consequently, the approach usually taken is to estimate K_0 from the proposed mathematical expressions (Brooker and Ireland 1965; Mayne and Kulhawy 1982; Shmidt 1983).

Historical Development:

The coefficient of earth pressure at rest (K_0) was introduced first by Donath (1891), who defined this coefficient as the ratio of the horizontal to the vertical earth pressure resulting in a soil from the application of vertical load under a condition of zero lateral deformation. Terzaghi (1920) conducted a significant work on K_0 and reported a value of $K_0 = 0.42$ for a coarse sand. Later in (1925) by using a modified equipment, he reported a value of $K_0 = 0.7$ for yellow residual clay and blue marine clay. Kjellman (1936) developed a complicated triaxial apparatus to perform one dimensional compression tests on sand. He reported values of K_0 varying between 0.5 to 1.5 and that it was a function of the stress history of the soil.

The best known expression for estimating K_0 was derived by Jaky (1948), which is a theoretical relationship between K_0 and the angle of shearing resistance of the soil:

$$K_0 = 1 - \sin \phi' \quad 2.1$$

This expression can be employed to estimate the value of K_0 for normally consolidated engineering soils and still widely used due to its practical significance and attractive simplicity. Fig. 2.4 shows that the relationship (2.1) is reasonable for cohesive and cohesionless soils.

If the soil deposits have undergone a complex stress history of loading and unloading, the prediction of in situ horizontal stress becomes a much difficult problem. Consider the simplified stress history as shown in Fig. 2.5 for a homogeneous soil deposit with horizontal ground surface. Stress-path OA represents virgin loading in which the soil was normally consolidated. Any reduction in the effective overburden stress (path ABC) results in overconsolidation of the soil and the value of K_0 becomes higher than the K_{0-nc} values obtained during virgin compression. Different investigators reported several expressions to quantify the coefficient K_0 for overconsolidated soil in terms of the magnitude of the OCR. They believe that if the degree of overconsolidation is introduced the value of K_0 can be determined exactly. However, the determination of OCR for cohesionless soils is rather difficult. This difficulty is due to the fact that it is impossible to obtain a sample of cohesionless soils with zero disturbance (Marchetti 1985).

One of the classic references for an observed K_0 -OCR relationship is the one presented by Brooker and Ireland (1965). They demonstrated that the stress history governs the value of K_0 , and that an increase in the OCR reflects as an increase in K_0 . Schmidt (1966,1967) and Alpan (1967) suggested that the increase in K_0 could be related to the overconsolidation ratio (OCR) by:

$$K_{0-oc} = K_{0-nc} (OCR)^b \quad 2.2$$

where b is an empirical exponent that varies between 0.4 to 0.5 (Alpan 1967; Schmertmann 1975) and even as high as 0.6 for very dense sands (Al-Hussaini and Townsend 1975). Ladd et al. (1977) pointed out that this exponent itself varies with OCR, and it seems to depend on the direction of the applied stresses.

The relationship K_0 -OCR was the subject of work conducted by different investigators (e.g.: Al-Hussaini and Townsend 1975; Saglamar 1975). The former concluded that the value of K_0 increases with increasing OCR. Their conclusion was obtained from laboratory tests on loose and dense dry sand.

Wroth (1975) confirmed the validity of the expression (1) proposed by Jaky in (1948) to calculate K_0 for normally consolidated soils and derived a relationship to compute K_0 for lightly overconsolidated soils:

$$K_{0-oc} = K_{0-nc} OCR - \left(\frac{\mu}{1-\mu} \right) (OCR - 1) \quad 2.3$$

where: K_{0-oc} , K_{0-nc} are the respective values of K_0 for overconsolidated and normally consolidated soils and μ is the poisson ratio. However, Wroth stated that this expression is only valid for lightly overconsolidated soils ($OCR < 5$). Meyerhof (1976) proposed a semi-empirical formula to estimate K_0 for overconsolidated soils, in which:

$$K_{0(oc)} = (1 - \sin \phi) \sqrt{OCR} \quad 2.4$$

In 1982, Mayne and Kulhawy proposed an expression to determine K_0 for overconsolidated soils in terms of the angle of shearing resistance (ϕ), the OCR, and a new stress history parameter OCR_{max} , in which:

$$K_0 = (1 - \sin \phi') \left[\frac{OCR}{OCR_{max}^{1 - \sin \phi'}} + \frac{3}{4} \left(1 - \frac{OCR}{OCR_{max}} \right) \right] \quad 2.5$$

OCR_{max} is defined as:

$$OCR_{max} = \frac{\sigma'_{v \max}}{\sigma'_{v \min}} \quad 2.6$$

where $\sigma'_{v \max}$ and $\sigma'_{v \min}$ are the maximum and minimum effective vertical stresses respectively. Equation (2.5) can be used to determine K_0 anywhere along the stress paths shown in Fig. 2.5 and to determine the probable bounds of K_0 in soil with more complex unload-reload histories. Results obtained by this equation are shown in Fig. 2.6.

The approach requires that only the stress history (OCR and OCR_{max}) and ϕ' for a particular soil be known. For natural soils, the current value of OCR may be determined from conventional consolidation tests or other methods. However, Mayne and Kulhawy (1982) stated that there appears to be no known technique of determining OCR_{max} for a specific soil deposit other than a good knowledge of local geology and stress history of the soil deposit.

Schmidt (1983) argued that horizontal pressures could be reduced with time due to aging and proposed the following simpler equation instead of (2.5) proposed by Mayne and Kulhawy (1982).

$$K_0 = \left[\frac{OCR}{OCR_{max} - 1} \right] \left[OCR_{max} - OCR + (OCR - 1) OCR_{max}^\alpha \right] \quad 2.7$$

where α is equal to $\sin \phi'$.

Clemence and Pepe (1984) reported that vibratory densification causes an increase in lateral stresses, which reflects in an increase in the value of coefficient K_0 . These lateral stresses at-rest condition are considerably higher than those expected for a normally consolidated sand. Later, Duncan and Seed (1986) reported a theoretical study on the effect of compaction in soil deposits. They concluded from their study that the sand compaction results in an increase of K_0 , OCR, and μ . The same conclusion was reached by Hanna and Ghaly (1992), in which the application of vibratory compaction represents a process of load application and removal. This process induces high horizontal stresses, which reflect their influence on K_0 . This results in K_0 value higher than that determined theoretically for a normally consolidated sand. In their experiment, the placement of a sand deposit in the laboratory in layers, and the application of compaction to every individual layer created a deposit in which the OCR increased with depth. In a natural stratum, the OCR decreases with depth. However, the authors do not propose any new expression or method to evaluate K_0 for overconsolidated sand.

No practical method is presented in the literature for estimating K_0 for lightly and heavily overconsolidated sand. There are some empirical or indirect methods (e.g.; Brooker and Ireland 1965; Mayne and Kulhawy 1982, Schmidt 1983) available for the determination of in situ stresses of lightly and heavily overconsolidated cohesionless soils. But all of these methods are dependent on a combination of laboratory tests. Based in literature, K_0 is affected by different parameters including the effective angle of shearing resistance, porosity, crushing, modulus of elasticity of the minerals particles, aging, densification, compacting method, stress history.

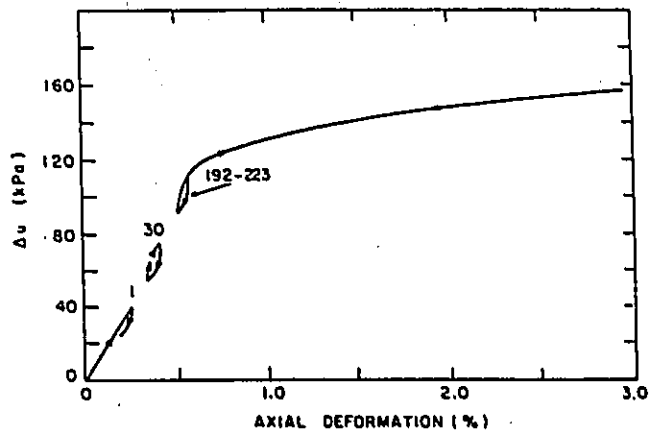
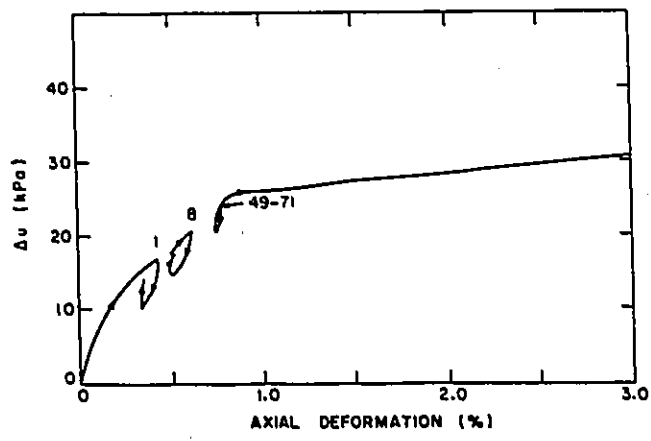
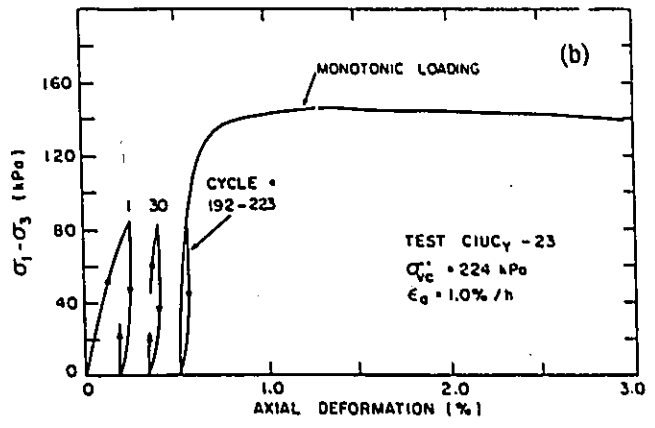
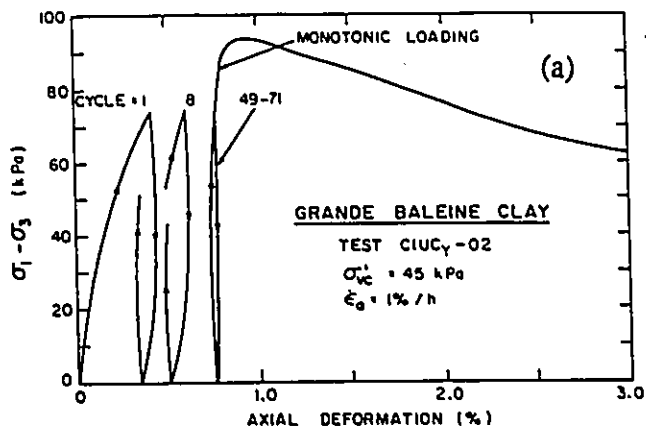


Fig. 2.1. Typical stress-strain-pore pressure response under repeated loading (after Lefebvre et al., 1989). a) for structured clay.
 b) for normally consolidated clay.

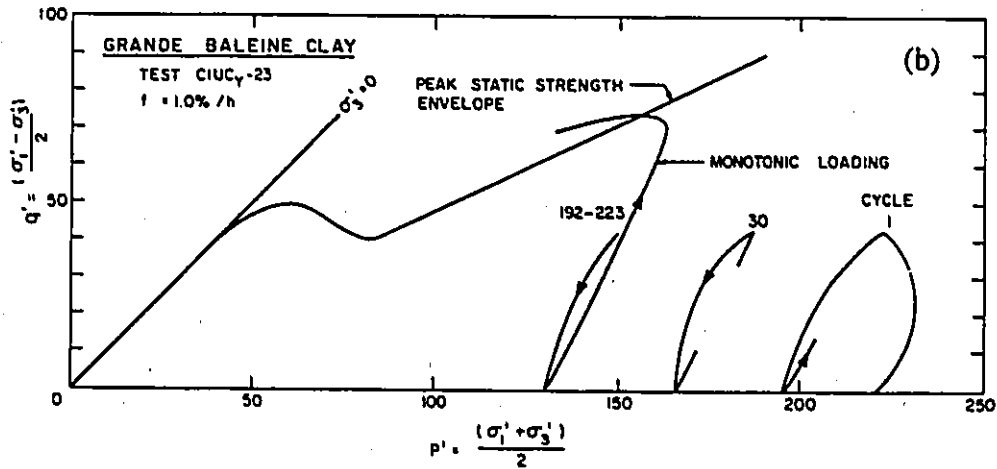
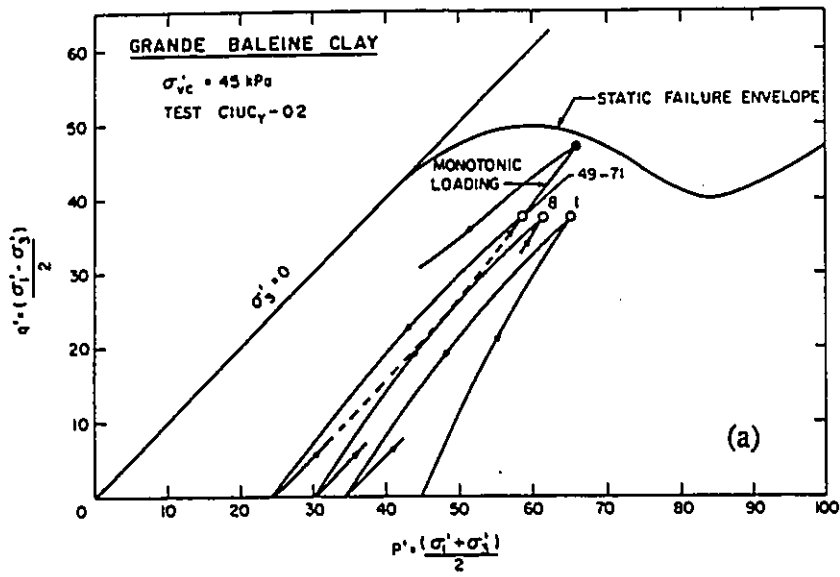


Fig. 2.2. Stress-path under repeated loading followed by monotonic loading after stabilization (after Lefebvre et al., 1989): a) for structured clay.
 b) for normally consolidated clay.

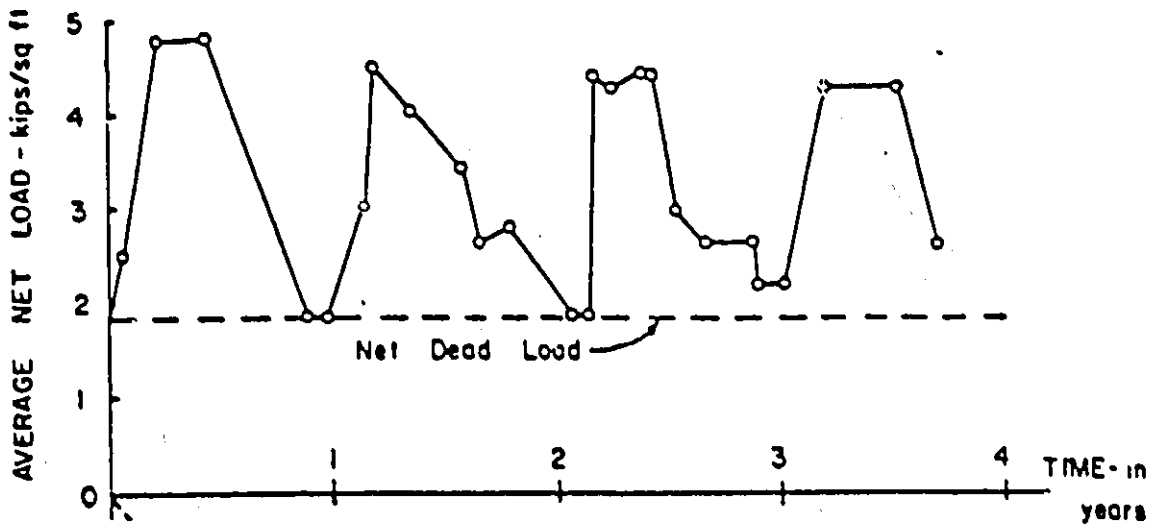


Fig. 2.3. Loading data-time after the construction of grain elevator for a period of 5 years (after Deere and Davisson, 1956).

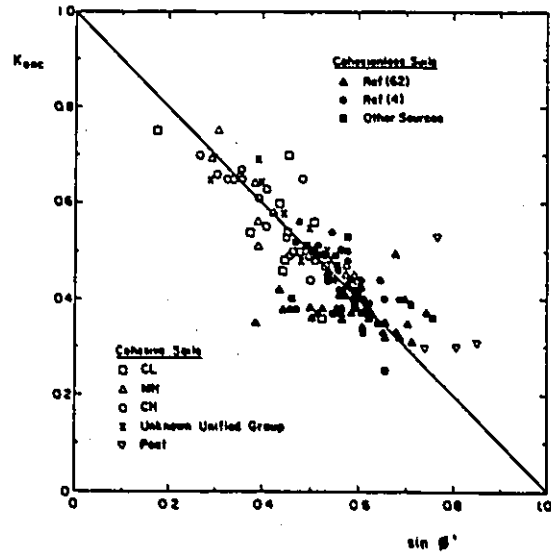


Fig. 2.4. Observed relationship between $K_{0,nc}$ and $\sin \phi$ for cohesive and cohesionless soils (after Mayne and Kulhawy, 1982).

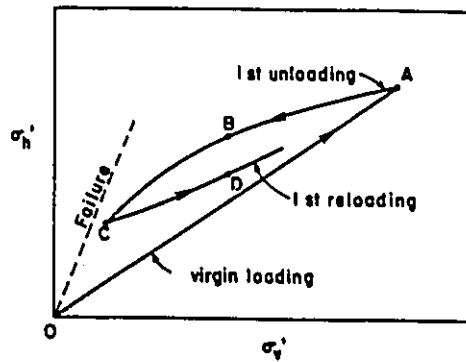


Fig. 2.5. Simplified stress history of soil under K_0 conditions (after Mayne and Kulhawy, 1982).

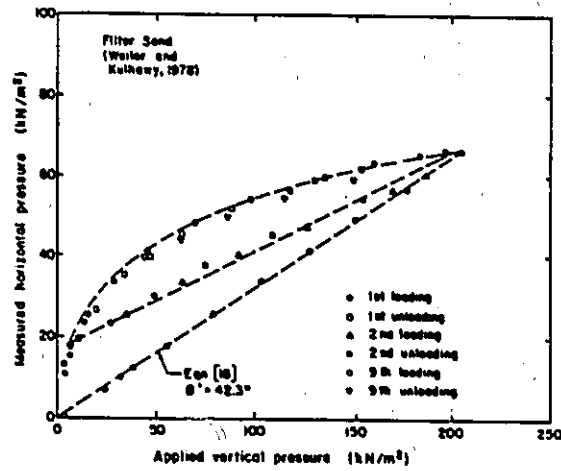


Fig. 2.6. Measured and predicted response of Filter sand during loading-unloading-reloading (after Mayne and Kulhawy, 1982).

CHAPTER 3

The Experimental Program

3.1 Introduction:

The objective of this experimental work was to quantify the undrained response of the two clayey soils under various combination of slow cyclic shear stresses. Thirty stress-controlled, consolidated undrained cyclic triaxial tests were performed on two clayey soils. The purpose of these tests was to examine the behaviour of these clayey soils under the change in the amplitude, frequency, number of cycles, fluctuation of pore pressure, and also to examine the effect of cycling on the overconsolidation of the material and postcyclic strength and the variation of CLRL with the amplitude of applied stresses. In addition to the consolidated cyclic undrained tests, a number of consolidated undrained static triaxial compression tests were conducted in order to provide a basis for interpreting the results of cyclic static tests.

The first clay used in this investigation is an overconsolidated crust clay, obtained from Fraser Farm, 30 km Southwest of the University of Ottawa. Hand-cut cubical samples were collected from this crust. The size of these cubes was approximately 225 mm. Above 2 m depth level, some rocks, roots, and worm-holes were observed. Because of the presence of these rocks, roots and holes, some scatter is to be expected in the test results. Therefore, most of the tests were conducted for the depth range of 2.7 m and 3.6 m. The limited number of cubes available in this range were not adequate enough to achieve all the objective of this research, hence a second clay was also used. The second kaolinitic clay was commercially obtained from Alberta. The size of

obtained from Alberta. The size of the two blocks obtained from kaolinitic clay is around 140 mm in height, 140 mm in width, and 300 mm in length.

The peak undrained strength was used as a reference failure criterion for the overconsolidated clay crust. For kaolinitic clay, a maximum axial strain of 5% was used as a failure criterion. Most of the tests conducted on these two clays were continued until failure of the specimen occurred. However, many samples did not fail under cycling and reached equilibrium conditions. For these samples, the available undrained shear strength was determined immediately after the end of repeated loading. For the samples used for other objectives such as to investigate the effect of cycling on postcyclic strength, the tests were stopped after a required axial strains were developed under cycling and repeated loading was followed by a monotonic one.

3.2 Description of the materials:

Undisturbed and remoulded block samples have been used in this study. The undisturbed samples refers to the overconsolidated clay crust, while the commercial kaolinitic clay was obtained in remoulded and reconstituted blocks.

3.2.1 Overconsolidated clay crust:

This soil is a clayey silt containing of occasional thin seams of silt and fine sand but does not show any detectable layering. The soil profile consists of clayey silt of dark grey colour which exhibits overconsolidation behaviour with an overconsolidation ratio (OCR) of 3.1 at 3.7 m depth and 5.2 at 2.7 m. The OCR increases linearly with decreasing the depth. This overconsolidation may be due to combined effect of erosion, desiccation, or chemical changes due to leaching. The physical characteristics of this soil are shown in Table 3.1. Detailed description is provided in Khan and Garga (1991).

Hydrometer analysis:

Hydrometer analysis is a widely used method of obtaining an estimate of the distribution of soil particle sizes from #200 (0.075 mm) sieve to about 0.001 mm. The hydrometer data obtained are plotted on a semilog-plot of percent finer versus grain diameters as shown in Fig. 3.1. This hydrometer analysis is done at 3.3 m depth and can be considered representative of soil between a depth of 2.7 m to 3.6 m. The clay fraction is 43%.

3.2.2 Kaolinitic Clay:

Two block samples were commercially obtained from this soil. The first block showed a slightly higher preconsolidation pressure (p_c) of 31.3 kPa compared to the second block in which p_c was equal to 26.3 kPa. This soil is a clayey soil with a brownish grey in colour and contains a trace of silt. The physical properties determined from laboratory tests on the block samples are presented in Table 3.1.

Hydrometer analysis:

The data obtained from this analysis are plotted on a semilog-plot of percent finer versus grain diameters as shown in Fig. 3.2. The clay fraction is 67%.

3.3. Equipment Used:

The equipment used comprised a hydraulic triaxial cell connected to an air pressure system and controlled by a closed-loop control system controlled by computer. This equipment is capable of generating both slow and fast cyclic stresses. An internal load cell were used to measure axial loads. Pressure transducers (resolution 0.3 kPa) were used to measure the cell pressure, pore water pressure at the base of the sample, and back pressure at the top of the sample. An automatic volume gauge transducer were used to measure the volume change. A displacement transducer (resolution 0.01 mm) connected externally to the cell, was used to measure the axial deformation. The radial strain was measured by a radial hall effect transducers was placed at mid-

height of the sample.

A 2 mm stainless steel tubing into the base pedestal connects the cavity behind the porous stone to the base pore water transducer. A similar arrangement in the cap connects the cavity behind the porous stone to the back pressure system. The displacement transducer was seated at the top of the cell diagonally opposed to an L-shaped arm attached to the ram.

The vertical load is applied to the sample from below the pedestal. Two bellofram rolling seals seated at each extremity of the ram permit the application of hydraulic pressures separately to the lower chamber and to the upper perspex cell. The ram is forced to move vertically, upwards or downwards, depending on the direction of the force resulting from differential pressure applied to the cell and to the chamber. The axial pressure is applied to the sample by the bottom platen which is fixed in the horizontal direction but is able to move axially.

Upward movement of the top of the sample is prevented by the internal load cell while downward movements can be prevented by means of some convenient coupling between the load cell and top cap. Thus, by changing the upper and the lower chamber pressures, it is possible to follow many desired stress paths, both in the compression and extension sides of the triaxial stress space. For cyclic loading, the ram moves vertically between two limits which are fixed depending on the test requirement. The ram pressure is applied at a constant rate.

Air pressure was used in the control of radial, vertical, and back pressures. The air pressure control system is formed by the main pressure system, air valves, and servo-motors. Changes in pressure are provided by the servo-motors which operate according to signals from the servo-amplifiers and rotate the air valve spindle through a reduction gear-box. Air-water interchange pressure cylinders were used to provide hydraulic pressure to the triaxial cell.

A volume gauge was used which has a total volume change capability of 100 cc. This volume gauge uses a piston fitted with a bellofram diaphragm. The vertical movement of the piston is calibrated to provide measurements of volume change. The calibration curve of this gauge is

linear only over the middle 55 cc. The combination of the initial and final curved portions, including the middle straight line portion of the calibration curve, has an "S" shape. This volume gauge, with a linear calibration of 55 cc, satisfied the requirement of these tests.

In addition to cyclic tests, the system is capable of performing any triaxial compression or extension stress path tests. It can be used for any stress-controlled, strain controlled, or combination of both stress and strain-controlled tests.

3.4 Test procedures:

3.4.1 Specimen preparation:

Block samples obtained from the two materials were waxed and then stored in high humidity room. A small block was cut from the larger one using a fine wire saw, care being taken to maintain the axis of the sample parallel to the vertical direction. The final trimmed size of the test specimens was 50.6 mm in diameter and 101 mm in high. The ends were cut parallel to each other and flat using a very thin wire saw. Considerable care was taken at this stage to guarantee that the end surfaces were as smooth and parallel as possible in order to minimize bedding errors and guarantee axial symmetry of loading. The specimen was then weighed.

3.4.2 Triaxial cell assembly:

After preparation, the sample was installed in a triaxial cell. In addition to the top and bottom drainage, the side drains were also used to accelerate consolidation. Then, the sample was covered by a thin membrane. When working with the hydraulic triaxial cell, care was taken at this stage to ensure that the piston at the chamber was at the lowest position and the load cell at the highest level. After installation of the sample, the cell was filled with distilled-water. Then, the initial isotropic stress conditions were applied to the sample isotropically. Generally an initial cell pressure of 15 kPa and a back pressure of 10 kPa was used before starting the saturation process. For the unsaturated samples, the sample was consolidated to the desired stresses directly.

3.4.3 Saturation of the specimen:

Saturation by increments of back pressure was used in this experimental work. The first two cell pressure increments were of 50 kPa, and a differential between cell and back pressures of 10 kPa was maintained after each cell pressure increment. The following cell pressure increments were of 100 kPa, and a differential of 10 kPa of back pressure was always maintained, as shown in Fig. 3.3. For both soils, only 300 kPa was required to achieve full saturation of the sample. The B value obtained at the end of this stage was around 0.99 for all the samples.

3.4.4 Consolidation:

All samples were either isotropically or anisotropically consolidated to bring the soil to the desired initial state of stresses before applying any undrained loading.

3.4.4.1 Isotropic consolidation:

Most of the samples were isotropically consolidated prior to undrained loading. After applying the cell pressure, the back pressure required to bring the sample to the desired effective stresses was applied in one step; the cell pressure being kept constant. After the pore pressure at the base and the top had equalized, the sample was left under drained conditions for an additional period of 24 hours.

3.4.4.2 Anisotropic consolidation:

After full saturation, the sample was consolidated anisotropically by applying the stress path method, by increasing the effective horizontal stress and keeping the vertical one constant (overconsolidated clay), until in-situ stress required was achieved. Therefore, the back pressure was increased to the value required to achieve the in situ stresses conditions.

For isotropically and anisotropically consolidations, the dissipation of water pressure build-up with time is of the form shown in Fig. 3.4, for both materials. To accelerate drainage during consolidation, both top and bottom drainage were allowed.

3.5 Conventional Oedometer Tests:

These tests are done on 50 mm undisturbed and remoulded samples of the both clays. Preconsolidation pressure, as well as the values of overconsolidation ratio (OCR), were obtained from these consolidation tests.

3.6 Monotonic and Cyclic Loading:

After consolidation, the rate of the applied load was fixed to 1 kPa/min. This rate was slow enough and is believed to simulate similar the real rate of applied loading and unloading for many problems.

Monotonic tests:

Nine samples were first tested under monotonic loading in order to evaluate their undrained static strength at failure (q_f). The nine samples comprised of six overconsolidated clay crust samples, two kaolinitic clay samples, and one from clay crust which was sampled in horizontal direction to simulate the slightly overconsolidated clay.

Cyclic tests:

Thirty samples were subjected to repeated loading under the same rate, except for the samples used to investigate the effect of the rate of loading. In a typical test, a specimen was subjected to a series of loading and unloading which alternated between two constant values of the stress difference ($\sigma_1 - \sigma_3$), and which were fixed according to the requirement of the testing conditions. The cyclic loading and unloading was continued until either the specimen failed under the applied stress or a condition of equilibrium is reached.

Table 3.2 shows the complete program of tests.

Table 3.1. General properties of the crust and kaolinitic clays.

Properties	Crust clay	Kaolinitic clay
Total density (KN/m ³)	18±0.1	19.7
liquid limit (%)	42±2	42
plastic limit (%)	20±2	20.4
plasticity index (%)	22±2	21.6
Water content (%)	41±1	26
Specific gravity	2.75	2.78
% < # 200 sieve	99	94
% < 2μ	43	67

Table 3.2. Complete program of testing on kaolinitic, crust, and highly overconsolidated clays.

Overconsolidated Clay Crust				
Test series	Sample number	Test type	Remarks	Parameter examined
T	T1, T1, and T2	CIUC	Static test	Determination of q_r .
	T11, T22, and T33	CAUC	Static test	Determination of q_r .
C1	C11	CIUC	Cyclic test	Effect of cycling at 50% q_r on postcyclic strength.
	C12	CAUC	Cyclic test	
C2	C21 and C22	CIUC	Cyclic test	Effect of cycling at low levels of CSR.
C3	C31, C32, and C33	CIUC	Cyclic test	Behaviour at high levels of CSR.
Kaolinitic Clay				
K	K1 and K2	CIUC	Static test	Determination of q_r .
S1	S11, S12, S13, S14, S15, and S16	CIUC CIUC	Cyclic test	Behaviour at high levels of CSR.
S2	S21	CIUC	Cyclic test	Effect of the variation of the CSR.
S3	S31, S32, S33, S34, S35, S36, S37, S38, and S39	CIUC CIUC	Cyclic test	Variation of the CLRL with the amplitude of applied stress.
S4	S41	CIUC	Static test	Frequency.
	S42	CIUC	Cyclic test	Frequency.
S5	S51	CIUC	Cyclic test	Fluctuation of water table.
S6	S61, S62, S63, and S64	CIUC	Cyclic test	Effect of cycling on postcyclic strength.
Lightly Overconsolidated Clay				
C4	C41	CIDE	K_0 test	Effect of cycling on overconsolidation of the soil
	C42	CIDC	K_0 test	
	C43	CAUC	Static test	
	C44	CIUC	Static test	

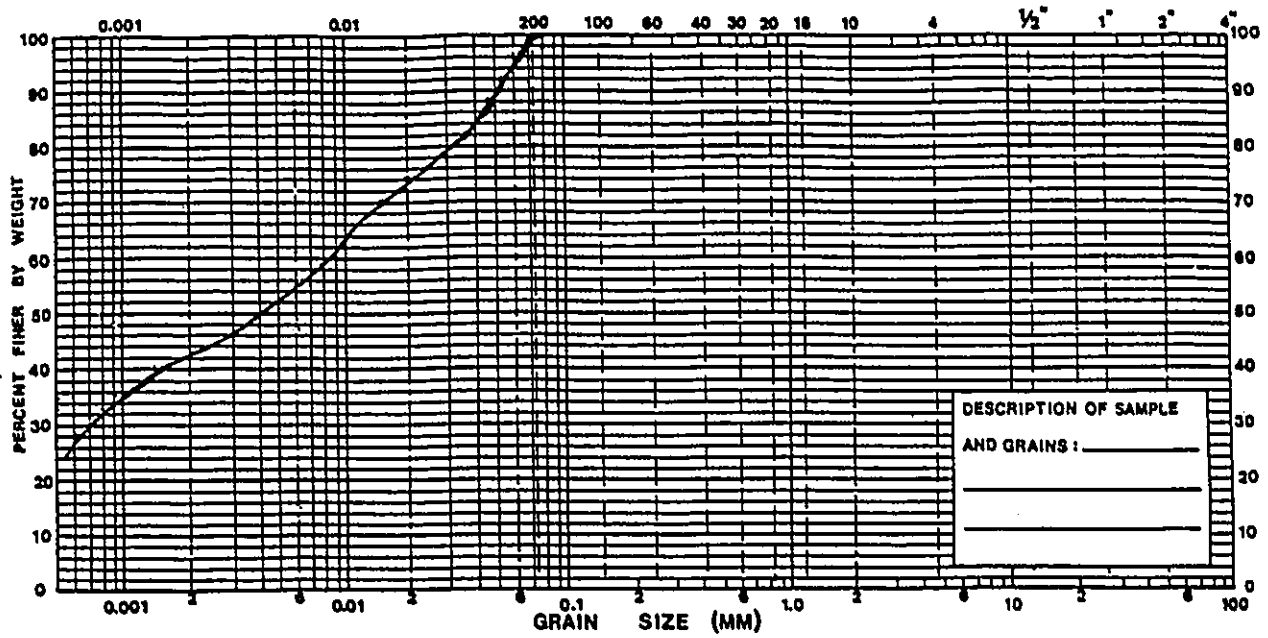


Fig. 3.1. Hydrometer analysis for overconsolidated clay crust (depth, 3.30m).

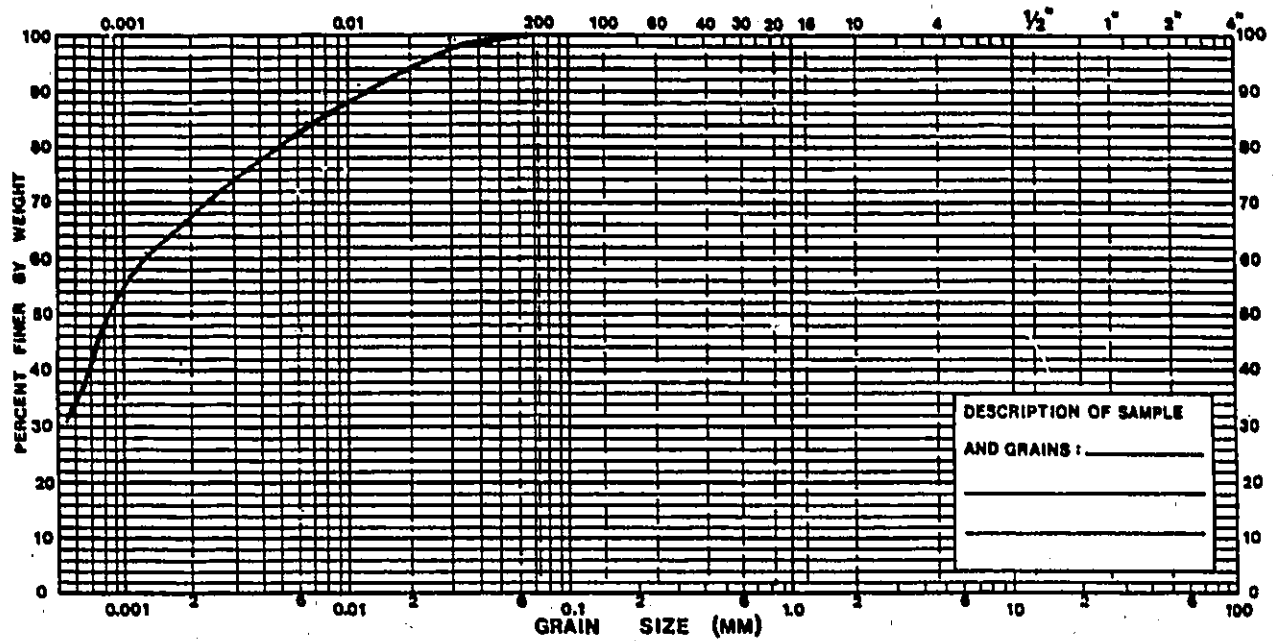


Fig. 3.2. Hydrometer analysis for Kaolinitic clay.

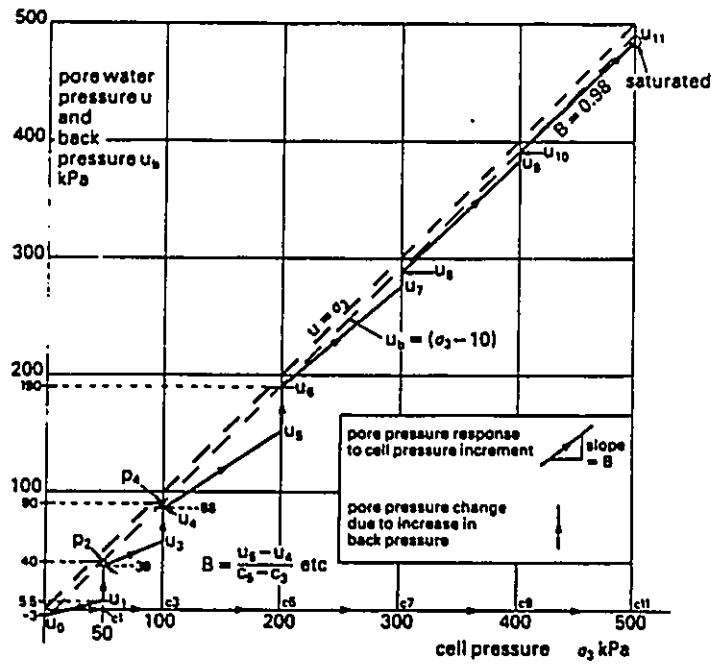


Fig. 3.3. Plot of pore pressure, back pressure, and cell pressure changes during saturation stage.

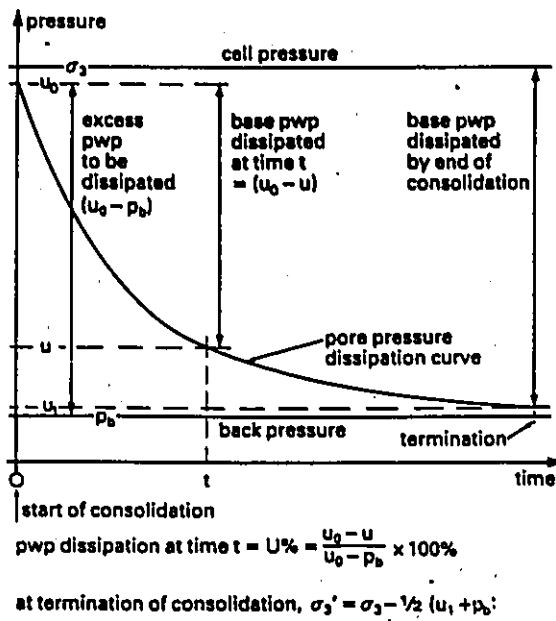


Fig. 3.4. Representation of pore pressure dissipation.

CHAPTER 4

Behaviour of the Kaolinitic Clay Under Static and Repeated Loading

4.1 Monotonic tests:

The two blocks of this commercially obtained clay showed different preconsolidation pressures. Hence, from each block, a sample was consolidated isotropically to an initial effective stress of 20 kPa and then taken to failure under monotonic loading. A summary of the testing conditions and test results is given in Table 4.1.

The response of the kaolinitic clay to static loading is unusual and similar to the response of Weald clay reported by Bishop and Henkel (1953). It was observed during testing that the shear failure occurs with significant bulging. Figs 4.1 and 4.2 show the stress strain, pore pressure-strain, and stress path curves obtained from these two tests, K1 and K2, respectively.

The behaviour of these two samples under monotonically loading can be summarized as follows:

- (1) The axial strain is apparent from the beginning of shearing and increases rapidly after it reaches 0.5%.
- (2) The pore pressure increases at the initiation of shearing. The maximum value of pore pressure is achieved at 0.7% axial strain and the pore pressure then starts decreasing until negative values are measured.

- (3) The maximum value of the positive pore pressure developed is around 13 kPa and 11 kPa in tests K1 and K2, respectively.
- (4) The static strength obtained at 5% axial strain is around 72 kPa for the first sample and 61 kPa for the second one. These values are considered as failure strengths.
- (5) At failure, a negative value of pore pressure of -4.2 kPa was measured in test K1 and -1.8 kPa in the test K2.

4.2 Repeated loading tests:

4.2.1 Test series S1 and S2:

The maximum and minimum levels of shear stresses applied in the cyclic tests have been expressed as a proportion of the undrained strength measured in monotonic loading test. The ratio is referred to as the cyclic stress ratio (CSR) and is defined as the repeated axial stress difference divided by the axial stress difference that caused failure in a static test. Two test series, S1 and S2, are presented and discussed here. These test series are used to examine the corresponding parameters indicated in Table 3.2.

Test series S1:

This test series comprises 6 tests. In each test, the specimen had the same consolidation history as that used to determine monotonic strength (test K1). The CSR used in these tests varied between a minimum value of 0.11 and a maximum value which is a proportion of the static strength ($CSR_{max}=0.5, 0.54, 0.64, 0.71, 0.77, 0.84, \text{ and } 0.93$). In each test, cycling was applied with a constant amplitude of applied stress until failure or equilibrium conditions was reached. The equilibrium conditions means that no additional axial strain or pore pressure was developed with additional cycles of loading. For the tests that reached equilibrium conditions, the repeated loading was followed by a monotonic one. A summary of the testing conditions and test results

are shown in Table 4.2.

Test series S2:

This test series comprises only one test. In this test, the specimen had the same consolidation history as that used to determine monotonic strength (test K2). The specimen was subjected to a total of 6 sets of cycles. In each set of cycles, cycling was continued until failure or equilibrium conditions was reached. In each set of cycles, a regular amplitude was maintained and cycling continued until failure or equilibrium conditions was reached. Summary of the testing conditions and test results are shown in Table 4.2.

4.2.2 Test results and discussion:

The typical response of the kaolinitic clay to undrained repeated loading at low and high cyclic stress ratios is shown in Fig. 4.3 (a) and (b), for the tests S12 and S14, respectively. These figures show the variation of the pore pressure and axial strain with time. As can be seen, for low cyclic stress ratio, as the number of cycles of loading increases the axial strains build up where the pore pressure decreases in the first few cycles before the equilibrium conditions are reached. For high cyclic stress ratio, the axial strains build up continuously whereas the pore pressure decreases as the number of cycles of loading increases until failure is reached.

Results of test series S1:

Sample S11:

This sample was repeatedly loaded 50 times. The stress-strain, pore pressure-strain, and stress-path curves obtained are shown in Fig. 4.4. It was observed that the sample had reached the equilibrium conditions after the first few cycles. With additional cycles no further increase in both axial strain and pore pressure were measured. However, it is interesting to note that pore pressure stabilized before axial strain. An axial strain of 0.18% and a change in pore pressure of -1.8 kPa were developed in the sample under cycling. As stated earlier, a repeated loading was

followed by a monotonic one. It was observed that the sample showed a very slightly higher strength than the one obtained in the static test.

Sample S12:

This sample was also repeatedly loaded 50 times. Fig. 4.5 shows stress-path, stress-strain, and pore pressure-strain curves obtained from this test. The pore pressure reached equilibrium after 9 cycles of loading, however, axial strains stabilized after 11 cycles of loading. An axial strain of 0.3% and a change in pore pressure of -2.8 kPa were developed under cycling. These values are higher than those obtained in test S11, but, nevertheless smaller when compared to those obtained at failure in the static test. Repeated loading again was followed by monotonic loading. It was found that the sample showed a postcyclic strength which was also very slightly higher than the one obtained in the static test.

Sample S13:

The sample was repeatedly loaded 50 times. Fig. 4.6 shows the stress-strain, pore pressure-strain, and stress path curves obtained from this test. A significant axial strain of 0.52% and a change in pore pressure of -6 kPa had developed in this test under cycling. After the first 13 cycles of loading, the pore pressure reach equilibrium. However, the axial strain reached equilibrium after 15 cycles. At the end of 50 cycles the test was stopped and the sample sheared monotonically. It was found that this sample showed a maximum deviatoric strength of 68.5 kPa which is less by 3.5 kPa compared to the static strength.

Sample S14:

This sample was repeatedly loaded to failure (50 cycles). Fig. 4.7 shows the stress-strain, pore pressure-strain, and stress-path curves obtained from this test. As can be seen in this figure, the rate of strain decreased in the earlier stage of the test, followed by a steady build up of strain at a constant rate preceding an increase in the latter stage as the sample tends to failure. Similar behaviour was observed for pore pressure. Fig. 4.7 demonstrates that the response of this clay to repeated loading can be divided in three stages as discussed subsequently.

Sample S15:

This sample was repeatedly loaded to failure in 8 cycles at a higher cyclic stress ratio that varied between 0.11 and 0.85. Fig. 4.8 shows stress-strain, stress-path, and pore pressure-strain curves obtained from this test. Also the response of this sample to repeated loading can be divided in three stages as in test S14, but here these stages can not be clearly distinguished.

Sample S16:

This sample was also repeatedly loaded to failure at a cyclic stress ratio that varied between 0.11 and 0.93. The upper limit of this CSR is close to unity which causes the failure of the sample only in two cycles.

The variation of the axial strains and pore pressures both measured at the maximum repeated stress with the number of cycles is shown in Fig. 4.9 for all levels of CSRs imposed on this clay. The axial strains increases with the number of cycles with a corresponding decrease in pore pressure. The cyclic behaviour clearly depend on whether the CSR is above or below a value of approximately 0.74.

Application of CSR greater than 0.74 causes the axial strain to increase and pore pressure to decrease until shear failure occurs. CSR less than 0.74 does not result in sudden failure after the maximum number of 50 cycles applied in these tests. It is difficult to evaluate CLRL precisely, however, from the test results the CLRL can be fixed at a level of approximately CSR=0.7. This CLRL is represented by a horizontal line in Fig 4.11(a). Below this line no sudden increase in deformation or decrease in pore pressure would occur regardless of the number of stress repetitions. Above the CLRL, each cycle of loading produces additional plastic deformation and the clay eventually fails.

4.2.3 Behaviour of kaolinitic clay below CLRL:

As mentioned before, the CLRL was found to be at CSR=0.7. The samples subjected to cyclic loading less than this level reached the equilibrium conditions, as the case of the samples S11,

S12, and S13. Samples subjected to cyclic loading above this limit failed (S14, S15, and S16).

Samples S11, S12, and S13 were subjected to 50 repeated loadings as shown in Figs 4.4, 4.5, and 4.6. An important feature of these figures is that stabilization of axial strains and pore pressures was apparent after a certain number of cycles. No increase in both axial strain and pore pressure was measured with additional cycles. Most of the axial strains and pore pressure developed took place in the first cycles of loading. It was observed for this clay that the axial strain reaches equilibrium before pore pressure does. The axial strain, pore pressure, and the number of cycles required to reach the equilibrium for these samples are a function of the cyclic stress ratio used.

In order to appreciate the significance of these results, it is useful to represent the stress paths followed in the tests in effective stress space. The results of tests S11, S12, and S13 are shown, plotted in this space, in Figs 4.4, 4.5, and 4.6. For these tests, the decrease in pore pressure in the first few cycles leads to the migration of the stress path to the right side before an equilibrium condition, shown by the closed stress loop, is reached.

The quantitative analysis of the results obtained from the tests S11, S12, and S13 demonstrates the behaviour of this clay, below a CLRL, can be predicted by some equations which are function only of the amplitude of applied stresses.

First, the relationships between the axial strains and p' , both measured at the maximum repeated stress, are used to investigate the influence of the amplitude of applied stress on the behaviour of this clay below the CLRL. Test results indicate that there is a linear relationship between the variation of p' and the axial strain developed at the end of each cycle of loading as shown in Fig. 4.12(a). This figure shows three lines. The ends of these lines represent the equilibrium points and the maximum axial strain that can be developed in the sample. The equations of these lines for tests S11, S12, and S13 are respectively:

$$\epsilon_1 = 0.087 p'^{-1.95} \quad 4.1$$

$$\epsilon_2 = 0.1 p'^{-2.49} \quad 4.2$$

$$\epsilon_3 = 0.11 p'^{-2.71} \quad 4.3$$

These equations indicate that, as the amplitude of applied stresses increases the slope of these lines increases.

Test results also indicated that, the variation of pore pressure with p' can be described by a linear relationships. Fig. 4.12(b) shows three lines, the end of each line describes the equilibrium point and the maximum pore pressure that can be generated under repeated loading. The equations of these three lines can be written as:

$$u_1 = -1.15 p' + 31.84 \quad 4.5$$

$$u_2 = -1.05 p' + 31.45 \quad 4.4$$

$$u_3 = -1.03 p' + 33.54 \quad 4.6$$

The ends of the lines shown in Figs 4.12(a) and (b) represent the equilibrium points at which no additional strain and pore pressure can be developed with additional cycles. The axial strain and pore pressure obtained at these points are the maximum values that can be developed in the soil sample. It was found that the axial strain and pore pressure obtained at these points vary linearly with the amplitude of applied stress (Fig. 4.13) and can be represented by the following expressions:

$$\epsilon_{\max} = 0.076 A - 2.44 = e_1 A - f_1 \quad 4.7$$

$$u_{\max} = -0.25 A + 7.65 = e_2 A + f_2 \quad 4.8$$

Here, the constants e_i and f_i are dependent on the testing conditions and can be determined easily by regression. By knowing the amplitude, the maximum strain and pore pressure developed in the sample can be easily determined using these equations.

Thus, equations 4.1, 4.2, 4.3 and 4.4, 4.5, 4.6 can be rewritten, in a general form, as follows:

$$\epsilon_i = a_i p'^{l_i} - b_i \quad 4.9$$

$$u_i = c_i p'^{l_i} + d_i \quad 4.10$$

Also a quantitative analysis shows that the coefficients a_i , b_i , c_i , and d_i vary linearly with the amplitude of applied stress (Fig. 4.14) as:

$$a_i = 0.0017 A + 0.022 = l_1 A + m_1 \quad 4.11$$

$$b_i = 0.06 A - 0.38 = l_2 A + m_2 \quad 4.12$$

$$c_i = -0.01 A + 1.52 = l_3 A + m_3 \quad 4.13$$

$$d_i = 0.2 A + 22.68 = l_4 A + m_4 \quad 4.14$$

Note that the coefficients l_i and m_i depend on the testing conditions. They can be determined very easily by a linear regression.

The effective stresses at the equilibrium point where no additional axial strain and pore pressure occur with additional cycling, σ'_1 and σ'_3 , can be determined as follows: First, the value of p' can be estimated using either equation 4.9 or 4.10 ($\epsilon_i = \epsilon_{\max}$ and $u = u_{\max}$). Then using the fact that:

$$p' = \frac{1}{2} (\sigma'_1 + \sigma'_3) \quad 4.15$$

and,

$$A = \sigma'_1 - \sigma'_3 \quad 4.16$$

The values of σ'_1 and σ'_3 can be determined.

The necessary number of cycles needed to reach equilibrium for both axial strain and pore pressure are plotted against the amplitude of applied stress in Fig. 4.15. From this figure it is evident that the number of cycles required to attain the equilibrium point for both axial strain and pore pressure depend linearly on the amplitudes, and can be written as:

$$N_e = 0.72 A - 21.66 = g_1 A - h_1 \quad 4.17$$

$$N_u = 0.64 A - 20.66 = g_2 A - h_2 \quad 4.18$$

where N_e and N_u are the maximum number of cycles required to reach the equilibrium for axial strain and pore pressure, respectively. The coefficients g_1 and h_1 are dependent on test conditions and can be determined by regression.

As a conclusion it appears that, knowing only the amplitude of applied stress, the maximum axial strain and pore pressure that can be developed in the sample, effective stresses at the equilibrium point, and number of cycles for axial strain and pore pressure to reach the equilibrium can be determined.

4.2.4 Behaviour of kaolinitic clay above CLRL:

The samples subjected to a cyclic stress ratio above CLRL will fail, as demonstrated by samples S14, S15, and S16. Details of these tests are shown in Table 4.2.

The response of the samples S11 and S15 to repeated loading is shown in Figs 4.7 and 4.8, respectively. The applied cyclic shear stress is shown together with the pore water pressure changes and axial strains. Axial strains build up and pore pressures decrease as cycling of shear stress leads the sample to failure. The rate at which the changes in behaviour occur is strongly dependent on the cyclic stress ratio.

When a soil sample is cyclically or repeatedly loaded, permanent pore water pressures will accumulate at the end of the cycle inducing the stress paths to migrate in the effective stress space. The direction of the migration depends on the positive or negative values of pore pressure developed in the sample. For kaolinitic clay, it was found that on increasing the number of cycles, a negative value of pore pressure was developed. As a consequence of the continuous build up of negative residual pore pressures, the stress path continuously migrates to the right side in stress space until the failure envelope is reached, as shown in Figs 4.7 and 4.8.

Based on the changes in the development of pore water pressure and strain, the behaviour of this clay under repeated loading can be divided into three stages: primary, secondary, and tertiary. These stages can be recognized very easily in test S14, as shown in Fig. 4.7. However, for the tests S16 and S15, this is difficult because of the small number of cycles required to reach failure.

Primary stage:

This stage is limited to few initial cycles. The rate of development of both pore pressure and strain is rapid at first and then slows down. The variation of both pore pressure and strain with the number of cycles is approximately linear as shown in Fig. 4.9 (CSR=0.78). In semi-log-plot, this variation can be described by a straight line as shown in Fig. 4.10. The effective stress paths

form closed loops and only a small reduction in strength of the soil occurs in this stage.

Secondary stage:

In this stage, both strains and pore pressure develop at a uniform rate depending on cyclic stress level, as shown in Fig. 4.9 (CSR=0.78, 0.85, and 0.93). In semi-log-plot the variation of pore pressure and axial strain with the number of cycles is linear (Fig. 4.10). Stress-strain loops and effective stress paths maintain their general shape. As a consequence of the continuous build up of negative residual pore pressures, the stress path continuously migrates to the right side in stress space. The strength of the soil is decreasing continuously at a small rate.

Tertiary stage:

In this stage, significant softening is initiated. The rate of increase in both axial strain and pore pressure accelerates with the number of cycles. In semi-log-plot, the changes of pore pressure and axial strains with number of cycles are linear (Fig. 4.10). In this stage, the closed loops become larger and the material fails. A large reduction in stiffness occurs in this stage and the migration of the effective stress path is noticed to cease.

The change of axial strains and pore pressures in the above three stages can be described by straight lines, as:

$$\epsilon = j_1 \log(N) + z_1 \quad 4.19$$

$$u = j_2 \log(N) + z_2 \quad 4.20$$

The absolute value of the slope of these lines decreases in the second stage and increases in the third one. The coefficient j_i and z_i are dependent on cyclic stress ratio.

The number of cycles in each stage were found to be a function of the cyclic stress level. As the cyclic stress ratio increases, the number of cycles in each stage decreases. Fig 4.16 demonstrates that the boundaries of the tertiary stage can be represented by two lines plotted from the origin of the stress space. In this figure, the initial boundary of the tertiary stage can

be called as a transformation line in which a major change on the axial strains start to occur in the soil sample which increases with cycling until failure. The final stage can be called as a cyclic failure line.

The variation of the CSR with the number of cycles obtained at failure is shown in Fig. 4.11.(a). This variation is an upward concave curve and similar to the S-N curve observed for ferrous metals (Larew and Leonard 1962). S-N curve shows the number of cycles required to failure as a function of the cyclic stress level which is generally expressed as S (a percentage of the static strength). As can be observed in Fig. 4.11(b), there seems to be a linear relationship between the number of cycles and CSR, when a semi-logarithmic interpretation is adopted. This introduces an additional capability to evaluate the number of cycles at failure for different CSR's and to derive a simple mathematical expression such as:

$$CSR = t - k \log (N) \quad 4.21$$

Here t and k depend on the test conditions. They can be determined by a linear regression analysis.

Note: soil samples reached failure conditions under cycling were showed a much higher negative pore pressure at failure compared to the static test.

4.2.5 Effect of the step increase in CSR:

Test results of test series S2:

This series comprises only one test. The sample used in this test was taken from the second block of kaolinitic clay and had the same consolidation history as the sample used in test K2. The objective of this test series is to examine the behaviour of this clay while changing the amplitude

of the applied stress.

The sample was repeatedly loaded 152 times at a CSR varying from 0.49 up to 0.85 in a total of 6 steps. In each step, a constant CSR was applied during a given number of cycles. In the first step, the CSR has a maximum value of 0.49 and a minimum of 0.26. Changing from one set of cycles to the next one, the maximum and minimum values of CSR increases and decreases by 0.065, respectively. The cycling was always carried out about the mean deviatoric stress of 23 kPa. In the fifth set of cycles, the cyclic stress ratio has a maximum and minimum values of 0.75 and zero, respectively. In the sixth set of cycles, in order to keep cycling only in compression side, the maximum value of CSR had increased to 0.85 whereas the minimum value was kept constant and equal to zero. Due to this CSR, the rate of development of both axial strain and pore pressure accelerates with cycling until failure envelope was reached.

Table 4.2 shows details of the sequence of loading and the number of cycles at each step. Plots of excess pore pressure and peak to peak strain with number of cycles are shown in Fig. 4.17.

In the first five sets of cycles, significant axial strain and negative pore pressure accumulated in the soil sample before equilibrium conditions is reached. In the last set of cycles, a cyclic stress ratio used is higher than a CLRL which causes the rate of the development of both axial strain and pore pressure to accelerate with the number of cycles until failure occurred. Fig. 4.17 demonstrates that the development of both axial strain and pore pressure in each step can be represented by different straight lines. Each step increase in CSR causes an increase in absolute value of the slope of these lines. A step increase in CSR shows that the clay behaviour is a function of CSR; cumulative strain and pore pressure developed in each set of cycles and with each increase in CSR regardless of past cyclic loading history.

Table 4.1. Summary of testing conditions and test results of the test series K.

Test number	w %	q'_1 kPa	p'_1 kPa	ϵ at failure %	u at failure kPa	Maximum positive u kPa	q_r kPa	P_c kPa
K1	26	0	20	5	-4.2	13.1	72	31.3
K2	26	0	20	5	-1.8	11.4	61	26.3

Table 4.2. Summary of testing conditions and test results of the test series S1 and S2.

Test number	q'_i	p'_i	CSR _{min}	CSR _{max}	N	ϵ_t %	u kPa	Failed	Postcyclic strength (kPa)
S11	0	20	0.11	0.54	50	0.18	-2.8	no	73.5
S12	0	20	0.11	0.63	50	0.30	-4.02	no	72.3
S13	0	20	0.11	0.70	50	0.52	-6.04	no	69
S14	0	20	0.11	0.77	50	4.22	-12.5	yes	-
S15	0	20	0.11	0.85	7	3.91	-15.04	yes	-
S16	0	20	0.11	0.93	2	2.11	-6.23	yes	-
S21	0	20	0.26	0.49	47	0.11	-2.8		
			0.19	0.55	30	0.10	-3.1		
			0.12	0.62	15	0.15	-6.07		
			0.06	0.69	16	0.32	-7.1		
			0.00	0.75	25	0.64	-8.2		
			0.00	0.85	19	3.61	-10.1	yes	-

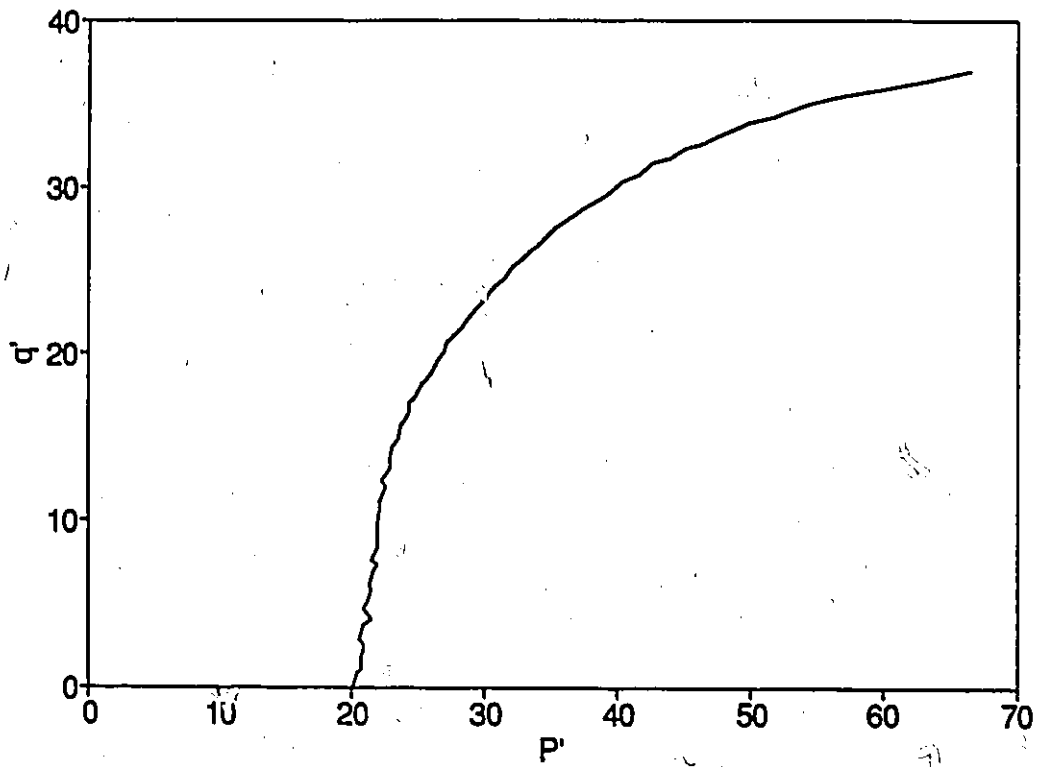
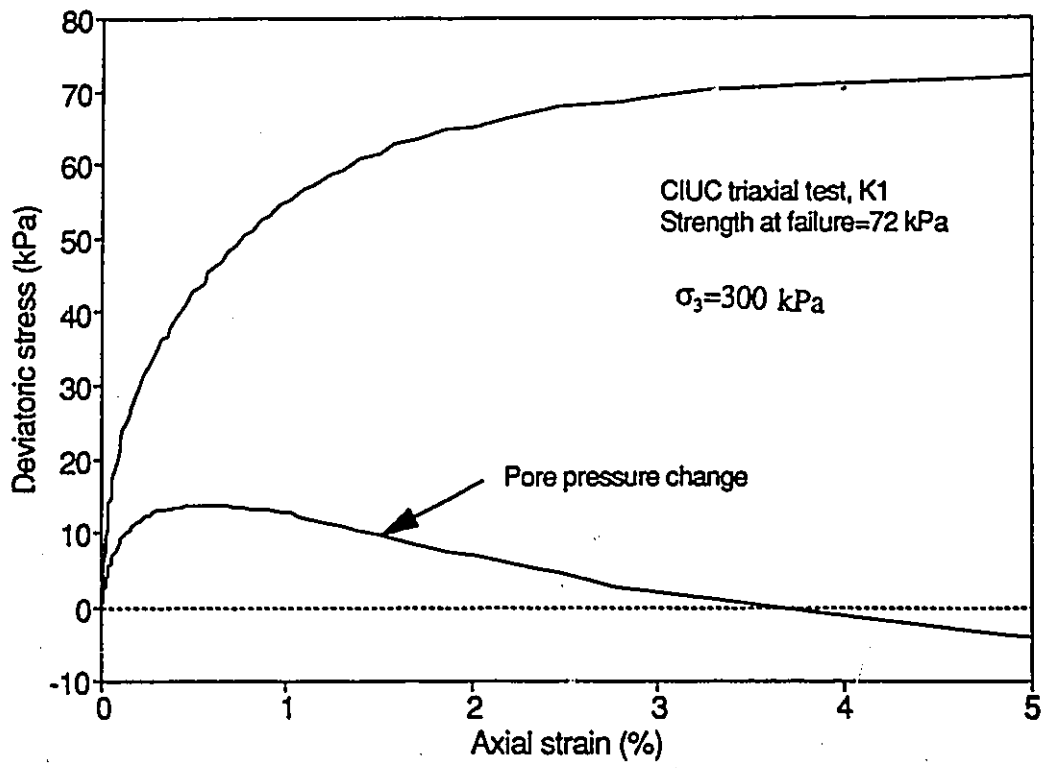


Fig. 4.1. Stress-strain, pore pressure-strain, and stress path curves for CIUC under monotonic loading: Test K1.

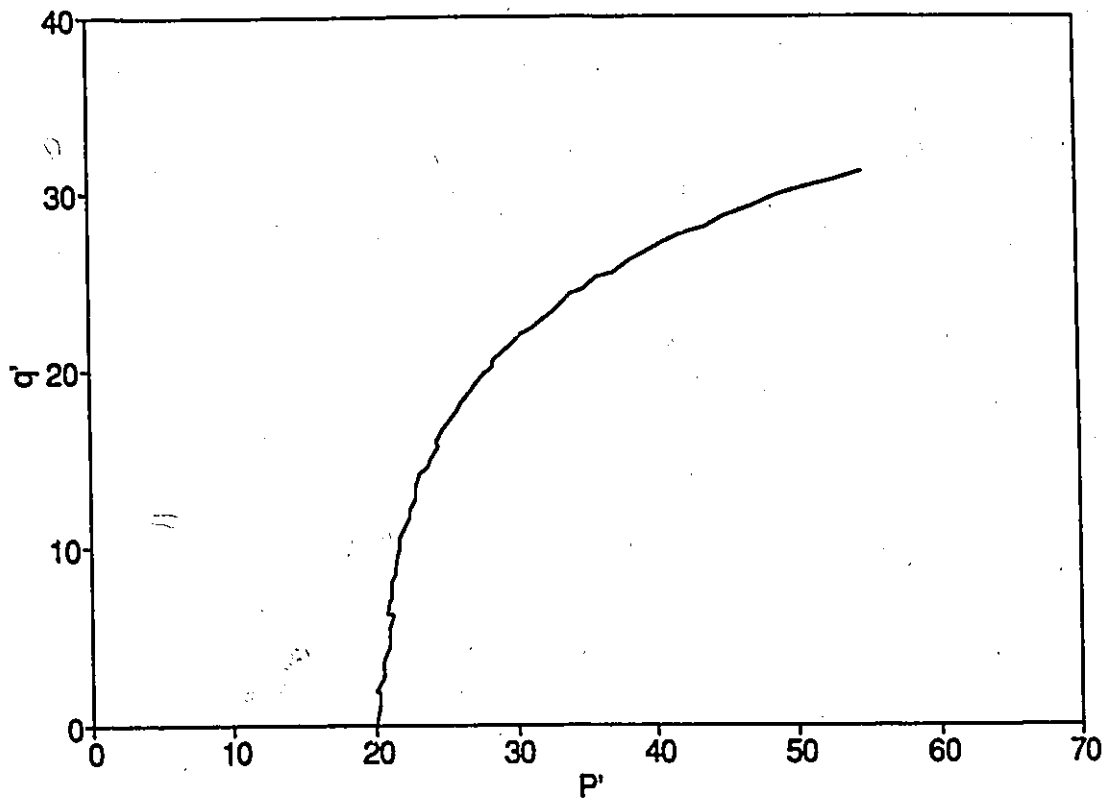
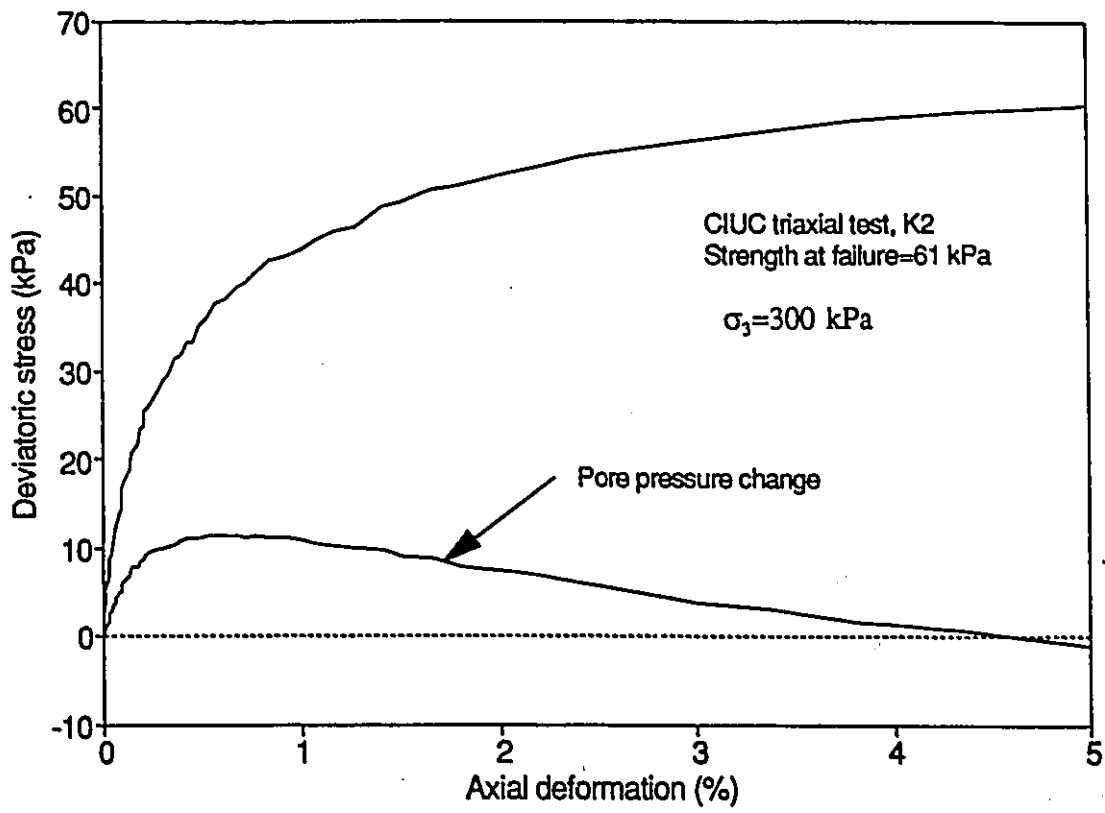


Fig. 4.2. Stress-strain, pore pressure-strain, and stress path curves for CIUC under monotonic loading: Test K2.

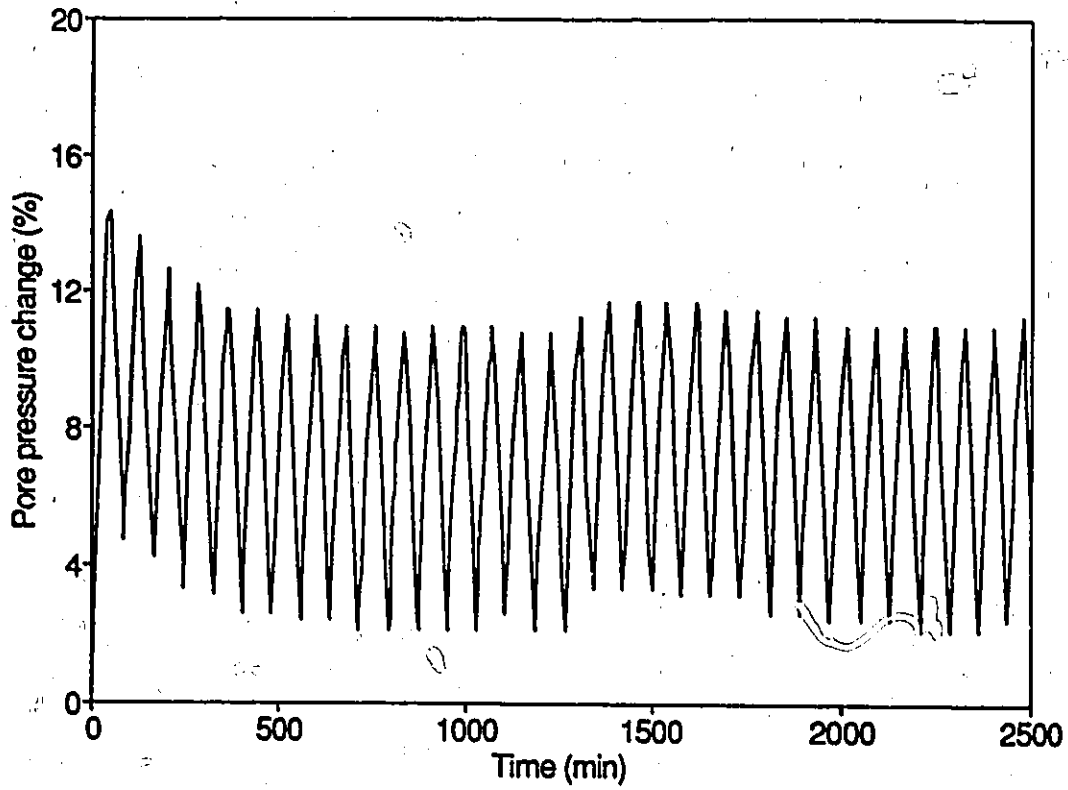
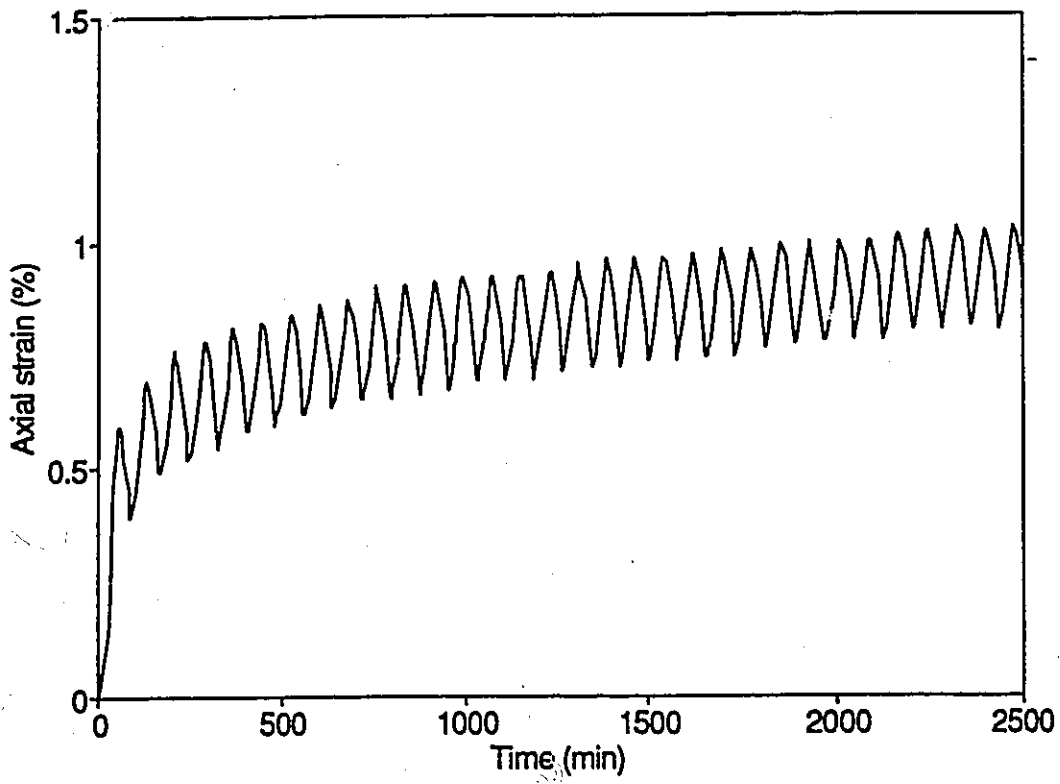


Fig. 4.3(a). Change in behaviour of kaolinitic clay during repeated loading at low levels of CSR.

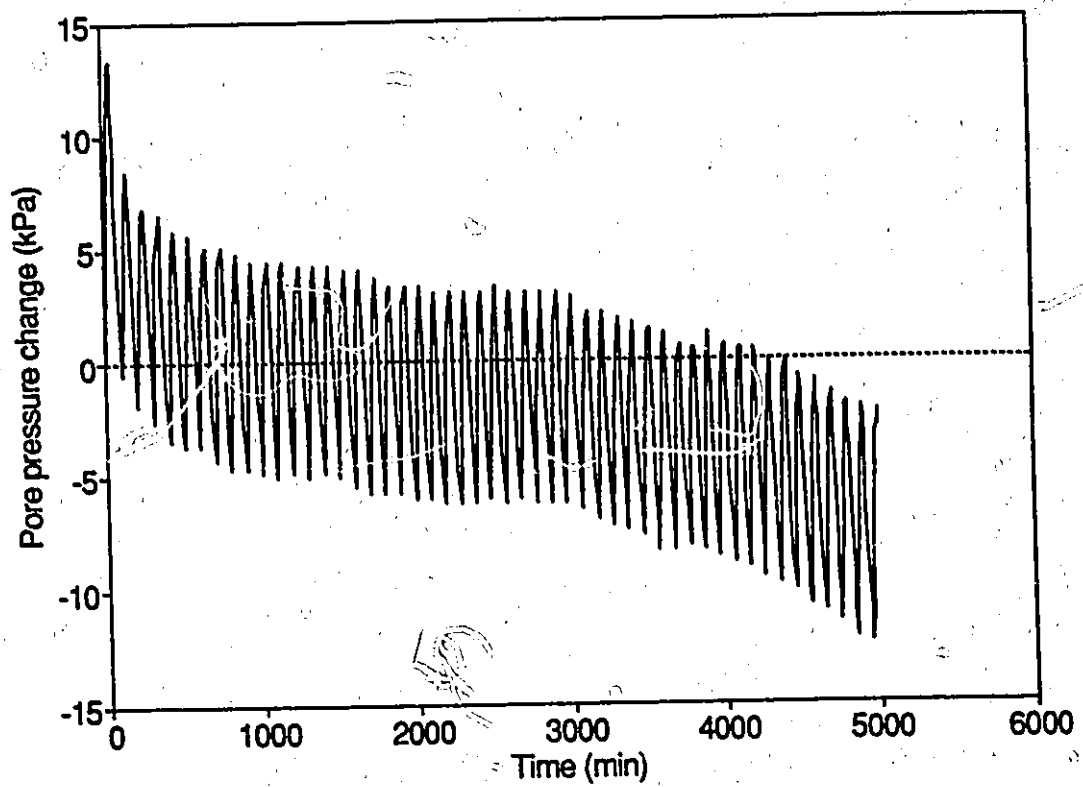
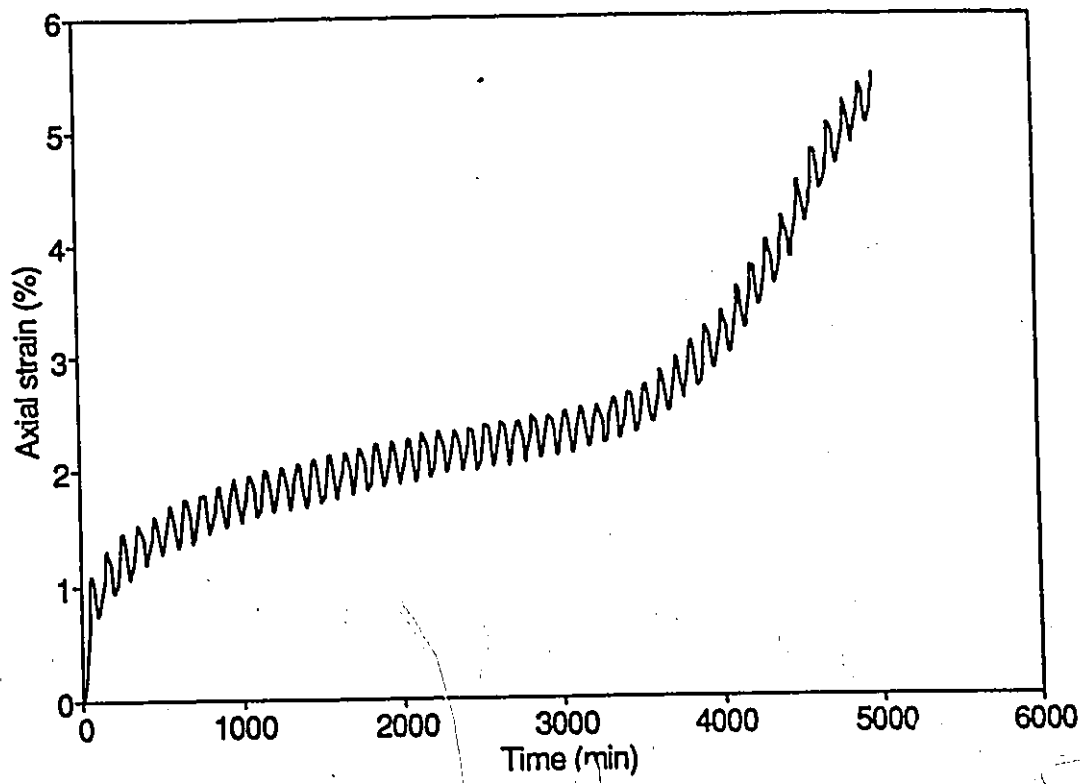


Fig. 4.3(b). Change in behaviour of kaolinitic clay during repeated loading at high levels of CSR.

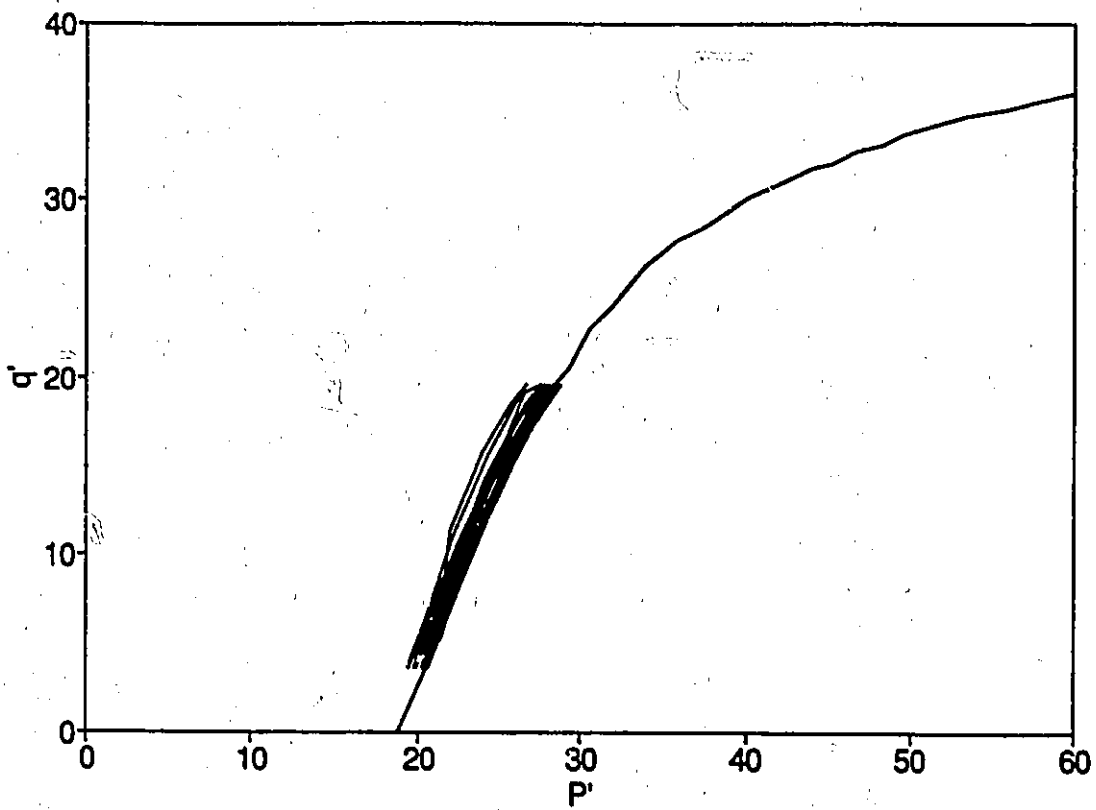
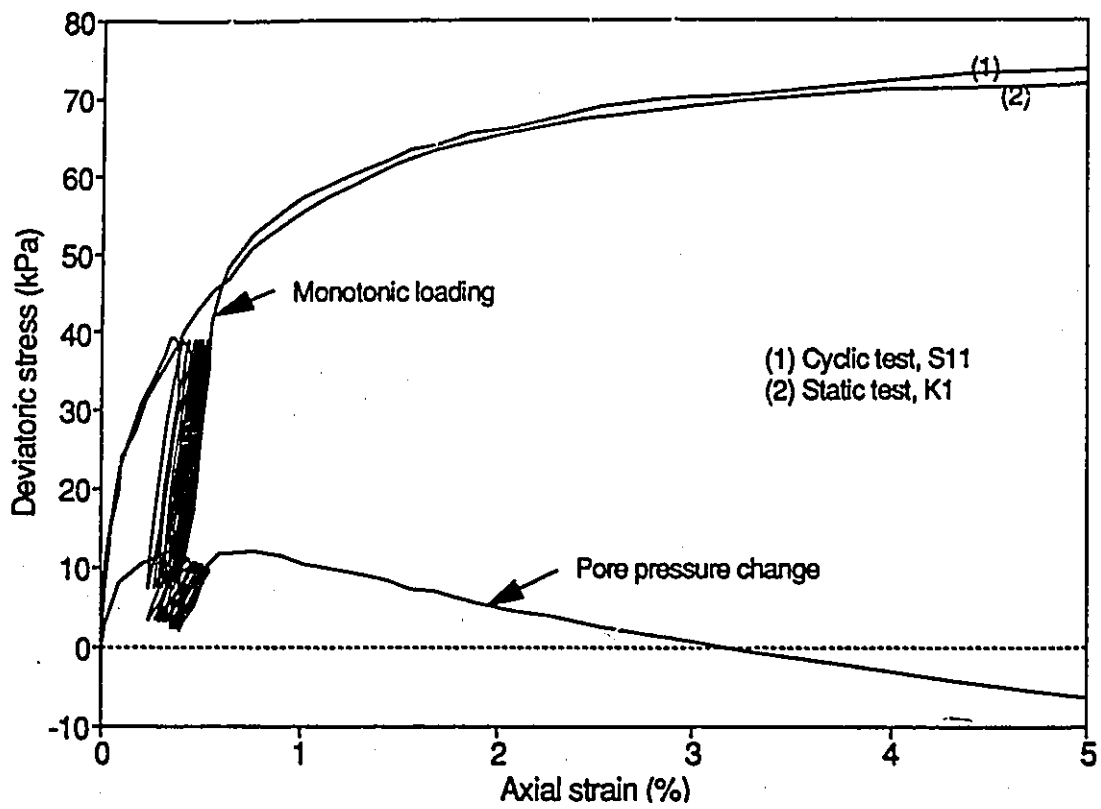


Fig. 4.4. Stress-strain, pore pressure-strain, and stress path curves for CIUC under one-way repeated loading: CSR=0.5, Test S11.

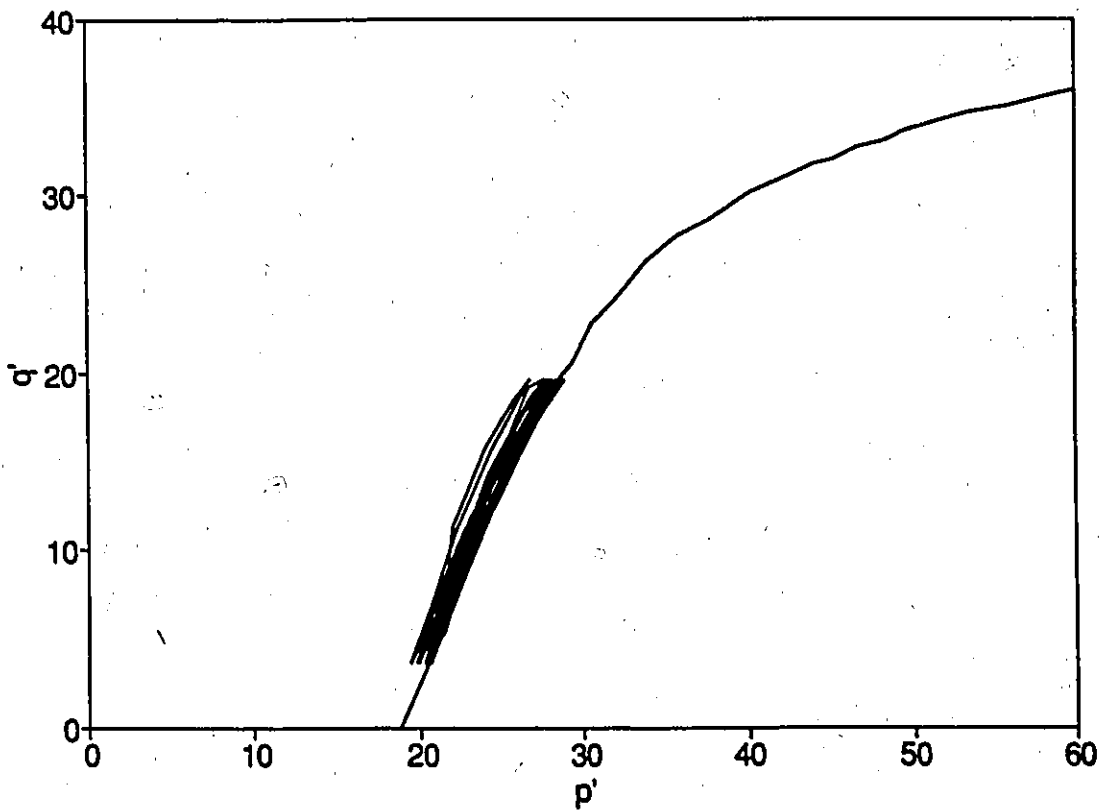
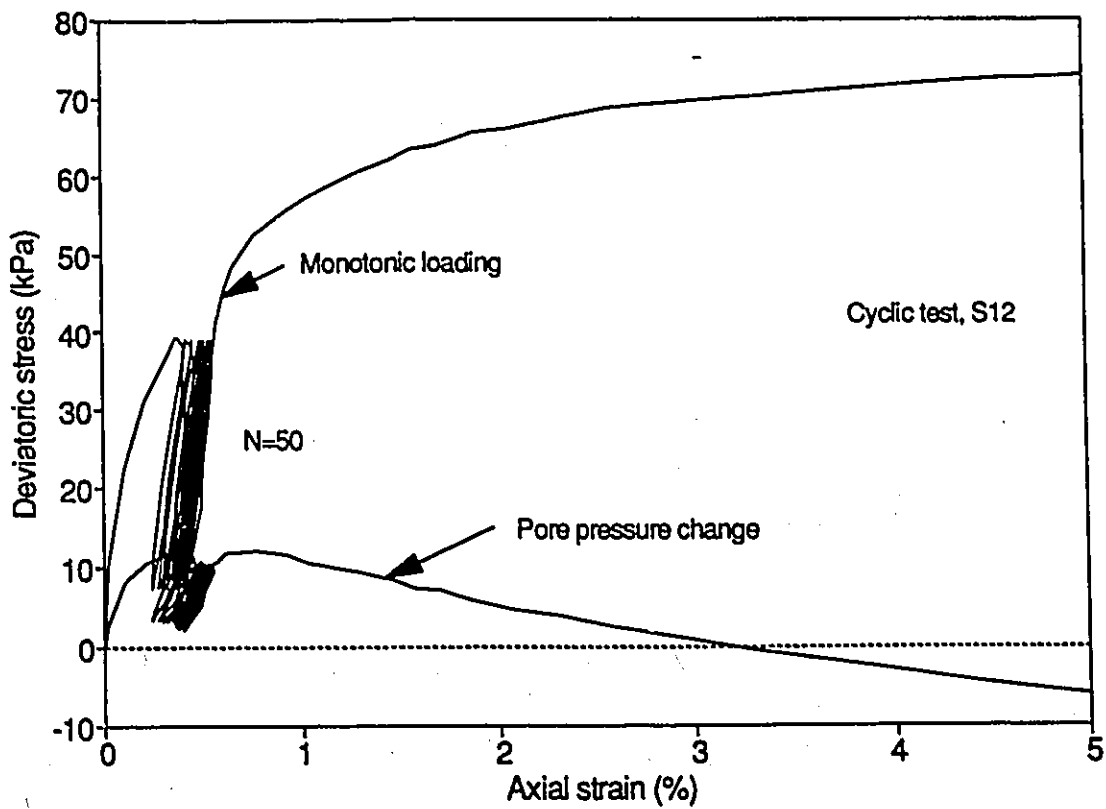


Fig. 4.5. Stress-strain, pore pressure-strain, and stress path curves for CIUC under one-way repeated loading: CSR=0.63, Test S12.

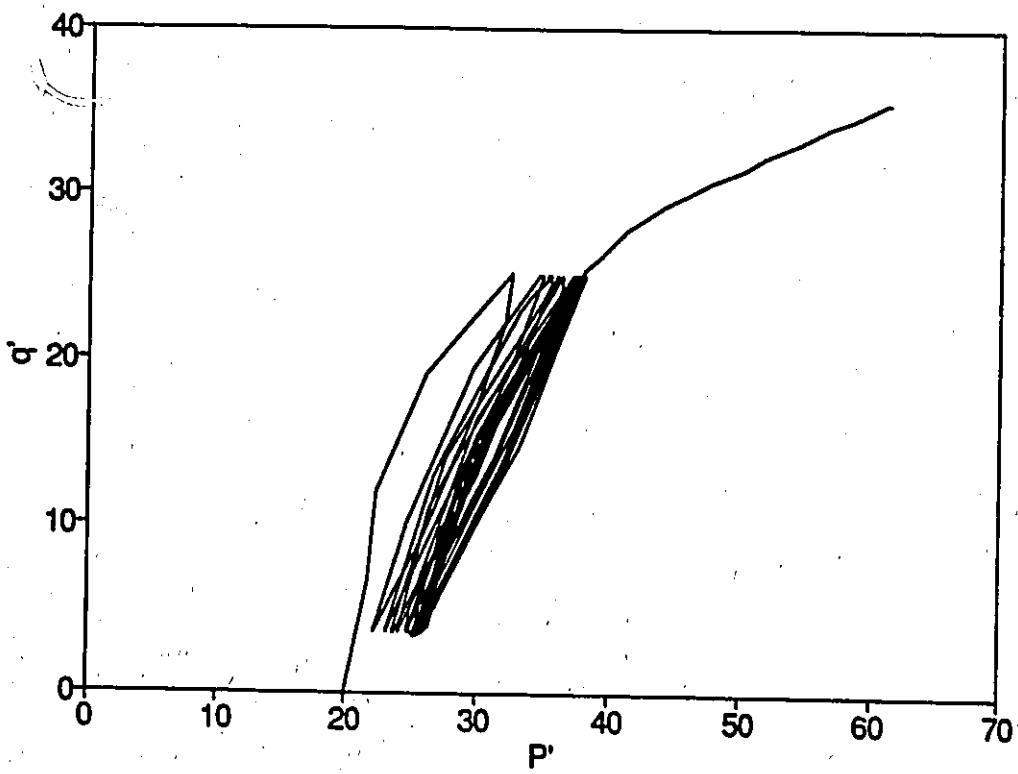
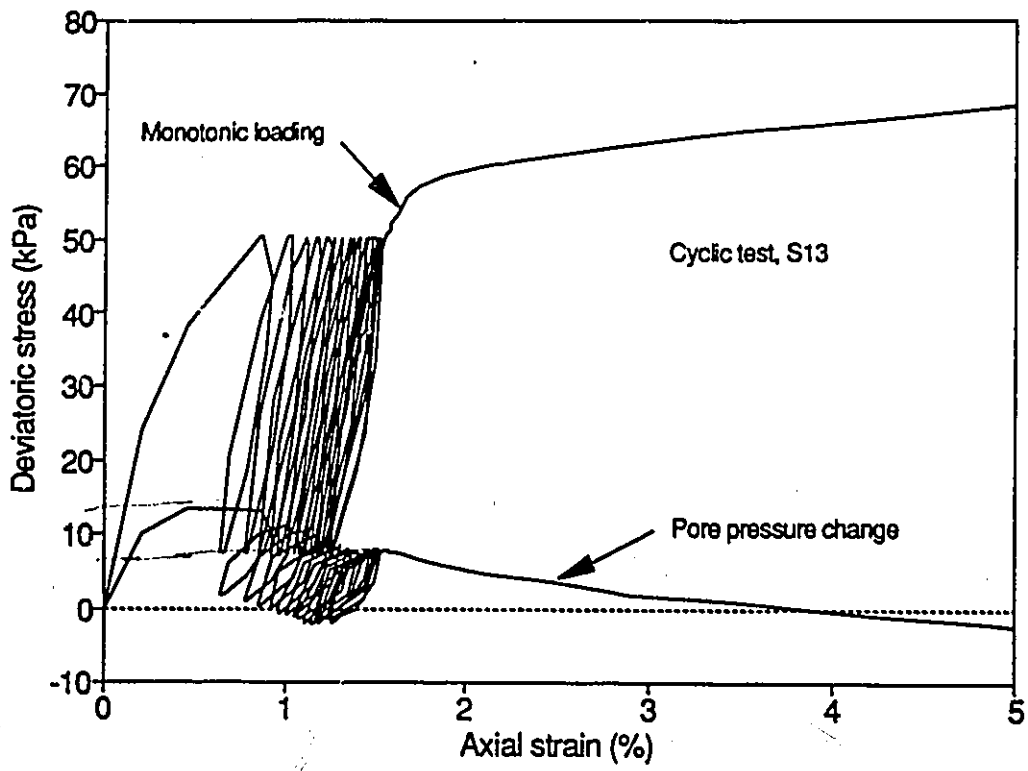


Fig. 4.6. Stress-strain, pore pressure-strain, and stress path curves for CIUC under one-way repeated loading: CSR=0.7, Test S13.

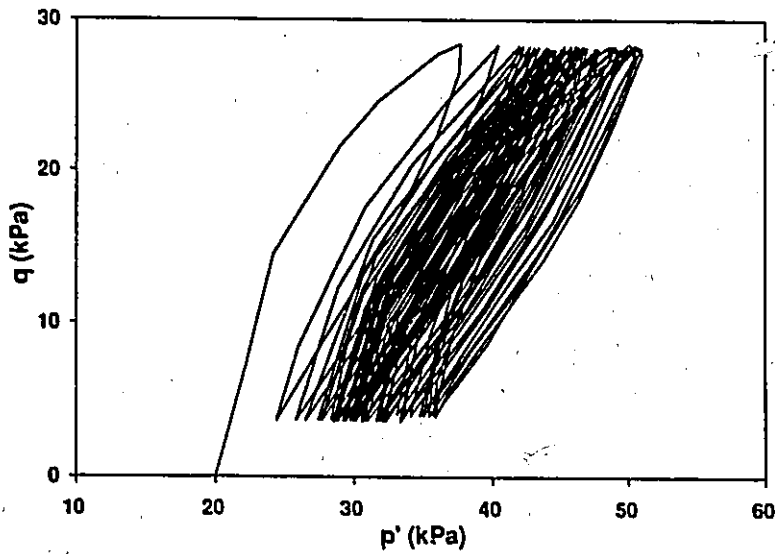
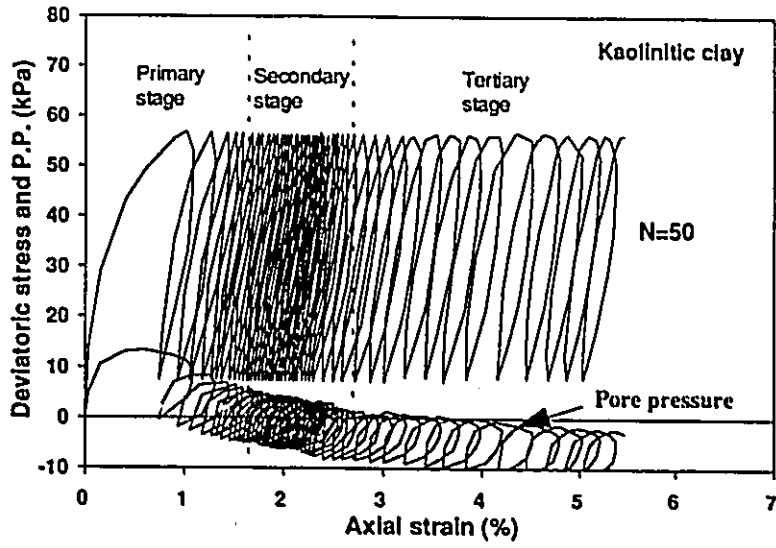


Fig. 4.7. Stress-strain, pore pressure-strain, and stress path curves for CIUC under one-way repeated loading: CSR=0.78, Test S14.

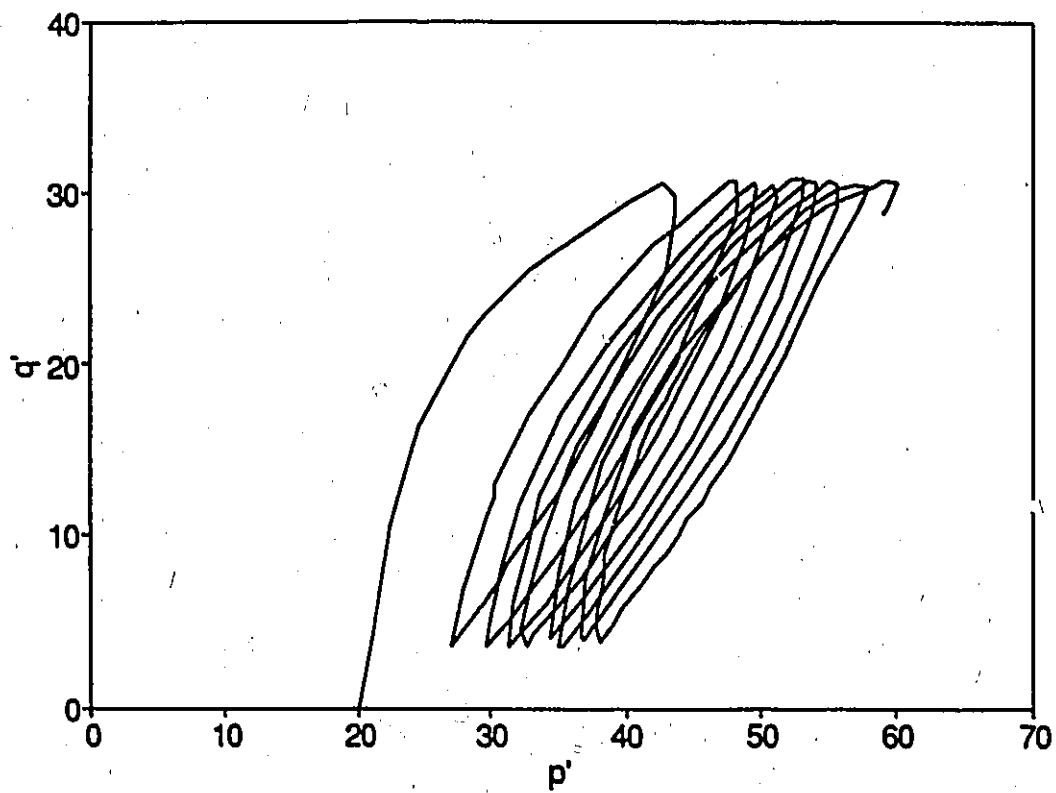
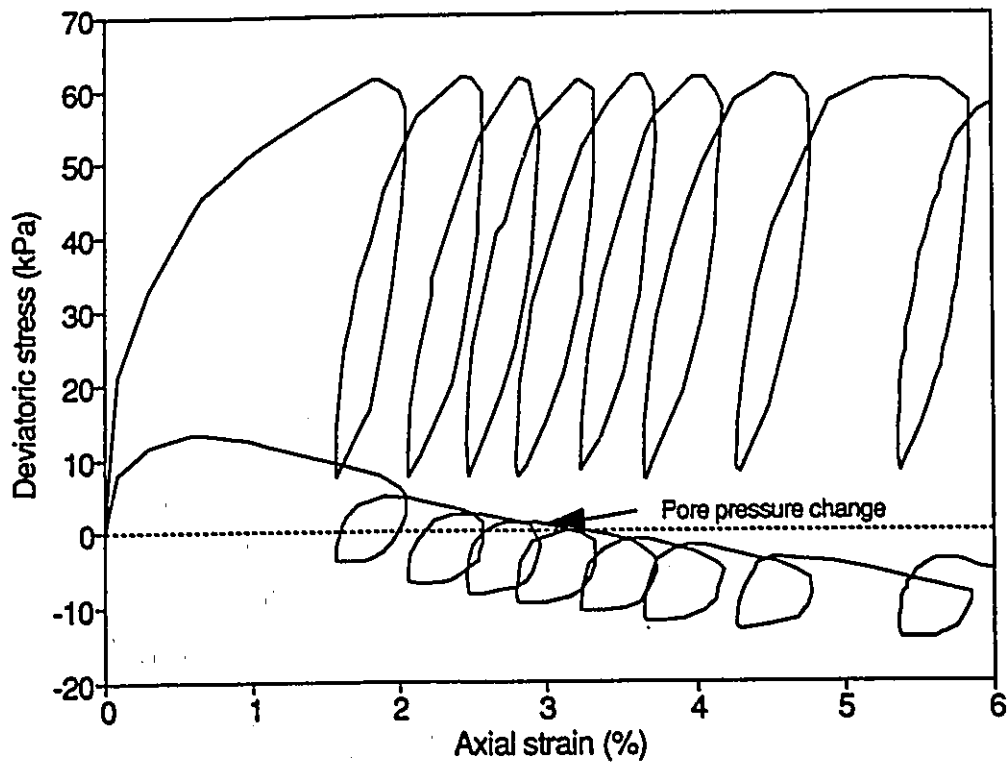


Fig. 4.8. Stress-strain, pore pressure-strain, and stress path curves for CIUC under one-way repeated loading: CSR=0.85, Test S15.

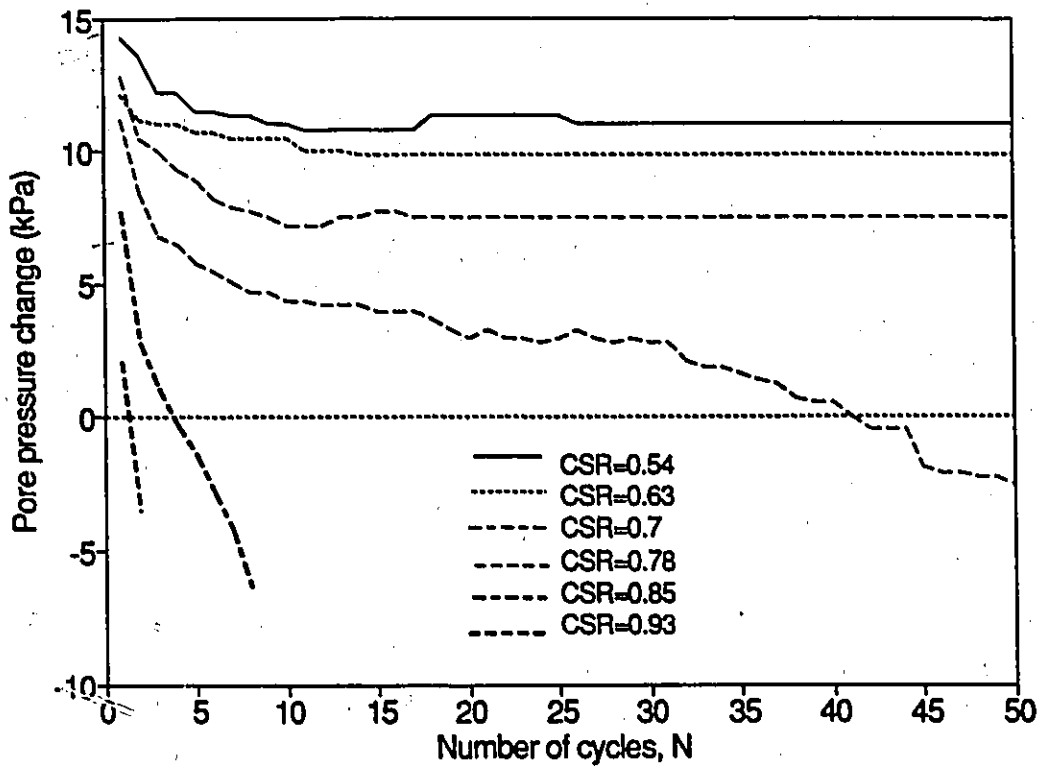
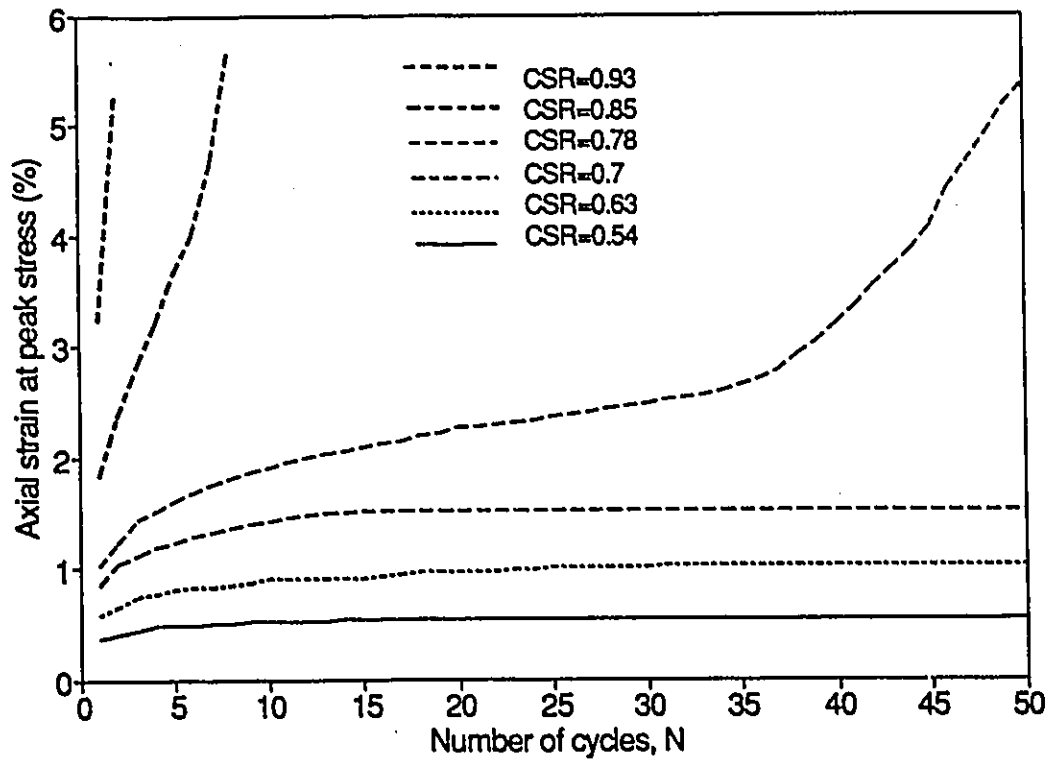


Fig. 4.9. Influence of the variation of the cyclic stress ratio on the peak strains and pore pressures: for test series S1.

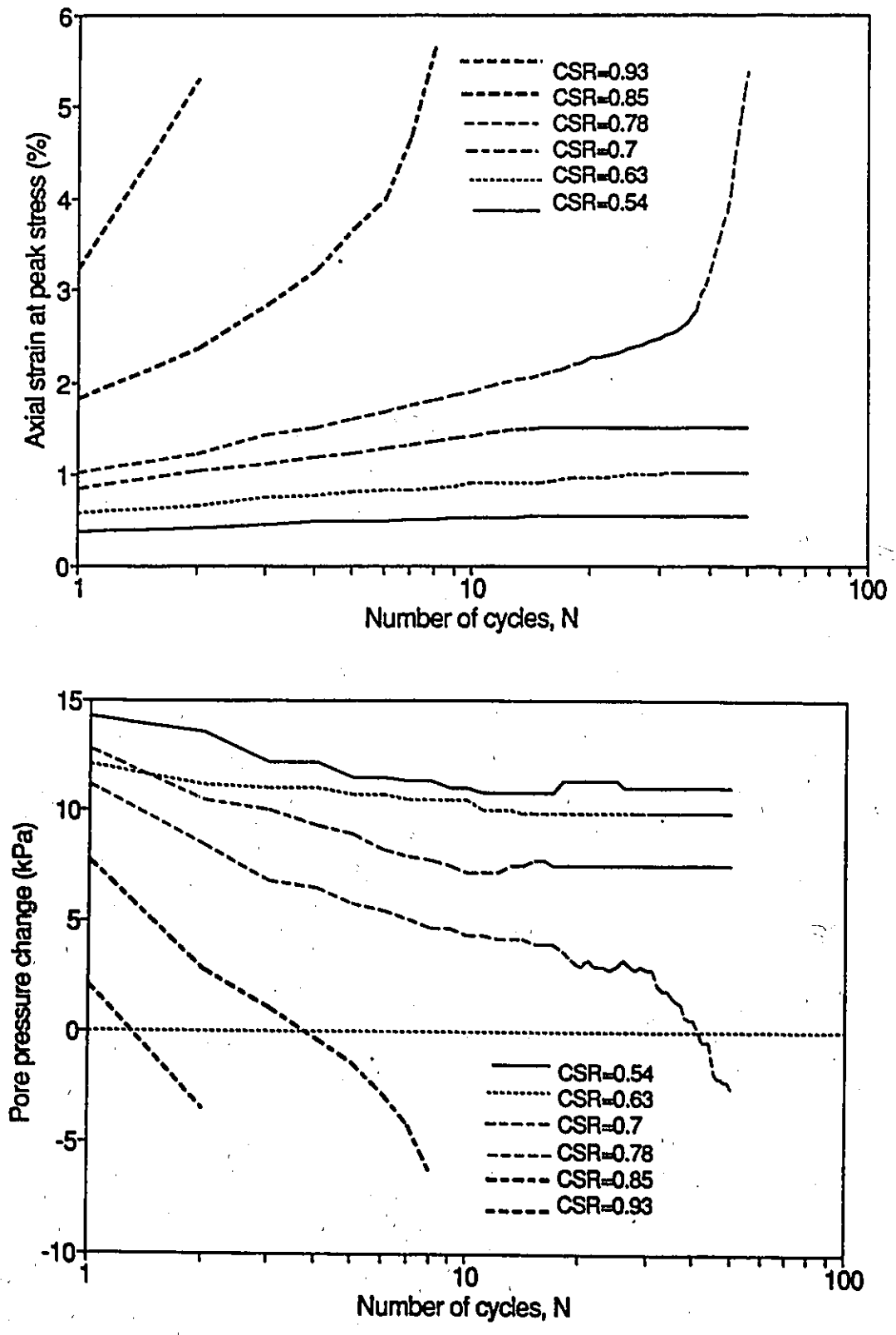


Fig. 4.10. Influence of the variation of the cyclic stress ratio on the peak strains and pore pressures for test series S1 in semi-log-plot.

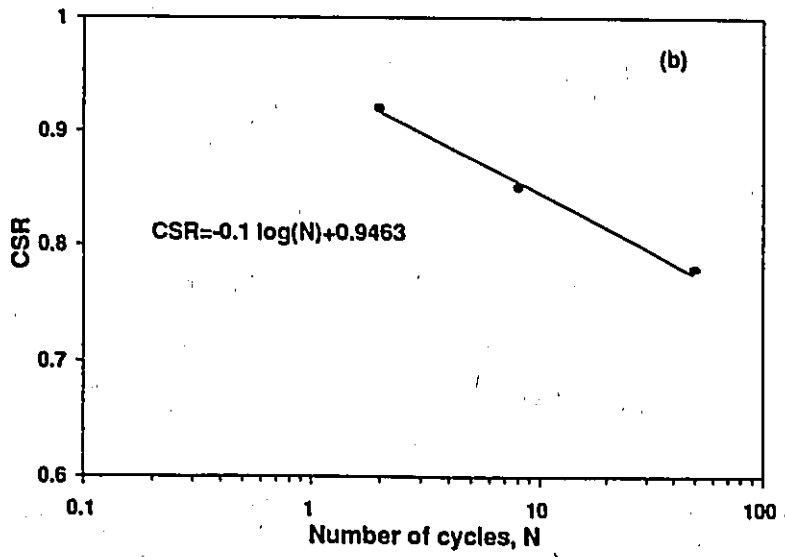
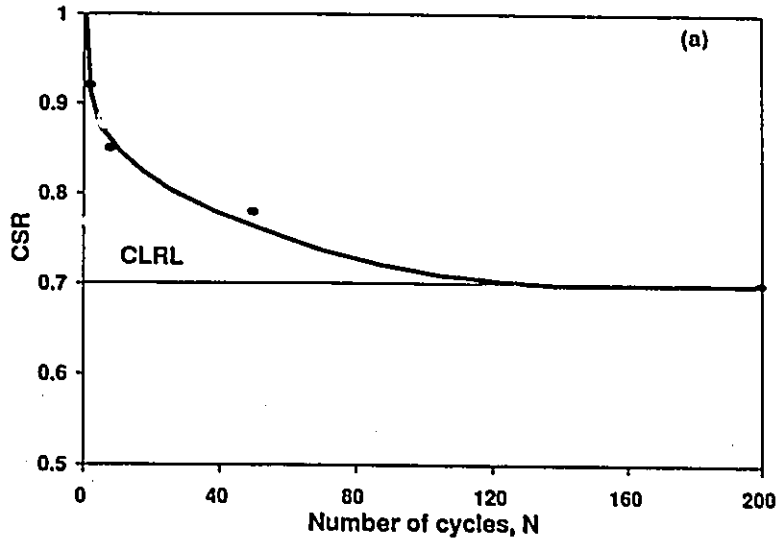


Fig. 4.11. CLRL (results obtained from test series S1).

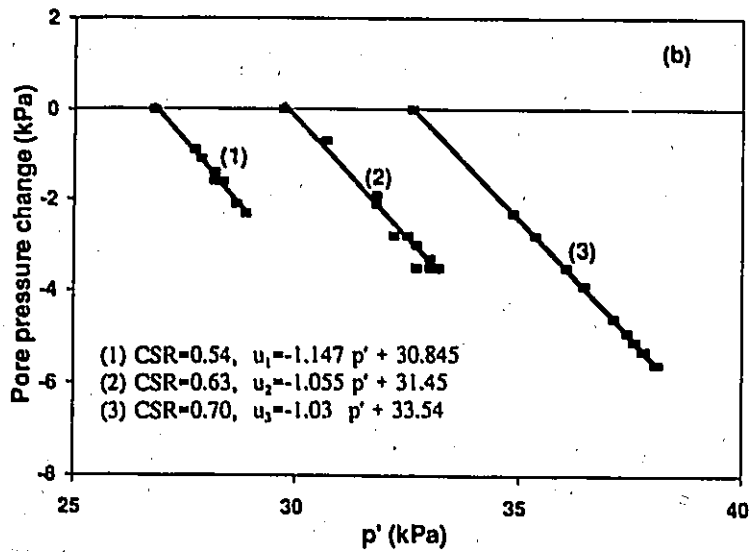
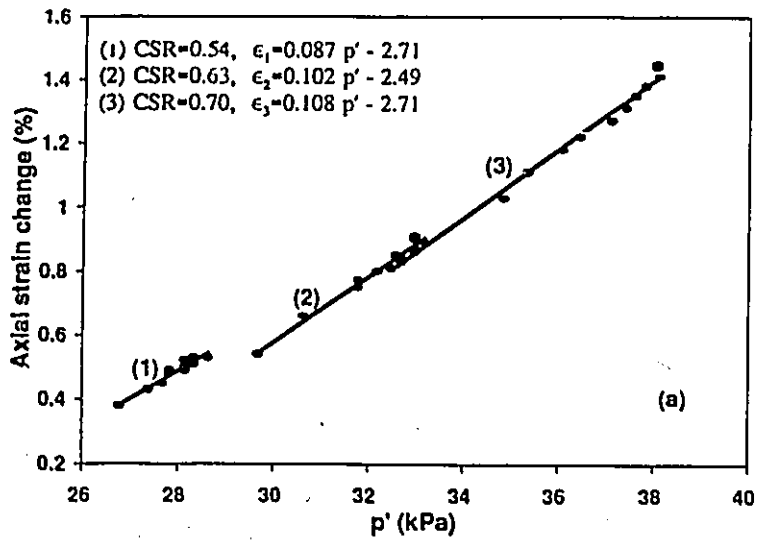


Fig. 4.12. Relationship between:
 (a) p' and axial strains measured at peak of cycles of loading.
 (b) p' and pore pressure measured at peak of cycles of loading.

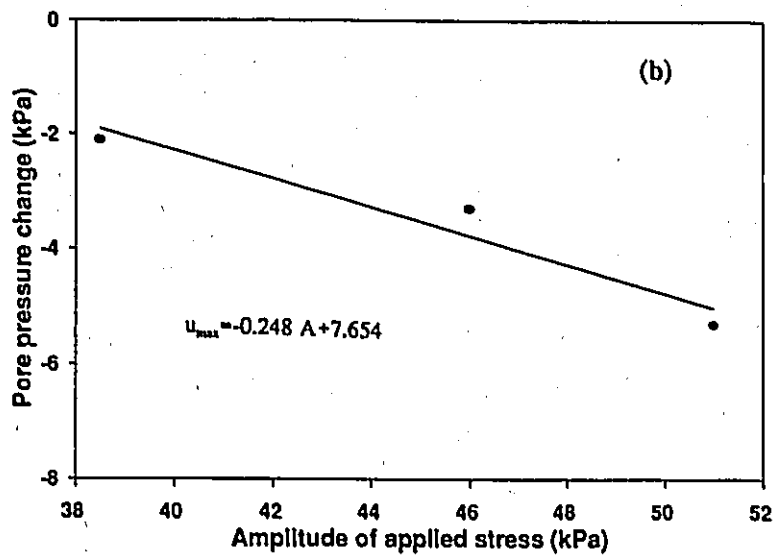
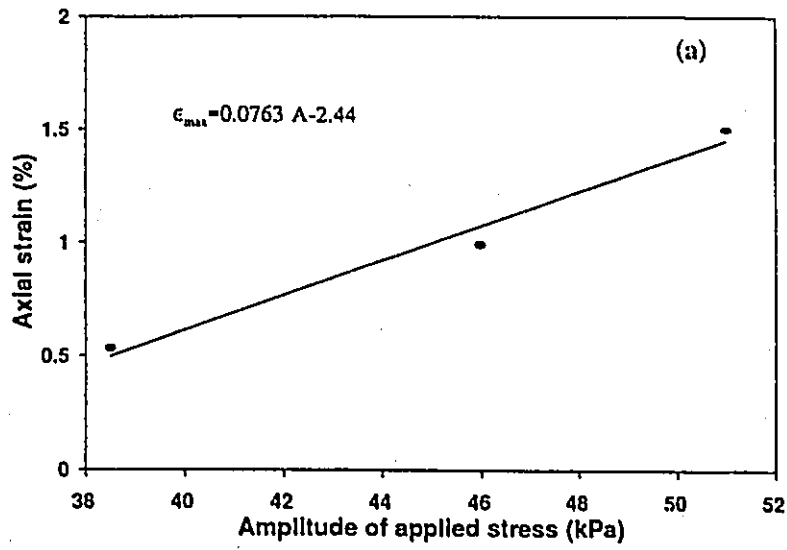


Fig. 4.13. Relationship between: (a) Amplitude of applied stress and a maximum axial strain measured in tests S11, S12, and S13. (b) Amplitude of applied stress and a maximum pore pressure measured in tests S11, S12, and S13.

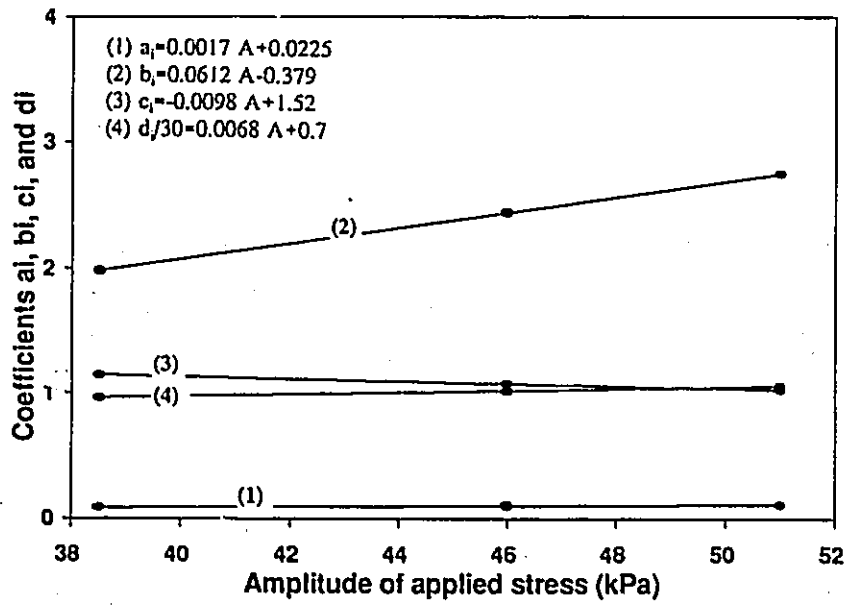


Fig. 4.14. Variation of the coefficient a_1 , b_1 , c_1 , and d_1 with the amplitude of applied stress.

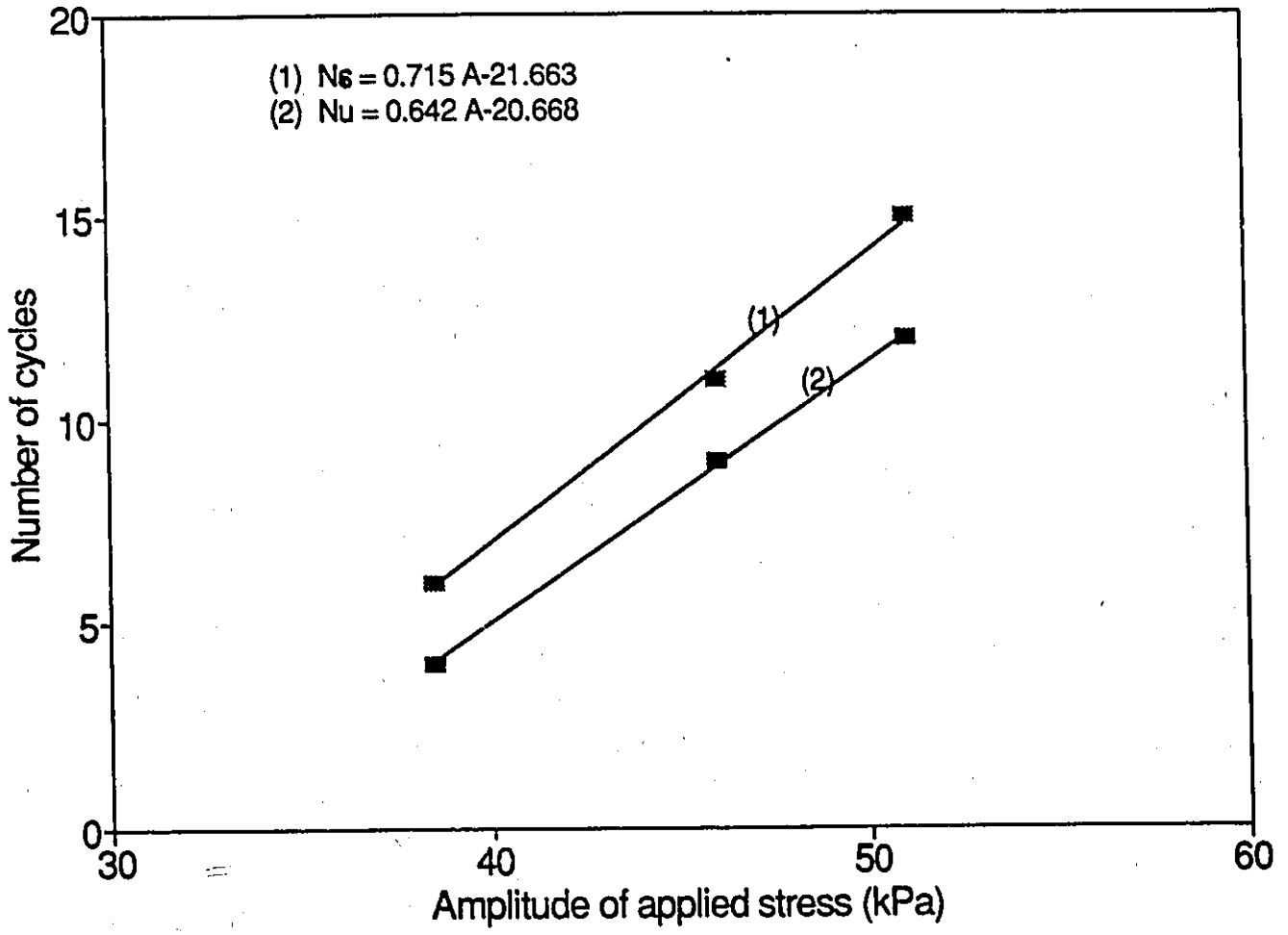


Fig. 4.15. Variation of N_s and N_u with the amplitude of applied stress.

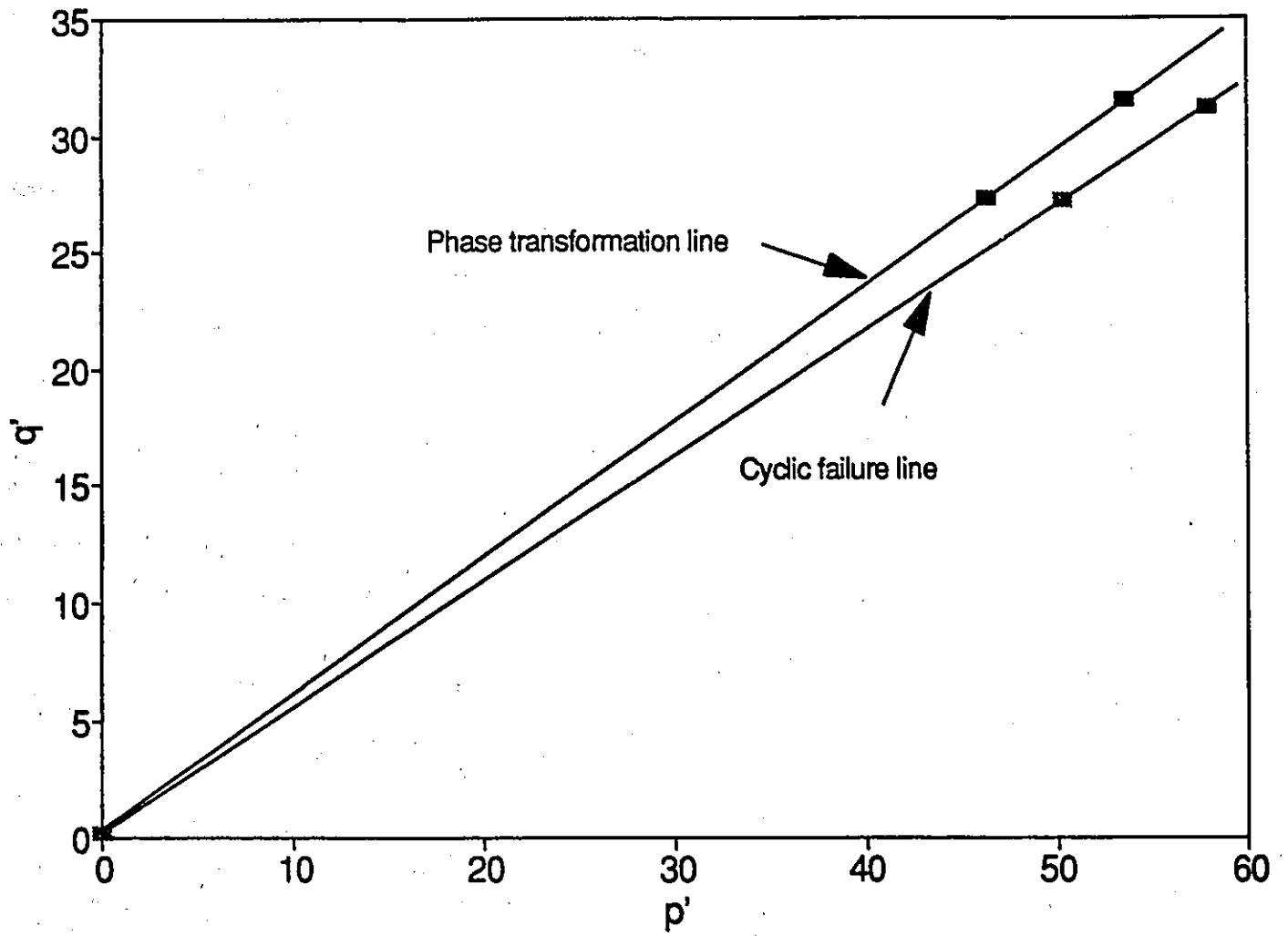


Fig. 4.16. Boundaries for the tertiary cyclic loading stage.

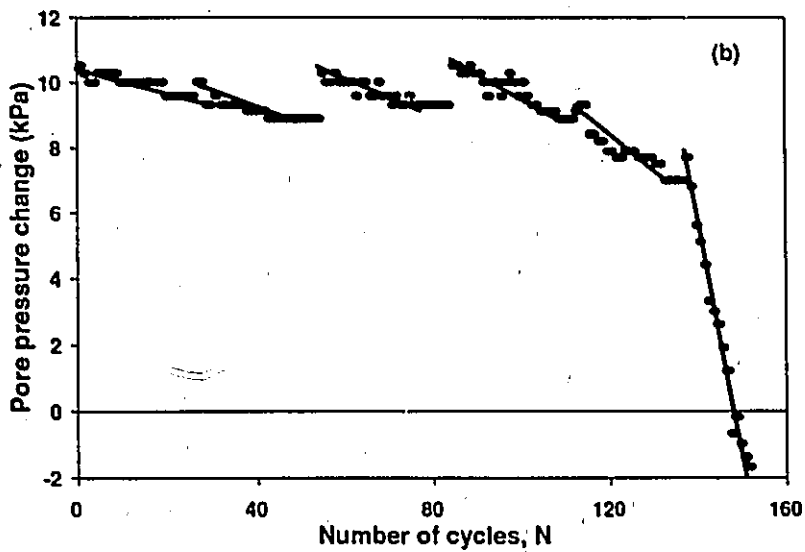
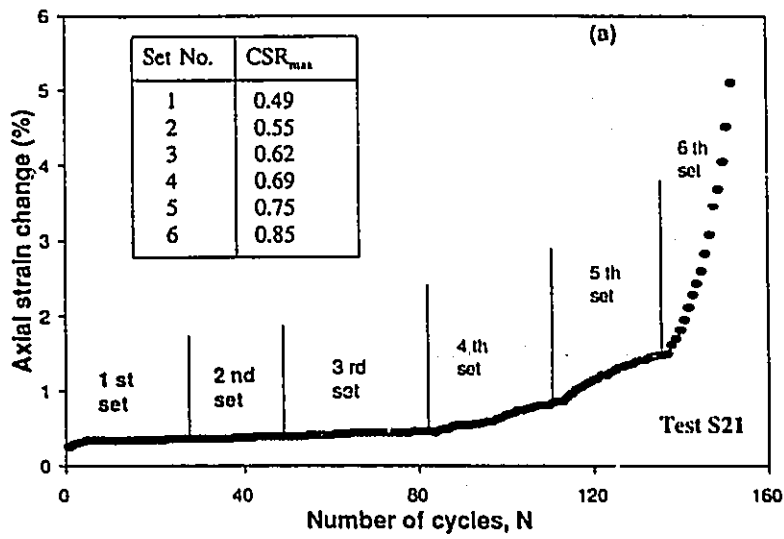


Fig. 4.17. Variation of: (a) axial strains measured at peak of cycles of loading with the number of cycles: Test S21. (b) pore pressure measured at peak of cycles of loading with the number of cycles. Test S21.

CHAPTER 5

Behaviour of the Clay Crust Under Static and Repeated Loading

5.1 Monotonic Tests:

Undrained triaxial tests were conducted on samples from the clay crust at depths of 2.7, 3.3 and 3.6 m. At each depth, two samples were taken to failure under static loading. The first sample was consolidated isotropically to in situ effective vertical stress while the second one was consolidated anisotropically to in situ effective stresses. This was to provide a basis for interpreting the results of cyclic tests which were done under similar conditions of testing and at the same depth. The rate of loading was always maintained constant and equal to 1 kPa/min.

The response of typical consolidated isotropically and anisotropically undrained tests at depth of 2.7 m (T1 and T11), as an example, are shown in Figs 5.1 and 5.2, respectively. In each plot, stress-strain, pore pressure-strain, and stress-path are shown. Similar curves were observed for other depths. The summary of the testing conditions and test results is given in Table 5.1. These test results demonstrate that, at the same depth of the crust, the anisotropically consolidated samples showed higher strength and higher pore pressure compared to the isotropically consolidated samples. The axial strain at peak deviatoric stress increases slightly with OCR.

5.2 Repeated loading tests:

5.2.1 Test series C1, C2, and C3:

Three test series conducted out on the clay crust are presented and discussed here. Each of these test series was done at a different depth of the crust and used to examine the corresponding parameter shown in Table 3.2. A summary of the testing conditions and test results is given in Table 5.2.

Test series C1:

This test series comprises two tests. The samples used in these tests were taken from a depth of 2.70 m of the crust ($OCR=5.2$). In the first test, the sample was consolidated isotropically to the in situ effective vertical stress (32 kPa) and in the second test, the sample was consolidated anisotropically to the in situ effective stresses (32 and 44.8 kPa). Both samples were subjected to about 70 cycles. An amplitude equal to 13% of the maximum deviatoric strength (q_f , obtained from the static test) was used in both tests. Cycling was carried out at mean stress of 45% and 55% of q_f for the first and second sample, respectively.

Test series C2:

This test series comprises two tests. The samples used in these tests were taken from a depth of 3.6 m of the crust ($OCR=3.2$) and consolidated isotropically to the in situ effective vertical stress (39 kPa). In the first test C21, the sample was subjected to a total of 6 sets of cycles as shown in Table 5.2. In the first set of cycles, the cyclic stress ratio used had a maximum value of 0.32 and a minimum value of 0.18. Changing from one set of cycles to the next, both of these values were increased by 0.07. A fixed number of cycles ($N=30$) and a constant amplitude of applied stress were applied in each set of cycles. However, in the last set of cycles, only one cycle of loading was required to reach failure.

In the second test, the sample was subjected only to the last 3 sets of identical cycles imposed on the first test. For this sample, in the last set of cycles, only two cycles were required to reach

failure.

Test series C3:

This test series comprises three tests. All the samples used in this test series were taken from a depth of 3.3 m of the crust ($OCR=3.9$) and consolidated isotropically to the in situ effective vertical stress (36 kPa). In the first test C31, the sample was repeatedly loaded 30 times. A cyclic stress ratio applied had a maximum value of 0.65 and a minimum value of 0.11. A constant amplitude was maintained along cycling. It was observed that after the first 22 cycles of loading, no additional residual pore pressure or axial strains were measured. The repeated loading was followed by a monotonic one.

In the second test C32, the sample was repeatedly loaded until failure. A cyclic stress ratio applied in this test has a maximum value of 0.75 and a minimum value of 0.11. A constant amplitude of applied stress was maintained along cycling. This amplitude caused the failure of the sample in 7 cycles.

In the last test C33, the sample was subjected to a high CSR. This CSR has a maximum value of 0.85 and a minimum value of 0.11. A constant amplitude was maintained. Due to this CSR, a large deformation and axial strain were expected in this test. It was observed that the soil sample reached the failure conditions in 5 cycles.

5.2.2 Test results:

The typical response of this clay to undrained repeated loading at high and low cyclic stress ratios, for tests C32 and C21 which taken as an examples, are shown in Figs 5.3(a) and (b), respectively. In both these figures changing of pore pressure and axial strains with time are shown. At high levels of cyclic stress ratio, the rate of development of both strains and pore pressure increase and becomes larger as cycling increases. At low levels of cyclic stress ratio, both axial strains and pore pressure build at a decreasing rate with cycling until equilibrium is reached.

Series C1:

In this series two tests were conducted: C11 and C12. The samples used in both tests were similar and had the same consolidation history as the samples used in static tests T1 and T11, respectively. Reference should be made to Table 5.2 for test conditions.

Figs 5.4 and 5.5 show stress-strain curves obtained from tests C11 and C12, respectively. For comparison, the stress-strain curve obtained from the static tests are also shown. During cycling, in both tests, the axial strains develop at a decreasing rate and only small strain of 0.08% were developed under cycling before stabilisation. This stabilisation indicates the critical level of repeated loading for this soil lies above 55% of q_r . On subsequent monotonic loading, both samples indicate a postcyclic strength which is very slightly higher than the static strength, indicating that the imposed cycling did not cause any destruction of the soil structure. It is possible that cycling causes an increase in the overconsolidation of the clayey soil which is reflected in the small increase in the strength of the material. Since a higher cyclic stress ratio of 0.55 was used in the anisotropically consolidated sample (C12) compared to the isotropically consolidated sample (test C11), it can be concluded that the anisotropically consolidated samples are more resistant to repeated loading.

Series C2:

Fig 5.6 shows the stress-strain, pore pressure-strain, and stress path curves obtained from test C21. In the first set of cycles, no significant axial strain was measured, however, an important change in pore pressure of 12 kPa was measured despite the small CSR used.

In the second set of cycles, a small increase in cyclic stress ratio of 0.1 was applied over that used for the first set of cycles. Due to this increase in CSR, an increase of 5.4 kPa was measured in pore pressure and a 0.08% in axial strain. After 16 cycles of loading, the rate of development of axial strains tended to zero, but the pore pressure did not. At the end of 30 cycles, the test was stopped and the cyclic stress ratio was increased.

In the third set of cycles, the pore pressure increased continuously with cycling and no

equilibrium conditions were observed. A total change of 6 kPa was measured. Only a small axial strain of 0.1% was measured in this set of cycles. After 20 cycles, the axial strain reached equilibrium.

In the fourth set of cycles, no increase in pore pressure was measured; however, the rate of development of axial strain was somewhat accelerated but after 26 cycles a state of equilibrium was reached. An increase of 0.18% of axial strain was measured in this set of cycles.

In the fifth set, application of a high cyclic stress ratio of 0.7 is used, higher than the CLRL, caused the rate of the development of axial strain to accelerate and no equilibrium condition was observed. Also no pore pressure increase was observed in the first 26 cycles. In the last 4 cycles, a maximum increase of 2 kPa in pore pressure was measured. At the end of 30 cycles, the test was stopped and the cyclic stress ratio was increased. In the last set of cycles, with a CSR of 0.8, no increase in pore water pressure was measured. However, the rate of axial strain accelerated and the sample failed in only 1 cycle.

In the stress space represented in Fig. 5.6, the development of pore pressure, especially in the first set of cycles, causes the migration of stress path to the left side. The failure envelope was reached at a value of $q/p' = 0.91$.

Fig. 5.7 shows the stress-strain, pore pressure-strain, and stress-path curves obtained from test C22. As mentioned earlier, in this test the sample was subjected to the last three sets of identical cycles imposed on the test C21. In the first set of cycles, both pore water pressure and axial strain develop at a decreasing rate, and significant pore pressure was developed (8 kPa). However, only a small increase in axial strain was measured (0.1%). Pore pressure did not reach equilibrium; however, the axial strain reached equilibrium after 20 cycles of loading. In the second set of cycles, an increase of 1.5 kPa in pore pressure was measured in the first few cycles and that is the maximum value that can develop in the soil sample. However, the rate of development of axial strain accelerated and no equilibrium conditions were observed. An increase of 0.21% of axial strain was measured in this set of cycles. Thus, it appears that the cyclic stress ratio used in this set is higher than the CLRL. At the end of 30 cycles, the test was stopped and

the cyclic stress ratio was increased.

In the last set of cycles, no increase in pore water pressure was measured. However, the rate of axial strain accelerated and the sample failed in two cycles.

In the stress space (Fig. 5.7), the build up of pore pressure in the first set of cycles causes the migration of stress-path to the left side. In the second set of cycles, the stress path is represented by closed loops and reaches the failure envelope at $q/p'=0.87$ in the third set of cycles. This value is less than the one observed at failure in test C21.

For an analysis of the variation of both axial strain and pore pressure measured at the maximum repeated stress with the number of cycles, reference should be made to Fig 5.8 (test C21). The changes of axial strain in each step with the number of cycles can be described by straight lines, and the slope of these lines increases with increasing CSR. However, the pore pressure increases with the number of cycles in the first three sets of cycles and then tends to stabilize.

In static test (T2), the pore pressure measured at failure is around 23.5 kPa; however in test C21 in which the sample was subjected to a total of 151 of cycles of loading, the pore pressure measured at failure is approximately 33 kPa and in the test C22 (62 cycles of loading) the pore pressure measured at failure was around 29 kPa. This indicates cycling at low levels of CSR causes the soil sample to develop more pore pressure. Similar behaviour was observed for axial strain, when at higher cyclic stress ratio, a higher value of axial strain at peak strength was reached. In stress space also, the higher the cycling the higher the value of q/p' at which the failure envelope was reached.

From the test results of these two tests, the following conclusions can be drawn:

- (1) Cycling below CLRL, causes a development of more than 90% of the total pore pressure that can develop in the soil sample.

(2) Cycling at low levels of CSR causes the stress path to travel beyond the slow monotonic loading effective stress failure envelope. For these samples the failure envelope is not identical.

Series C3:

Fig. 5.9 shows the stress-strain, pore pressure-strain, and stress-path curves obtained from test C31. Under cycling, both axial strain and pore pressure accumulate at a continuously decreasing rate. An axial strain of 0.77% and change of pore pressure of 23 kPa were developed in the sample under cycling. Both these values are very close to those obtained in static test at failure (T3). At the end of cycling, repeated loading was followed by a monotonic one. It was observed that this cycling causes a loss of strength of 11 kPa comparing to the static strength. This loss of strength demonstrates that the cyclic stress ratio used is above a CLRL and the sample will fail under cycling but at larger number of cycles. Lefebvre et al. (1989), concluded from their tests (on sensitive clay) that cycling below CLRL causes no decrease in static strength of the soil. Therefore, from the test results of the test C31, a CLRL can be fixed at a level slightly less than 0.65, and a level of 0.60 is suggested.

At failure in test C31, the sample showed an axial strain of 1.2% but no increase in pore pressure when compared to the static test. As shown in Fig 5.9, the stress path migrates to the left side and the characteristic stress ratio was reached at value of $q/p'=0.75$.

Fig. 5.10 shows the stress-strain, pore pressure-strain, and stress-path curves obtained from the test C32. As mentioned earlier, only 7 cycles of loading were required to reach failure. Both the axial strain and pore pressure accumulate at an increasing rates until failure envelope is reached. A total of axial strain of 1% and a change of pore pressure of 24 kPa were developed in the sample under cycling. Comparing these changes with the ones obtained in the static test, it is noted that the axial strain is higher; however no increase in pore pressure was measured. The stress-path reaches failure envelope at $q/p'=0.75$. A similar behaviour was observed in test C33.

The sample showed a higher strain and no increase in pore pressure at failure compared to the static test. The failure was also reached at $q/p'=0.75$.

From these tests, the following conclusions can be drawn:

- (1) When a cyclic stress ratio used is above a CLRL, no increase in pore pressure is measured when compared to monotonic tests. However, the axial strain is large. The stress path reaches failure at equal values of q/p' , but these values are less than those obtained in the static test. The failure envelope for these samples is identical and is bounded by monotonic loading effective stress failure envelope.
- (2) Since the pore pressure developed under cycling is the same as that in the static test, the reduction in postcyclic strength is a function of the amount of cyclic straining under cycling.

5.2.3 Behaviour of overconsolidated clay crust below the CLRL:

It was concluded from previous test series that the CLRL exists for this soil. Below the CLRL, only a small axial strain developed in the soil sample. The magnitude of this strain is function of the CSR used. However, more than 90% of the total pore pressure that can develop in the soil sample under cycling occurs in this stage. The remainder develops when the CSR becomes higher than the CLRL.

It is further found that with each step of increase of CSR, an additional axial strain always developed in the soil sample. The variation of the axial strain with the number of cycles can be described by a straight lines, as shown in Fig. 5.8. The slope of these lines increases with increasing in CSR.

5.2.4 Behaviour of overconsolidated clay crust above the CLRL:

In this stage, the rate of the development of the axial strain accelerates with cycling until failure occurred. The samples cycled in this stage failed at an axial strain greater than the one obtained in the static test. However, the development of the pore pressure under cycling depends on whether or not the clay is subjected to cycling below the CLRL. When the soil sample is subjected to cycling below a CLRL, as in the case of test series C2, most of the pore pressure that can develop in the soil sample develops in this stage. The remainder develops after when the CSR becomes higher than the CLRL. The soil sample fails at higher values of q/p' compared to the one obtained in the static test.

If the soil sample is subjected only to cycling at higher values of CSR (above CLRL), cycling causes only a development of the same amount of pore pressure as the one measured in the static test. The failure envelope is reached at lower values of q/p' compared to the one obtained in the static test. The failure envelope for all specimen cycled in this stage is identical. The variation of cyclic stress ratio with the number of cycles shows an upward concave curve, similar to the one observed for kaolinitic clay. The effective stress-path migrates to the left side and the closed loops become larger until failure envelope is reached.

5.2.5 Kaolinitic clay versus clay crust:

Since the kaolinitic clay is a normally consolidated clay and the crust is an overconsolidated clay, a difference in the response of these clays under static and repeated loading is expected. Therefore, a comparison of the behaviour of these clays under static and cyclic loading in terms of the development of both axial strain and pore pressure seems necessary. The effect of cycling on both the OCR and strength of the soil and the sensitivity of these soils to the variation of the CSR are discussed here.

The CLRL divides the response of both these clayey soils under cycling, in terms of the rate

of development of axial strains, in two different stages. Below a CLRL, under cycling, only a small axial strain can develop in the soil sample before the equilibrium conditions are reached. The magnitude of this axial strain is a function of the cyclic stress ratio and the OCR of the material. Above a CLRL, the rate of development of axial strains increases with cycling until failure envelope is attained. In this stage and for the same material, the larger the amplitude of applied stress, the less the number of cycles required to reach failure. When cycling at the same CSR, the more overconsolidated the soil, the lower is the axial strain produced and less the number of cycles required to reach failure. However, according to the data presented in chapters 4 and in this chapter, a critical factor appears to be whether or not the repeated loads lead to a pore pressure build up which brings the soil to failure.

For kaolinitic clay, the change in pore pressure under cycling is similar to the change in axial strain. Below CLRL, a significant negative pore pressure developed in the soil sample before equilibrium conditions is reached. In this stage, the behaviour of this soil under cycling can be described by some equations which are function only of the amplitude of applied stress. On cycling at higher values of CSR (greater than a CLRL), a negative residual pore pressure is associated with each additional cycle of loading until failure is reached. For this clay, cycling at any CSR causes more development of negative pore pressure at failure.

For the overconsolidated clay crust, the change in pore pressure is dependent on stress history that the soil sample was subjected to. If cycling is at low levels of the CSR (below the CLRL), more than 90% of the total pore pressure that can develop in the soil sample, develops in this stage as shown in Figs. 5.6 and 5.7. This increase in pore pressure causes the migration of stress path close to the failure envelope before equilibrium conditions are reached.

If cycling occurs at higher values of CSR greater than CLRL, the rate of development of pore pressure increases with cycling until failure. In this case no increase in pore pressure is observed compared to the one measured in the static test.

For both clays, it was observed that cycling below CLRL causes a very slightly increase in the strength of the soil. This increase may be caused by the fact that cycling at this level causes no

destruction in soil structure but causes an increase in overconsolidation of the material which is reflected in a small increase on the strength of the soil.

The effect of a step increase in CSR on the behaviour of both clays was investigated. For kaolinitic clay, a step increase in CSR causes an accumulation of positive axial strain and a negative pore pressure in the soil sample (below CLRL). When CSR becomes higher than CLRL, the rate of development of both axial strain and pore pressure increases with the number of cycles until failure occurs. For the overconsolidated clay crust, a step increase in CSR (below CLRL) causes a small change in axial strain and an increase of more than 90% of the total pore pressure that can develop in the soil sample. When CSR becomes higher than CLRL, the rate of development of axial strain increases with cycling; however, no increase in pore pressure is observed.

Table 5.1. Summary of the testing conditions and test results of the test series T.

Test number	Depth m	w %	q'_i kPa	p'_i kPa	OCR	ϵ_r %	u_r kPa	$(q/p')_r$	q_r kPa
T1	2.78	39.0	0.0	31.00	5.2	1.00	23.0	0.78	98.5
T11	2.78	39.0	-6.9	37.95	5.2	0.96	29.5	0.74	104.7
						0.60			
T2	3.33	40.3	0.0	36.0	3.9	0.67	24.8	0.79	90.0
T22	3.33	40.3	-5.4	41.4	3.9		30.1	0.75	100.6
						0.67			
T3	3.60	41.0	0.0	41.00	3.2	0.65	23.5	0.75	83.5
T33	3.60	41.0	-2.1	43.05	3.2		27.4	0.74	88.6

Table 5.2. Summary of the testing conditions and test results of the test series C1,C2, and C3.

Test number	Depth m	q'_i	p'_i	CSR _{min}	CSR _{max}	N	ϵ_t %	u kPa	$(q'/p')_r$	failed	Postcyclic strength kPa
C11	2.7	0	31	0.39	0.52	707	0.07	-	0.78	no	100.2
C12	2.7	-7	38	0.49	0.62	0	0.09	-	0.74	no	106.5
C21	3.6	0	41	0.18	0.32	30	0.05	12			
				0.23	0.42	30	0.08	5.4			
				0.36	0.51	30	0.10	6			
				0.46	0.61	30	0.18	1			
				0.55	0.70	30	0.48	-1			
				0.66	0.80	1	0.80	1.5	0.91	yes	-
C22	3.6	0	41	0.46	0.61	30	0.10	8.0			
				0.55	0.70	30	0.21	1.5			
				0.66	0.80	2	2.30	-1	0.87	yes	-
C31	3.3	0	41	0.11	0.65	30	0.80	9.4	0.75	no	76
C32	3.3	0	41	0.11	0.75	7	1.10	6.8	0.75	yes	-
C33	3.3	0	41	0.11	0.85	5	1.10	5.1	0.75	yes	-

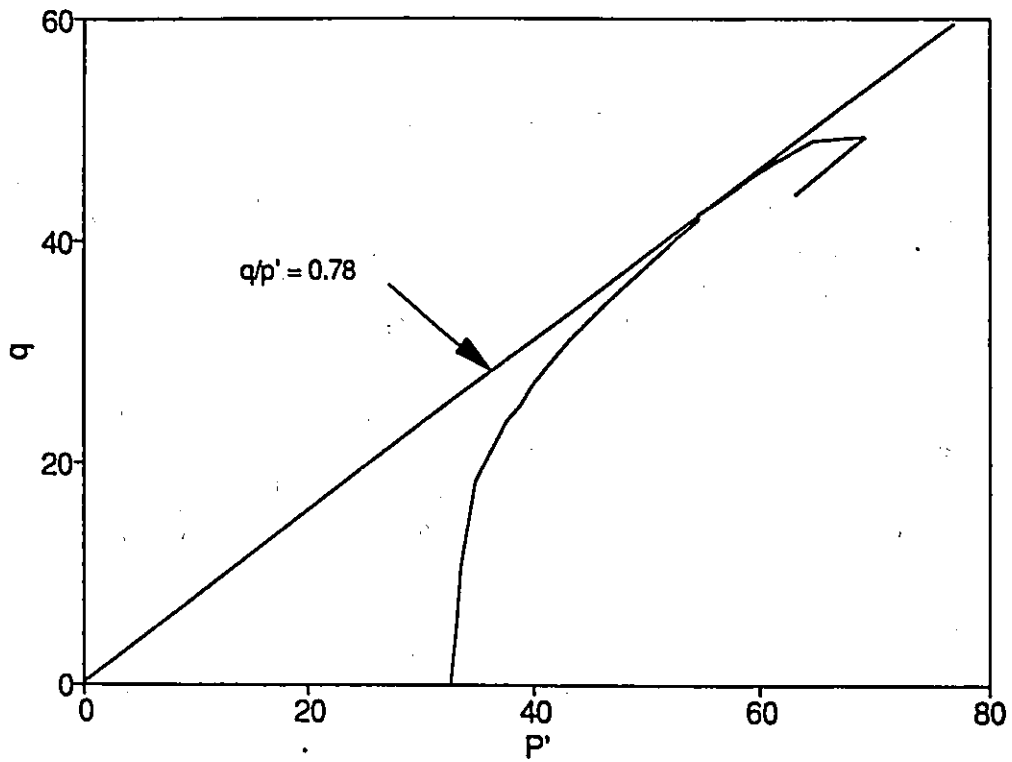
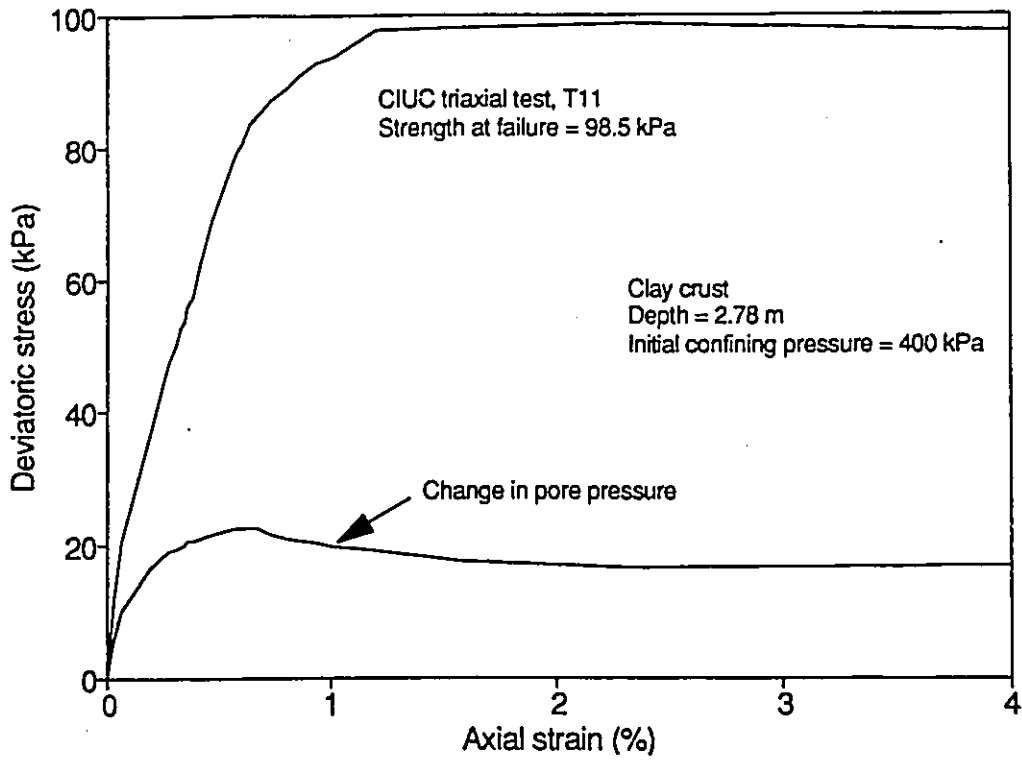


Fig. 5.1. Stress-strain, pore pressure-strain, and stress-path curves for CIUC under monotonic loading: Test T11.

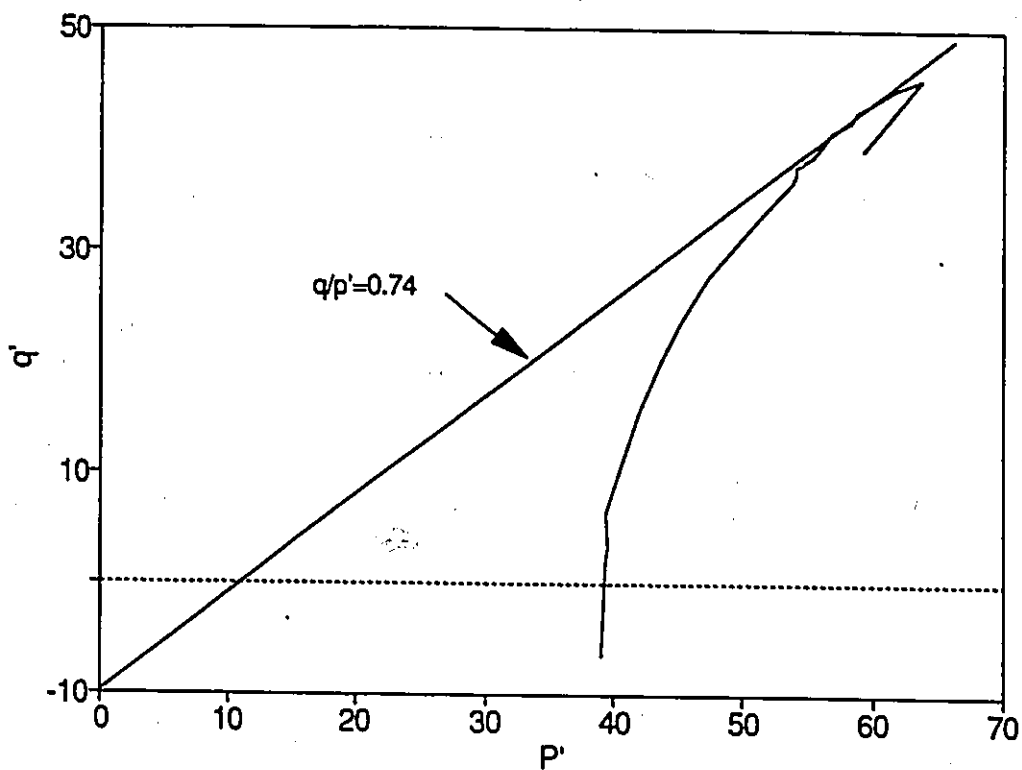
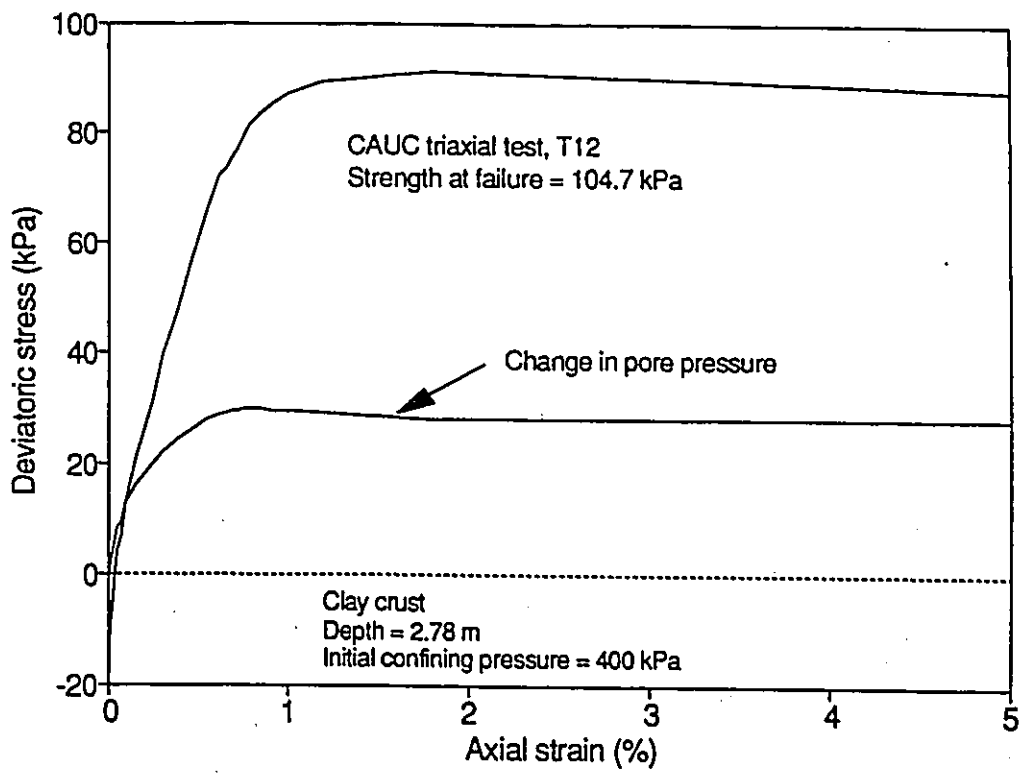


Fig. 5.2. Stress-strain, pore pressure-strain, and stress-path curves for CAUC under monotonic loading: Test T12.

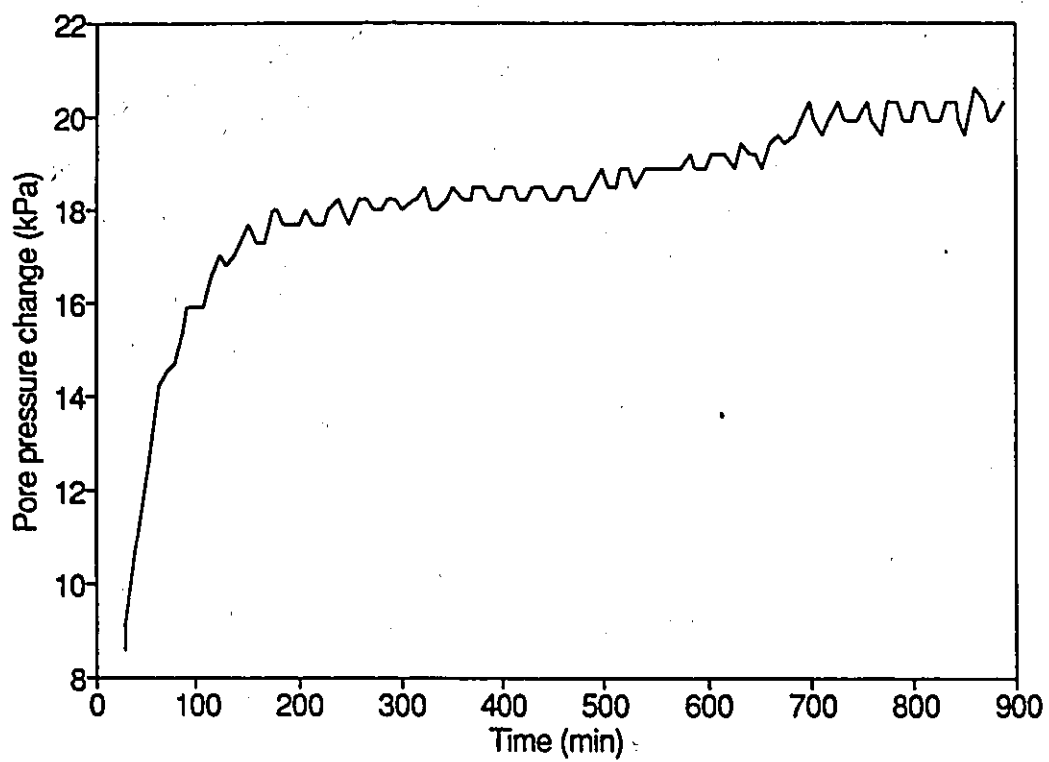
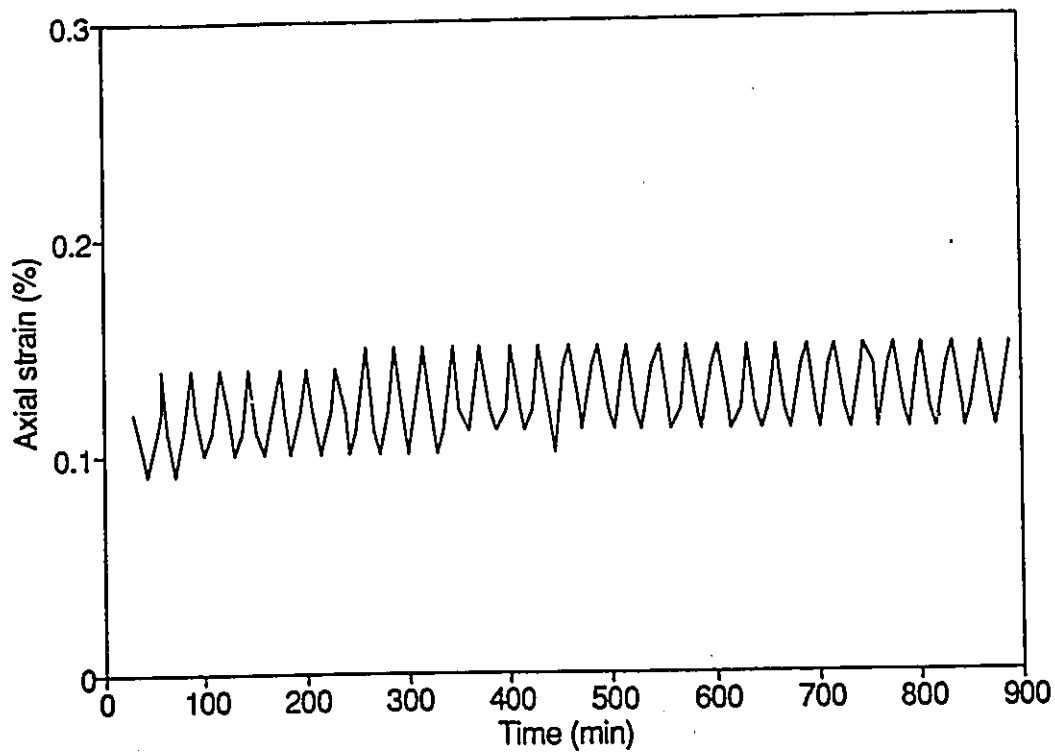


Fig. 5.3(a). Change in behaviour of clay crust during undrained loading at low levels of CSR: Test C21, CSR=0.25.

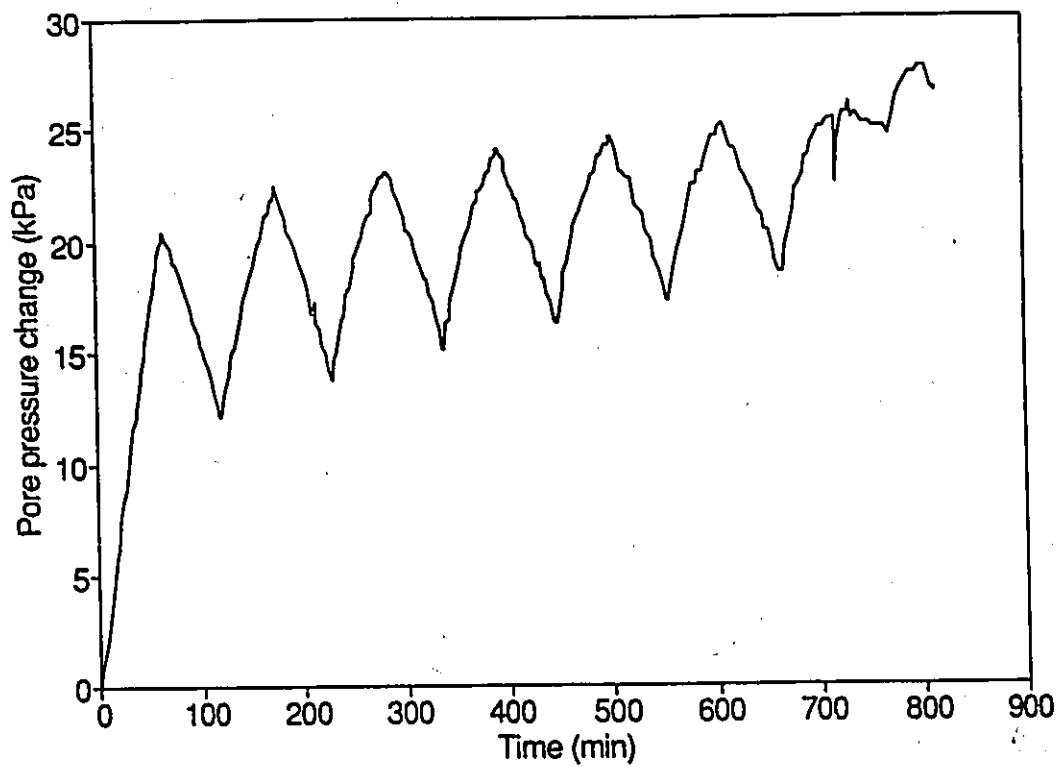
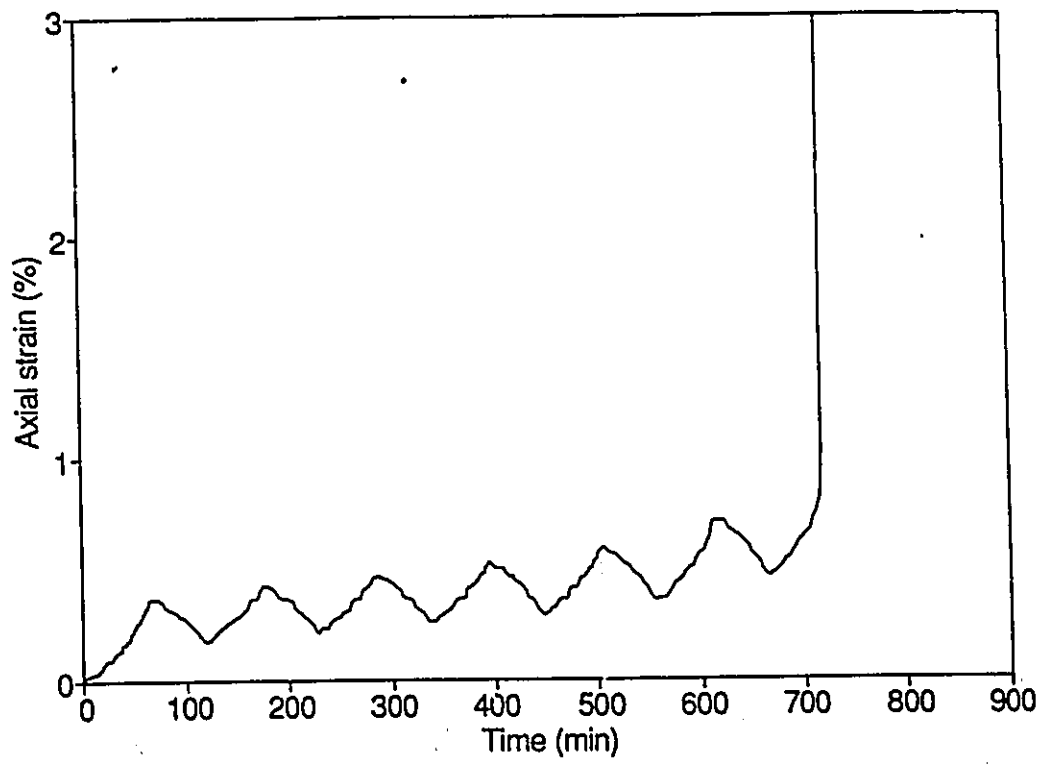


Fig. 5.3(b). Change in behaviour of clay crust during undrained loading at high levels of CSR: Test C32, CSR=0.75.

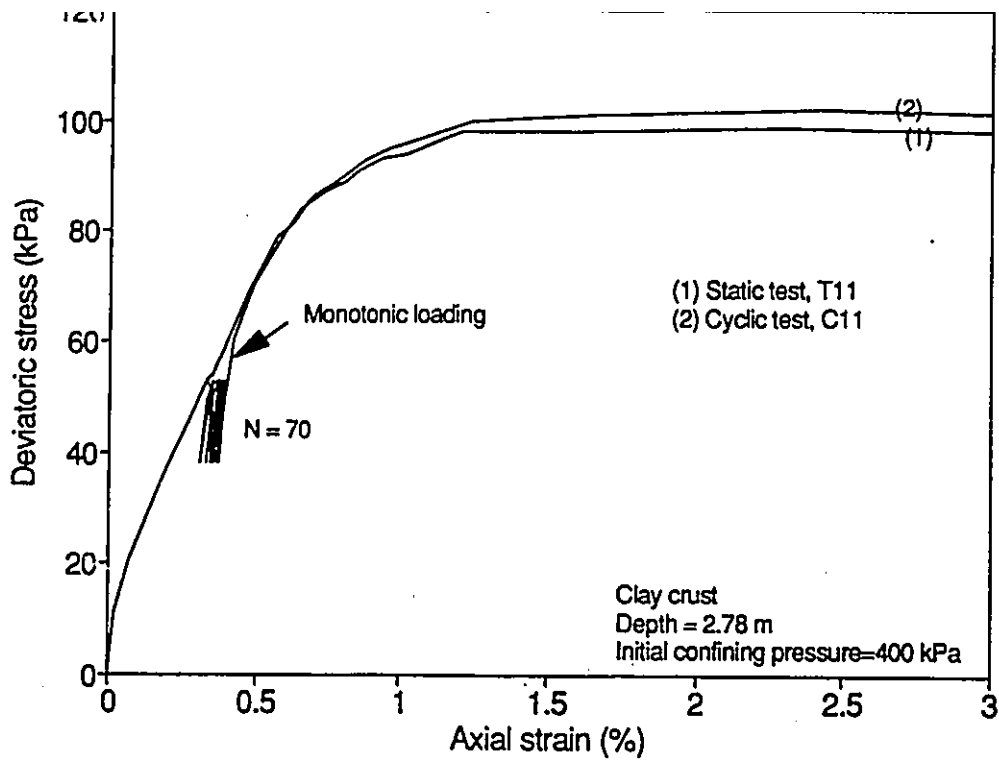


Fig. 5.4. Stress-strain, pore pressure-strain, and stress path curves for CIUC under one-way repeated loading: Test C11, CSR=0.52.

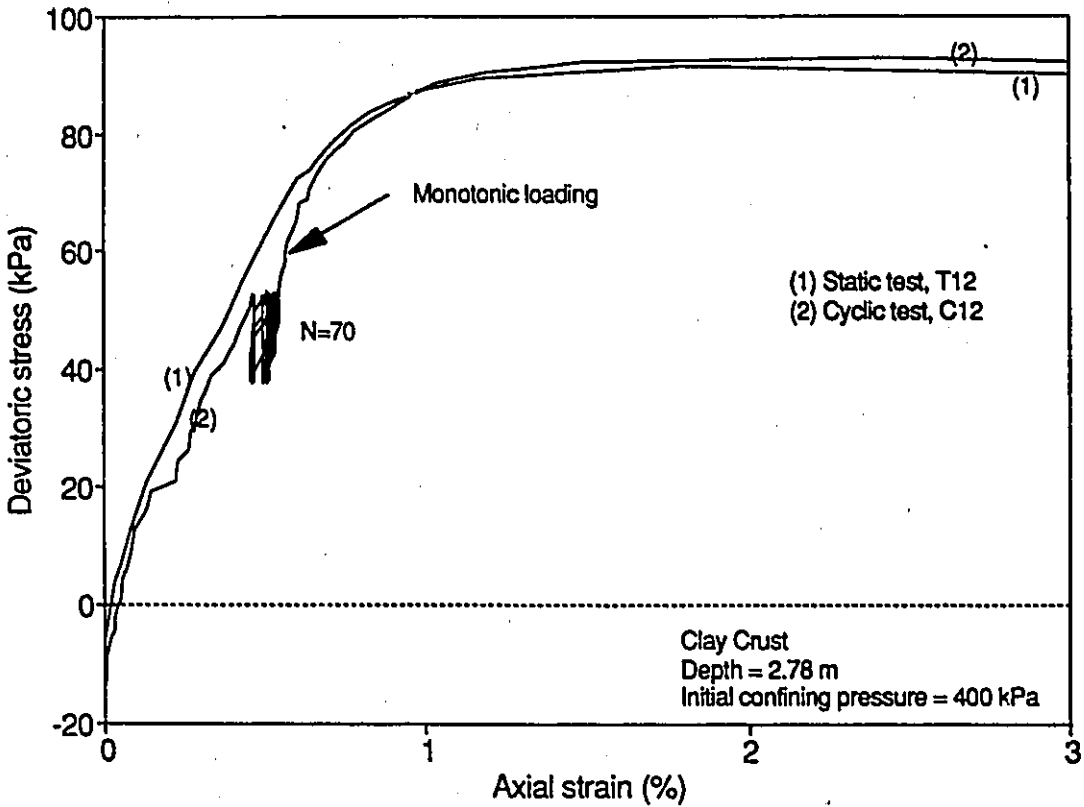


Fig. 5.5. Stress-strain, pore pressure-strain, and stress path curves for CAUC under one-way repeated loading: Test C12, CSR=0.62.

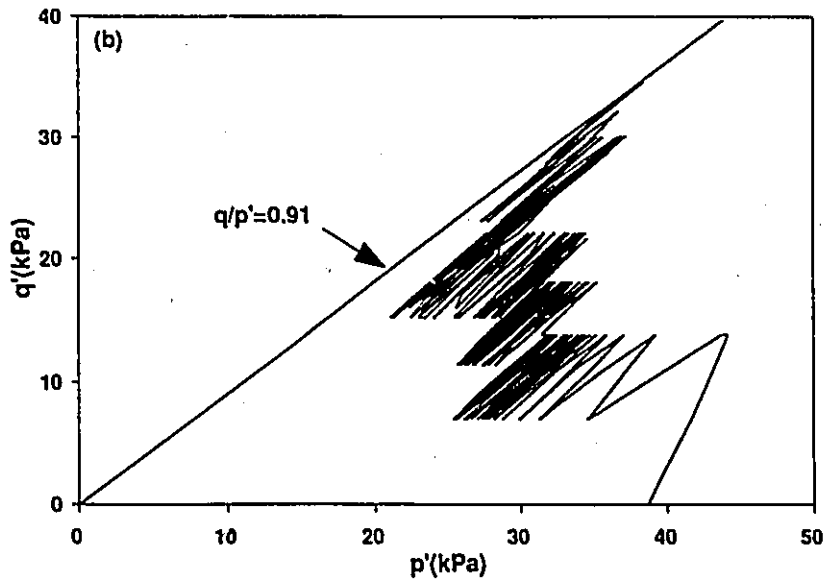
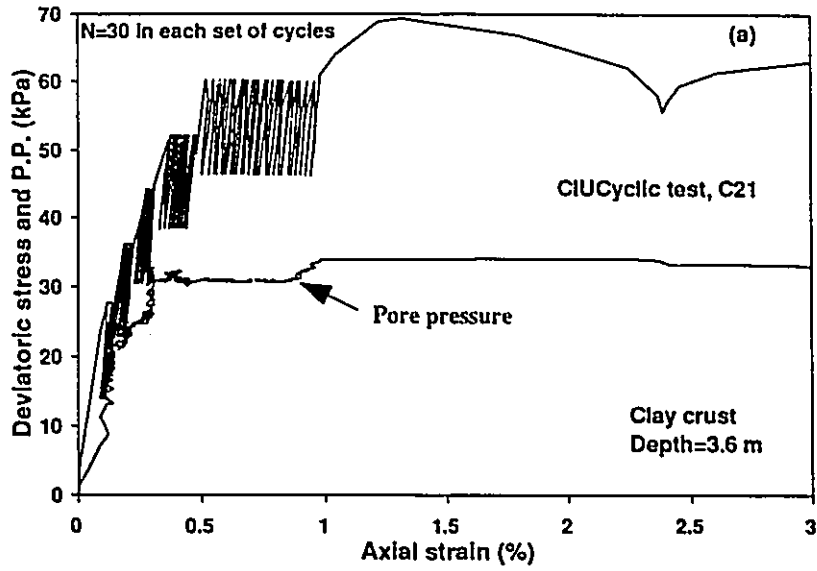


Fig. 5.6. Stress-strain, pore pressure-strain, and stress path curves for CIUC under one-way repeated loading at different CSRs: Test C21.

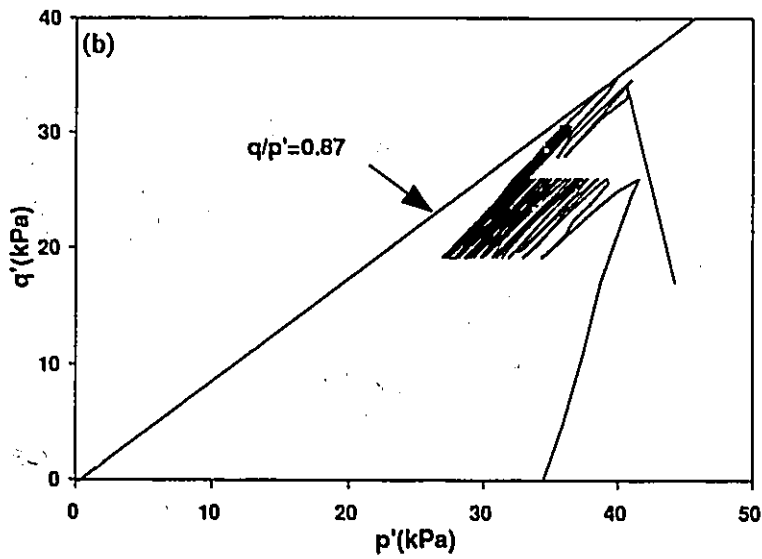
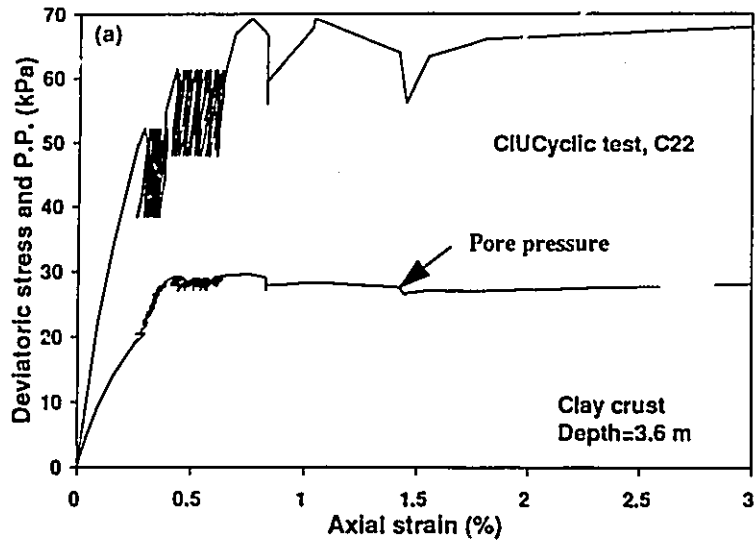


Fig. 5.7. Stress-strain, pore pressure-strain, and stress path curves for CIUC under one-way repeated loading at different CSRs: Test C22.

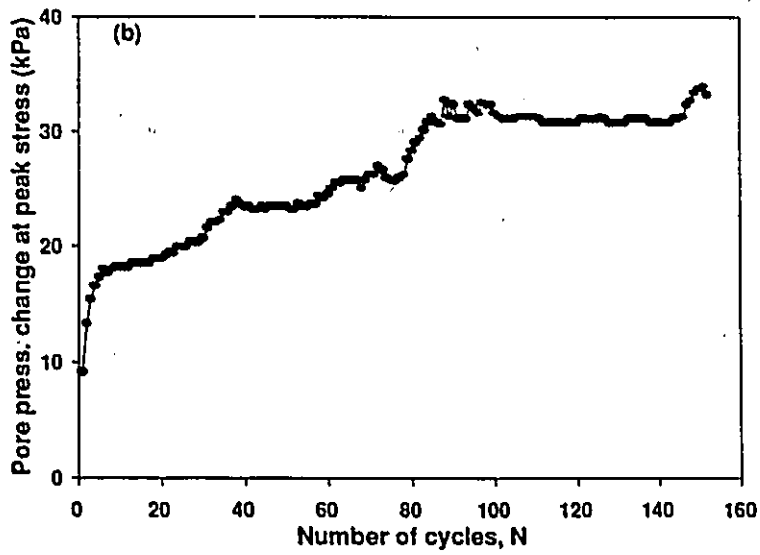
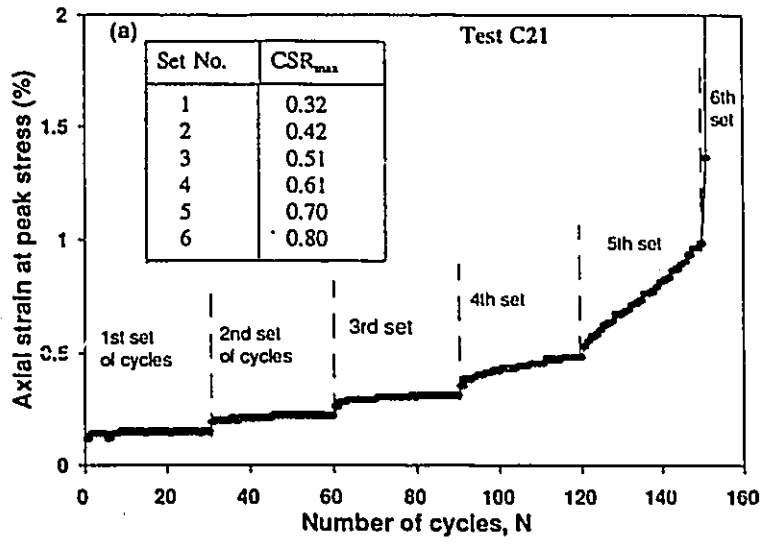


Fig. 5.8. Variation of both axial strains and pore pressure measured at peak of cycles with the number of cycles: Test C21.

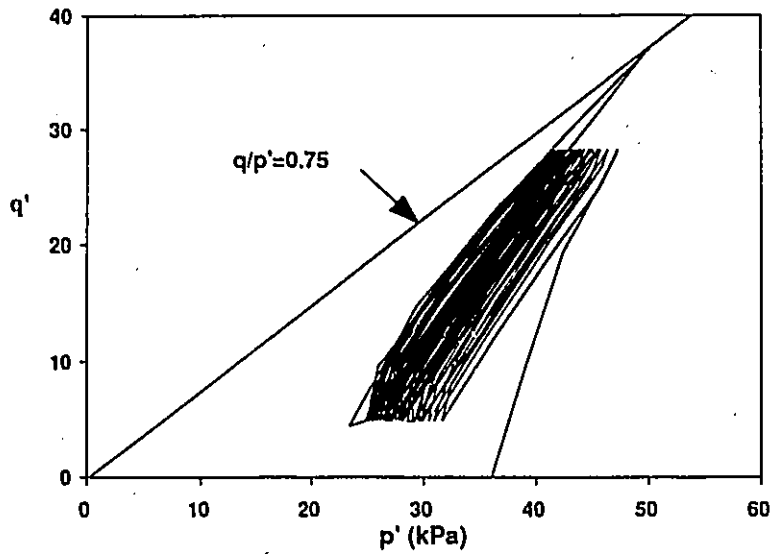
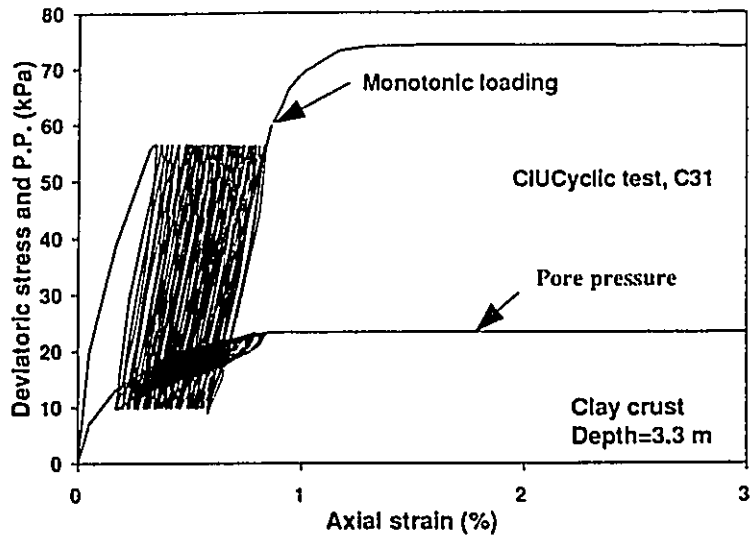


Fig. 5.9. Stress-strain, pore pressure-strain, and stress path curves for CIUC under one-way repeated loading: Test C31, CSR=0.65.

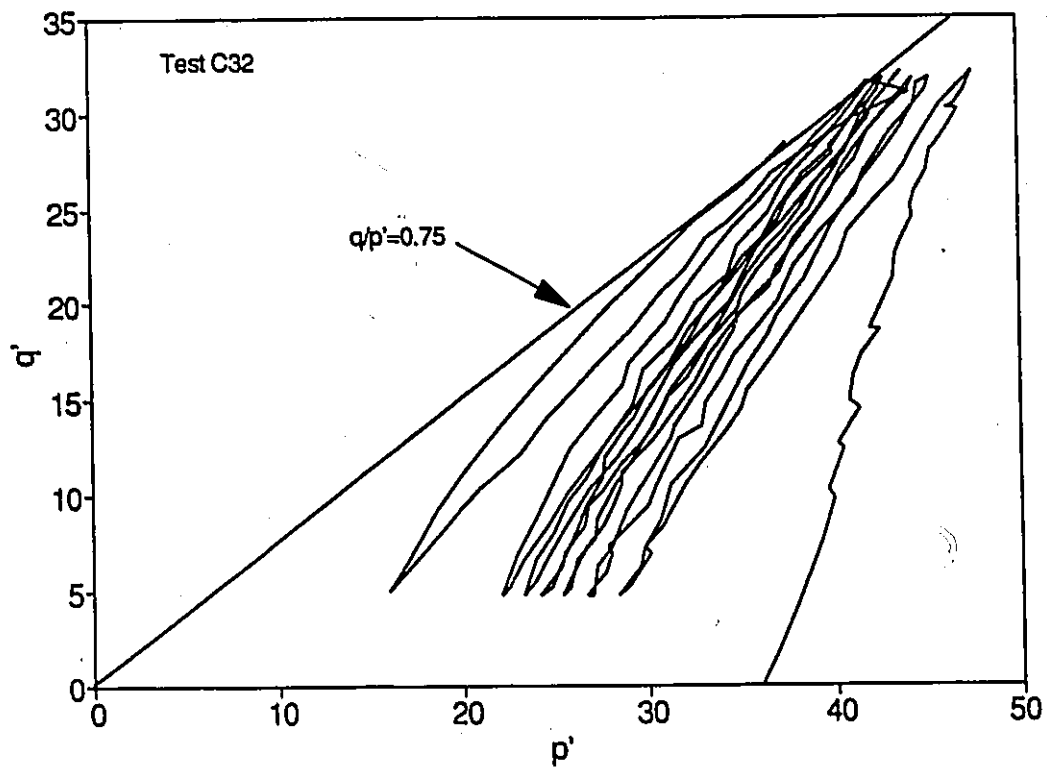
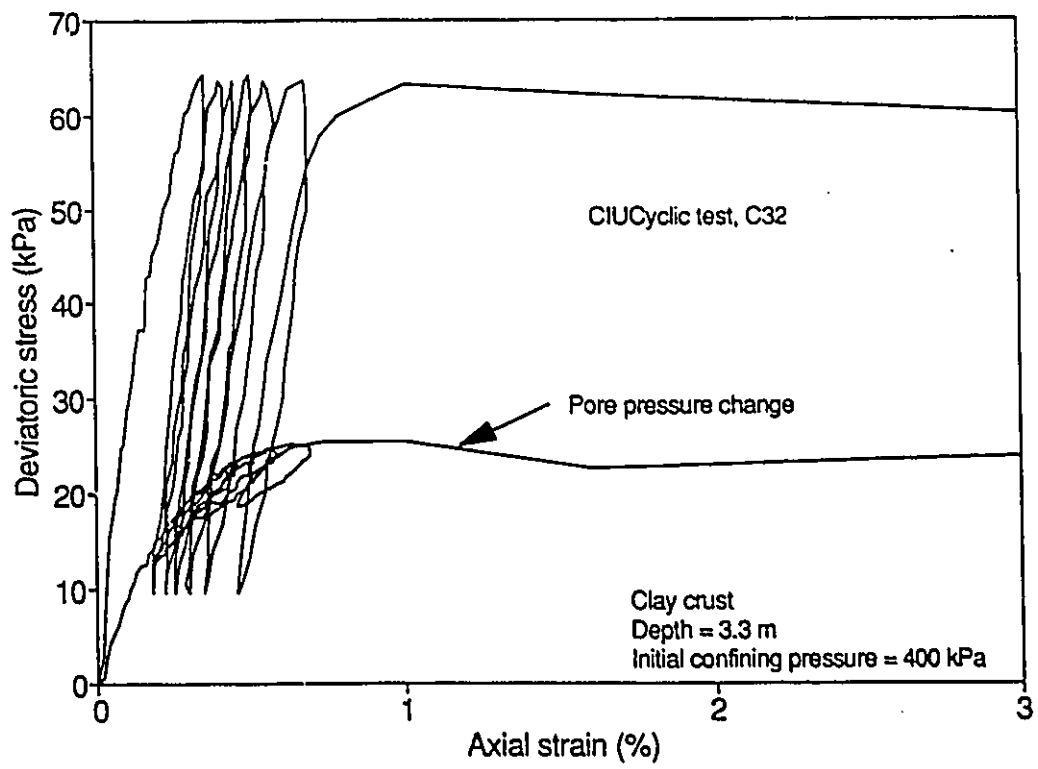


Fig. 5.10. Stress-strain, pore pressure-strain, and stress path curves for CIUC under one-way repeated loading: Test C32, CSR=0.75.

CHAPTER 6

Further Consideration on the Effect of Cycling on Behaviour of Clayey Soils

6.1 Variation of the CLRL with the Amplitude of Applied Stress

Several experimental works have been carried out to explore the concept of CLRL or threshold limit, below which the soil will not suffer failure regardless of the number of cycles. The published data and the data reported in chapters 4 and 5 indicate the existence of CLRL for most soils at different testing conditions. In general, a CLRL is evaluated by a series of stress controlled tests. However, other investigators, e.g. Procter and Khaffaf (1984), used the strain controlled tests. They defined the CLRL by performing strain controlled tests at a low level of strain and observing the strength reduction as the test progressed.

The most common definition for the CLRL in terms of the axial strains is that the CLRL is a limit below which a state of non-failure conditions will be reached. In this state, the stress-strain curve follows a closed hysteresis loop. Above the CLRL, each additional cycle of loading produces additional plastic deformation and the clay eventually fails. This behaviour was observed on both kaolinitic and clayey crust soils (as reported in Chapters 4 and 5). The apparently complex behaviour of soils under repeated loading is related to the conditions under which the repeated load leads to a pore pressure build up that brings the soil to the effective stress failure envelope.

The reported data in the literature showed that the CLRL is affected by different parameters, such as OCR, type of cyclic loading (one-way or two-way), frequency, plasticity of the soil. However, the amplitude of applied stress can be considered also from these parameters which has an effect on CLRL.

Theoretically, it is very easy to demonstrate that as the amplitude of applied stress decreases, the CLRL increases. However, the mode of this change can not be demonstrated theoretically and requires experimental work. No experimental work has been conducted to investigate how the CLRL changes with the amplitude of applied stress. The approximate evaluation of the CLRL for a specific amplitude of applied stress requires at least three tests.

Here, a test series (S3) was conducted on kaolinitic clay to investigate the questions raised above. The CLRL is evaluated for 4 different amplitudes of applied stresses.

Test series S3:

This test series is divided in three groups. Each group of tests contains three tests and is used to evaluate CLRL for a specific amplitude of applied stress. The samples used in these groups of tests are similar and had the same consolidation history as the sample used in the static test (K1).

Based on equilibrium conditions, failure conditions, and postcyclic strength, the CLRL was evaluated. The test results obtained from these test series are plotted in Fig. 6.1. This figure shows the variation of the CLRL with the amplitude of applied stress, in which:

$$CLRL = CSR_{\max} \times q_f$$

and the amplitude of applied stress changes between two limits L_1 and L_2 , in which:

$$L_1 = CSR_{\min} \times q_f$$

$$L_2 = CSR_{\max} \times q_f$$

where:

q_f = maximum deviatoric stress obtained in static test K1 (72 kPa).

CSR_{\max} = maximum cyclic stress ratio correspond to CLRL.

CSR_{\min} = minimum cyclic stress ratio considered.

In Fig. 6.1, the upper limit was taken to be linear. Therefore, the discussion must be only in terms of the lower limit. As can be observed in Fig. 6.1, there seems to be a linear relationship between the CLRL and the amplitude of applied stress used (lower limit). This relationship may be valid only for the homogeneous clayey soils such as the case of the kaolinitic clay used in this investigation. However, for non-homogeneous soils the change of CLRL with the amplitude of applied stress may not be linear. Fig. 6.1 demonstrates the existence of two zones. The zone between the lower and upper limits is the stabilization zone. Above the upper limit is the failure zone. The space of these zones is affected by different parameters including frequency, pulses shape, and the OCR of the material.

Note that the above results are valid only for a uniform amplitude of applied stress.

6.2 Effect of the frequency on the behaviour of soils

It seems likely from the data reported in literature that the change in frequency has more effect on the more plastic clays. Also, the slower cycles of loading cause more damage than the faster one because it gives the clay more time to follow the applied load and thus are likely to produce greater strains and greater pore pressures. Because of the slow rate of loading used in this investigation, it is of interest to study the effect of frequency. This slow rate probably allows pore pressure equalization along the specimen and permits an accurate measurements of pore pressure at the ends of the specimen. Hence, a reliable assessment of the effect of the frequency on

behaviour of soils can be made. To achieve this objective, a test series S4 (see Table 3.2) was conducted on kaolinitic clay.

Test series S4:

This test series comprises only two tests. The samples used in both tests are similar and had the same consolidation history as the sample used in static test K1. In the first test S41, the sample was sheared monotonically to failure under a rate of loading equal to 0.5 kPa/min and compared to test K1 (rate = 1 kPa/min). In the second test S42, the sample was repeatedly loaded at a frequency of 0.001 Hz and compared to the test S14 in which the sample was repeatedly loaded to failure at a frequency of 0.00017 Hz. Note that the same amplitude of applied stress was used in both tests S42 and S14.

Fig. 6.2 shows the stress-strain, pore pressure-strain, and stress-path curves obtained from both undrained static triaxial compression tests S41 and K1. This figure demonstrates clearly that the decrease in the rate of loading leads to a decrease in static strength, and less development of positive pore pressure. Also no negative pore pressure develops at failure in the test S41.

Fig. 6.3 shows the stress-strain curve obtained from the test S42. Also shown in this figure is the stress-strain curve obtained from the test S14. As observed in Fig. 6.3, despite the development of a large axial strain of 3.2% in the soil sample (test S42) under cycling, the equilibrium condition was reached after a larger number of cycles of loading (90 cycles). Also a higher postcyclic strength were measured in this test compared to the static test at a rate of loading of 1 kPa/min. These test results demonstrated that the frequency has an effect on behaviour of soils. Under the same conditions of testing, only increasing the frequency from 0.00017 Hz to 0.001 Hz, a state of failure and non-failure conditions were reached. As previously mentioned, the behaviour of this clay above a CLRL is divided in three stages, primary, secondary, and tertiary. Fig. 6.3 demonstrates the increasing in frequency increases the number of cycles in the primary stage.

6.3 Effect of the fluctuation of pore pressure on strength of the soil

It is known that the fluctuation of pore pressure has an effect on the overconsolidation of soils. Rising of water table causes a reduction in the effective overburden stress. This reduction results in an increase of the overconsolidation ratio which has a pronounced effect on the value of K_0 . The stress-path may undergo Path ABC as shown in Fig. 6.4. A subsequent, dropping of water table causes a decrease in overconsolidation ratio and the stress-path as represented by path CD. Subsequent unloading and reloading by seasonal water table fluctuation is likely to cause the stress path to occur within the loop ABCDA. In this section, the effect of the fluctuation of water table is studied and the objective is to examine whether the fluctuation of water table has an effect on the strength of the soil.

Test series S5:

A repeated loading sequence involving triangular variation of back pressure at a frequency of 0.0007 Hz and a constant confining pressure was applied on a sample of kaolinitic clay. The sample used in this test was taken from the second block of commercially acquired kaolinitic clay and had the same consolidation history as the sample used in test K2. This sample was subjected to a total of 70 cycles of change in back pressure, as shown in Fig. 6.5. The amplitude of applied stress is approximately 12 kPa which corresponds to a rise of the original water table by 1.2 m. At the end of cycling, enough time was provided to ensure that the pore pressure developed during cycling in the soil sample was dissipated. Then, the drainage valves were closed and the sample was taken to failure under monotonic loading at a rate of loading of 1 kPa/min.

Stress-strain, pore pressure-strain, and stress-path curves obtained from this test and the corresponding static test are shown in Fig. 6.6. As can be observed in this figure, clearly a loss of strength of approximately 13% was caused by cycling of back pressure. In the stress space, the failure envelope was reached at different values of q/p' . A lower value of q/p' is obtained for the soil sample with previous cycling. The pore pressure-strain curves obtained from both tests were identical. Therefore, the reduction in postcyclic strength may be related directly to some strains induced in the soil sample during cycling.

The increase in the level of back pressure reduces the effective stresses applied to the soil sample and may also induce an increase in pore pressure inside the soil sample. This pressure may cause some rearrangement of the particles of the soil. However, in this test, only a small change in back pressure of 12 kPa was applied to the soil sample. This small change may not have a significant effect on the rearrangement of the particles. The effect of the water table on strength of the soil can be related to the reduction in effective stresses applied to the soil sample during cycling. An increase in back pressure causes a reduction in the effective stress and the soil sample dilates. Unloading of back pressure causes an increase in the effective stress and the soil sample is compressed. Thus, both dilation and compression of the soil sample are associated with each cycle of loading and the tangent modulus decreases and the failure envelope is reached at lower values of q/p' . The reason for this behaviour are not clear. The identical pore pressure-strain curves obtained from both tests demonstrate the existence of a relationship between pore pressure and axial strains.

6.4 Effect of cycling on overconsolidation of the material

It is reported in literature that loading and unloading leaves a residual pore pressure in the soil, makes a soil behave as an overconsolidated soil (e.g. Wroth and Loudon 1967). Also Lefebvre et al. (1989) observed in their triaxial tests on normally consolidated clay that cycling causes an apparent overconsolidation of the material. The test results obtained from both kaolinitic clay and overconsolidated clay crust reported in chapters 4 and 5 demonstrate that cycling below CLRL causes an increase in the overconsolidation of the material. This is demonstrated by the fact that the postcyclic strength obtained from the samples which reached the equilibrium conditions is always very slightly higher than the one obtained in the static test. The stress path reaches the failure envelope at different values of q/p' . The maximum value is obtained for the samples subjected to more cycling. However, kaolinitic clay is a normally consolidated clay and a clay crust is an overconsolidated clay. Therefore, the verification must be done for a slightly overconsolidated clay (test series C4).

The samples used in this test series were trimmed from the crust in horizontal direction at a depth of 3.20 m to simulate a lightly overconsolidated clay. Therefore, the in situ effective vertical stress becomes the "horizontal stress" and vice versa.

First, the in situ stress ratio ($\sigma'_{110}/\sigma'_{v0}$) was determined which found equal to 0.75 (test C41). During this stage, the vertical stress was increased slowly (0.02 kPa/min) so that there was no excess pore water pressure developed. The lateral-displacement transducer activated an increase in the horizontal stress to maintain the conditions of zero lateral strain. In the test C42, the sample was consolidated isotropically to the value of 0.3 times the in situ effective vertical stress. Then, the specimen were subjected to two sets of cycles in undrained conditions, as shown in Fig. 6.7. In the first set of cycles, 11 cycles were applied to the sample at a frequency of 0.00025 Hz. In the second set of cycles, 70 cycles were applied to the sample at a frequency of 0.00035 Hz. The amplitude of applied stress was kept small to ensure that no destruction of the soil structure is caused by cycling. This cycling causes only a development of a total axial strain of 0.49% and a change in pore pressure of 6 kPa. These values are very small compared to the ones measured at failure in the static test (5% in axial strain and 26 kPa in pore pressure). At the end of cycling, both horizontal and vertical effective stresses were reduced to a value of 0.3 σ'_{v0} , and then the pore pressure accumulated under cycling was allowed to dissipate. Then, the value of the in situ stress ratio $\sigma'_{110}/\sigma'_{v0}$ was determined which found equal to 0.82. This test results indicate that cycling causes an increase in the in situ stress ratio. Since the pore pressure developed under cycling was allowed to dissipate, this increase in the in situ stress ratio can be related to the plastic strain developed in the soil sample.

Two other tests were conducted on this clay (tests C43 and C44). In the test C43, the sample was taken to failure at a rate of loading (1 kPa/min), where in the test C44, the specimen was subjected to the same stress history as the one imposed on test C42. In the latter test, after cycling the specimen was consolidated to the in situ stresses after cycling and then was taken to failure at a rate of loading of 1 kPa/min. Fig. 6.8 shows the stress-strain, pore pressure-strain, and stress-path curves obtained from both undrained triaxial static tests C43 and C44. This figure

demonstrates that cycling causes a very small increase in strength of the soil and less development of the pore pressure. In stress-space, the shape of the stress path for static loading of sample with previous cyclic loading migrates to the right side compared to the static test without previous cycling. This stress-path moves towards the right direction, resembling the stress-path observed for highly overconsolidated soils.

It can be concluded from the test results reported in this thesis on the effect of cycling on overconsolidation of soils that, repeated loading below the CLRL, causes an increase of the overconsolidation of soils. This increase can be related to both axial strains and residual pore pressure developed under cycling.

6.5 Effect of cycling on postcyclic strength

It is well known that when the deviator stress is applied to the clay samples, there is an immediate straining of the soil and an increase or decrease in the pore pressure. As a consequence of this, a loss in strength of the soil occurs which is the most dramatic effect of cycling on the behaviour of clayey soils. The question here is whether this loss of strength can be related to the increase in axial strain, pore pressure, or to both of them. The reported data in literature indicate that the reduction in postcyclic strength is function of the amount of cyclic straining a clay sample suffered before it is loaded monotonically to failure (Thiers and Seed, 1969). Later, this strain-dependent hypothesis was confirmed by different investigators including Lee and Focht (1976), Lee (1979), and Anderson et al. (1980).

The test results obtained from both kaolinitic and crust clays demonstrate that the pattern of axial strain under cycling is quite similar for most clayey soils. However, the change in pore pressure may vary from one soil to another. Also, as explained before, the loss of strength in kaolinitic clay caused by the fluctuation of water table may be related to the strain induced in the sample during cycling. From these two reasons, it can be concluded that the reduction in postcyclic strength can be related to the axial strains that the soil sample suffer before it is loaded

monotonically to failure. It is of interest to study the reduction in postcyclic strength after identical kaolinitic clay samples are subjected to varying axial strains under cyclic loading.

Fig. 6.9 shows the results of such tests (test series S6) where postcyclic strength after loading above the CLRL was determined after the application of arbitrarily chosen strains of 1.8%, 2.9%, and 4.2% had been imposed on the samples. These strains, although arbitrarily chosen were nevertheless selected to bring the sample to the primary, secondary, and tertiary stage of the stress-strain behaviour. In each test of test series S6, after a fixed axial strain was reached, the test was stopped and the sample was taken immediately to failure under monotonic loading.

Fig. 6.9 shows that the postcyclic undrained static strength decreased as a result of increased strains on cycling. In this figure, curve 1 shows the stress-strain curve for kaolinitic clay. Curve 2 shows the postcyclic strength after the sample had been subjected to a cumulative strain of 1.78%. A loss of strength of 1.5 kPa is observed. In a similar fashion, curves 3 and 4 show postcyclic strength after cumulative cyclic strains of 2.9% and 4.2%, respectively. These postcyclic strength decrease by 5 kPa and 9.5 kPa when compared to the static strength.

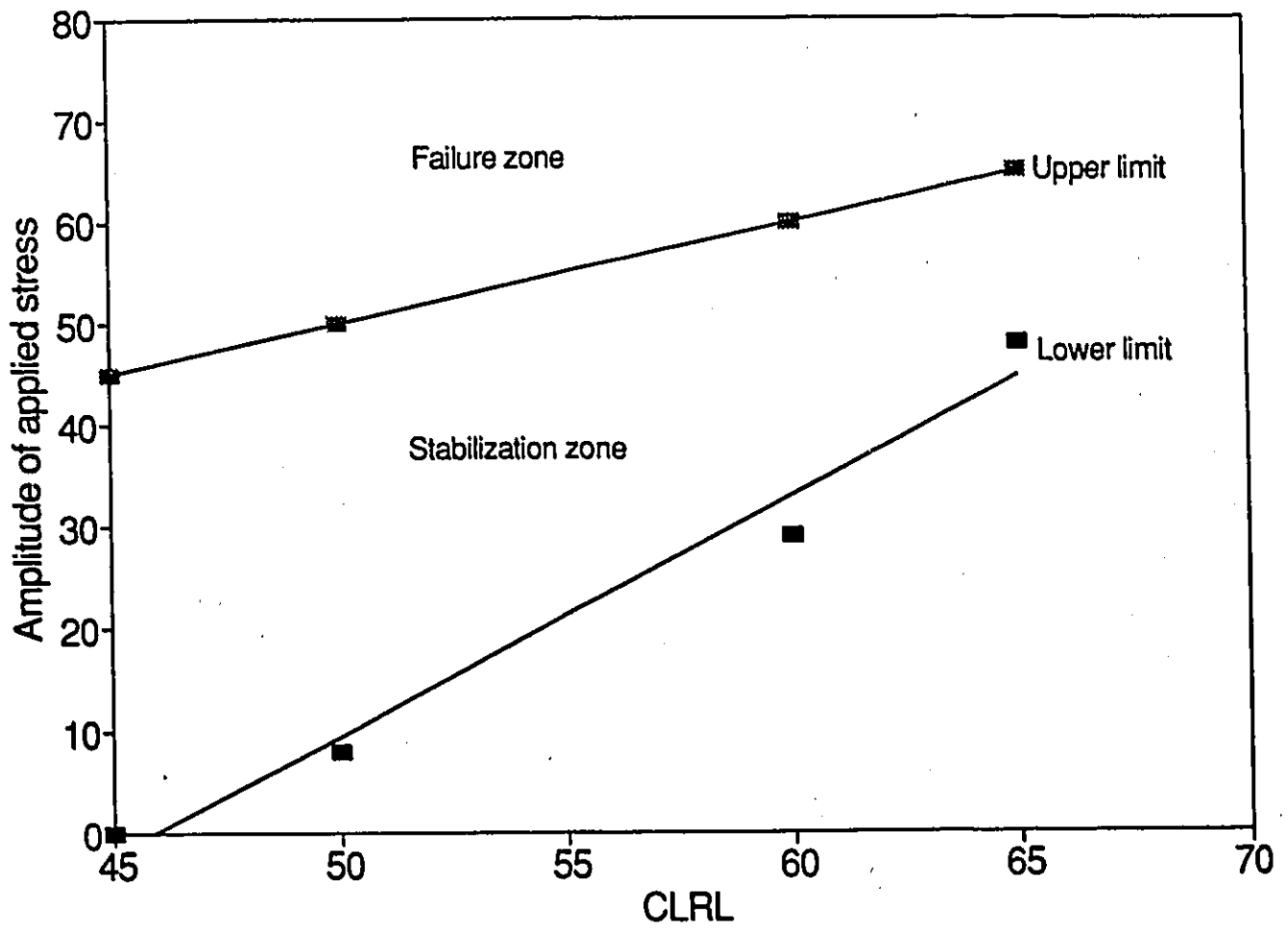


Fig. 6.1. Variation of the CLRL with the amplitude of applied stress.

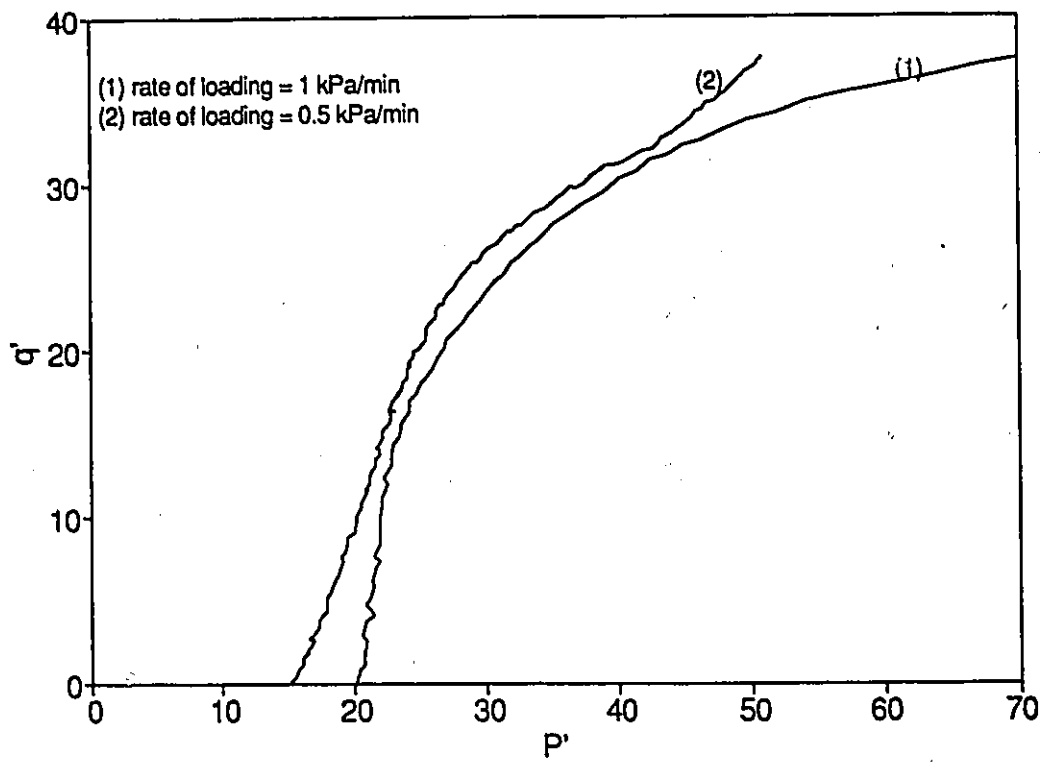
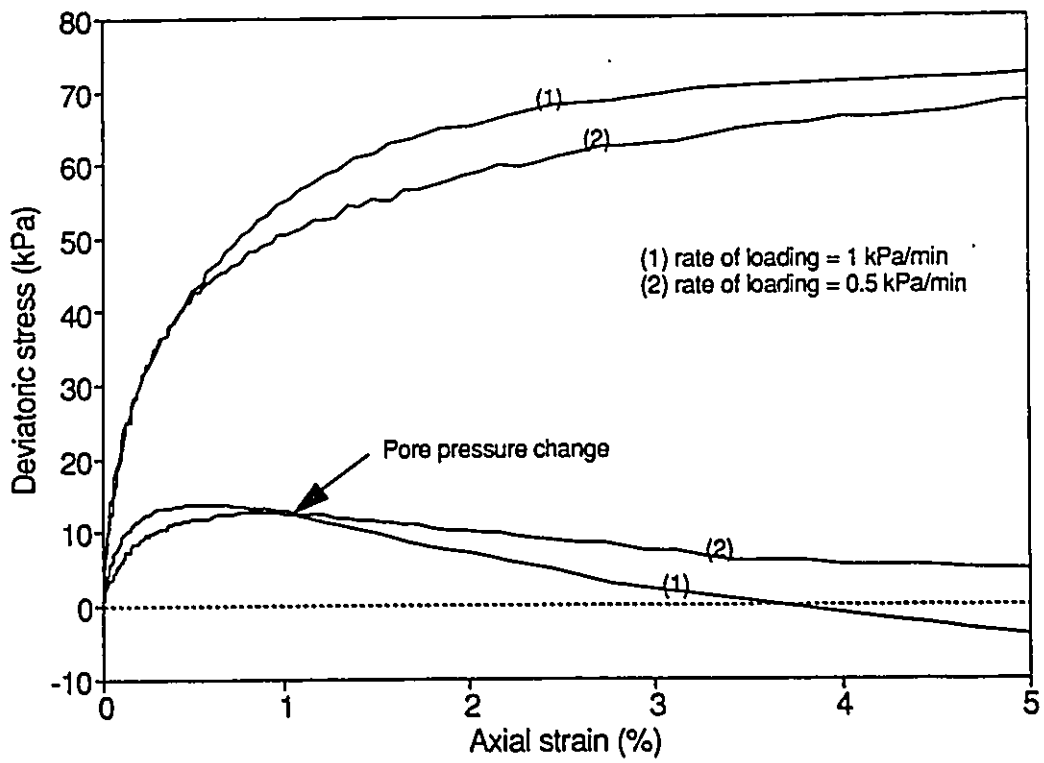


Fig. 6.2. Stress-strain, pore pressure-strain, and stress-path curves for CIUC tests under monotonic load: Tests K1 and S41.

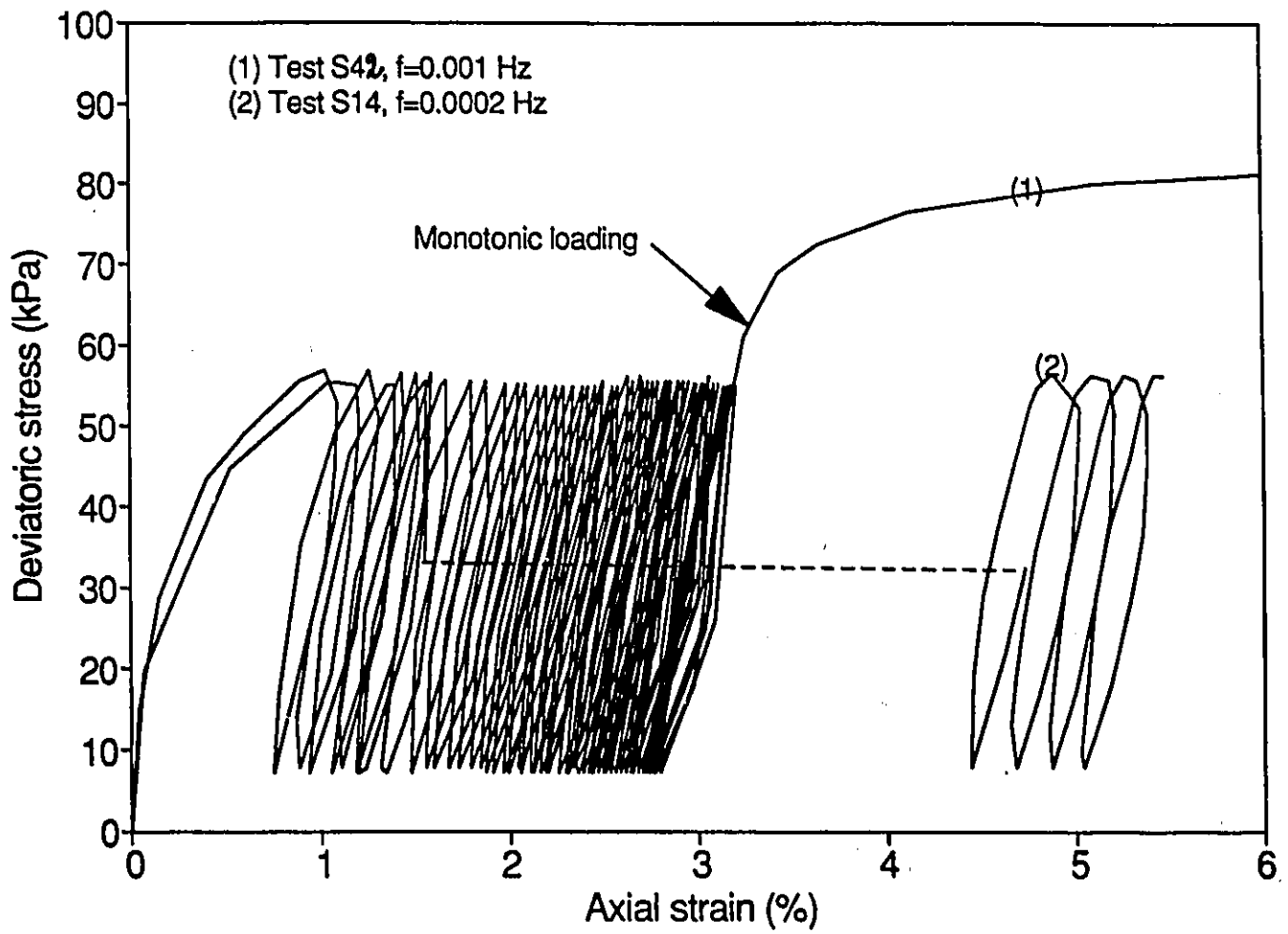


Fig. 6.3. Stress-strain curve for CIUC test under one-way repeated loading: Test S42.

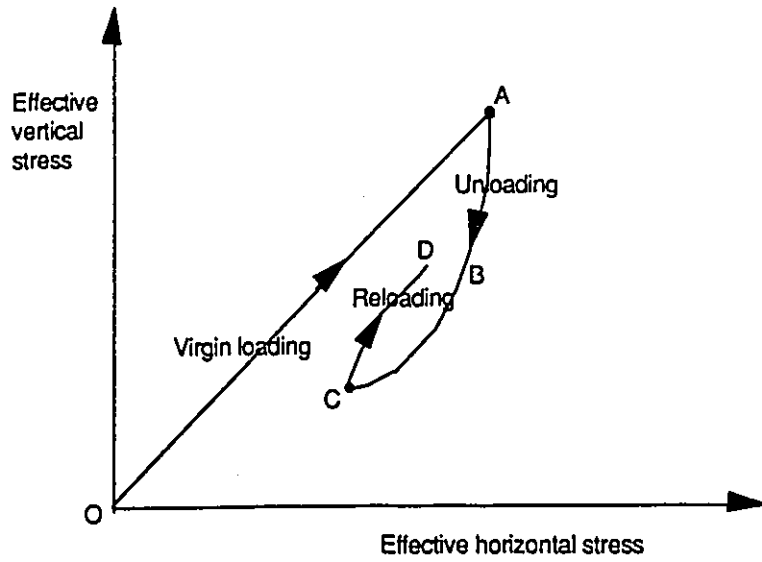


Fig. 6.4. Simplified stress history of soil subjected to fluctuation of water table.

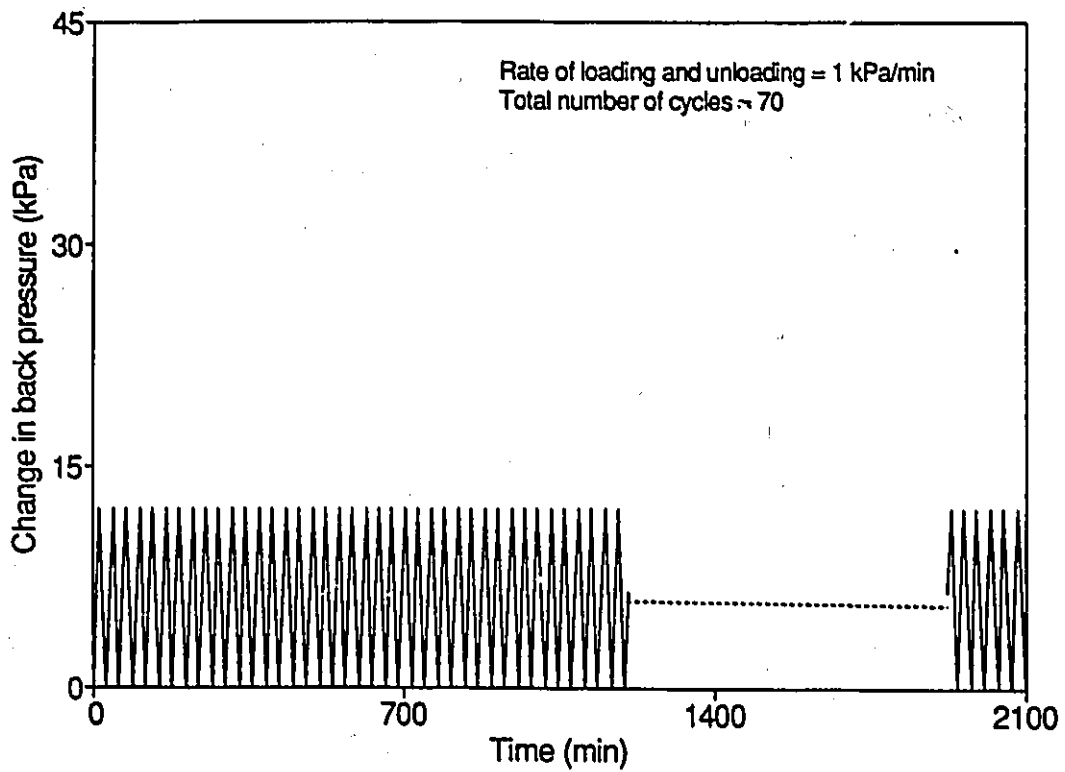


Fig. 6.5. A stress history applied to the sample S51.

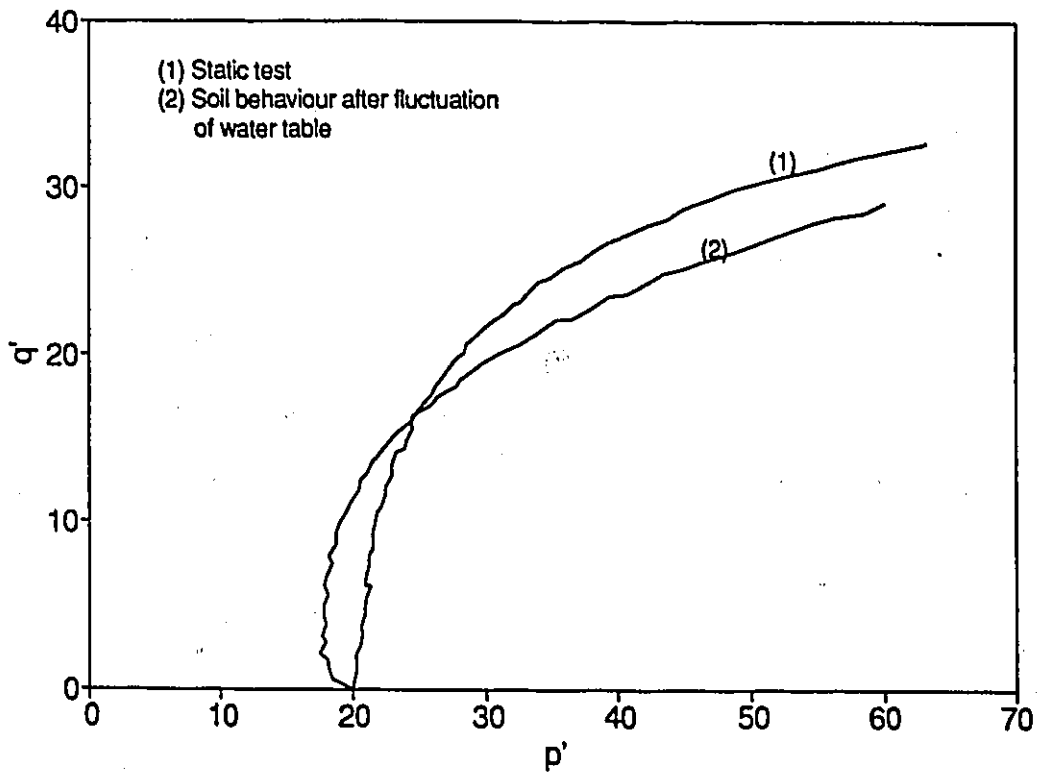
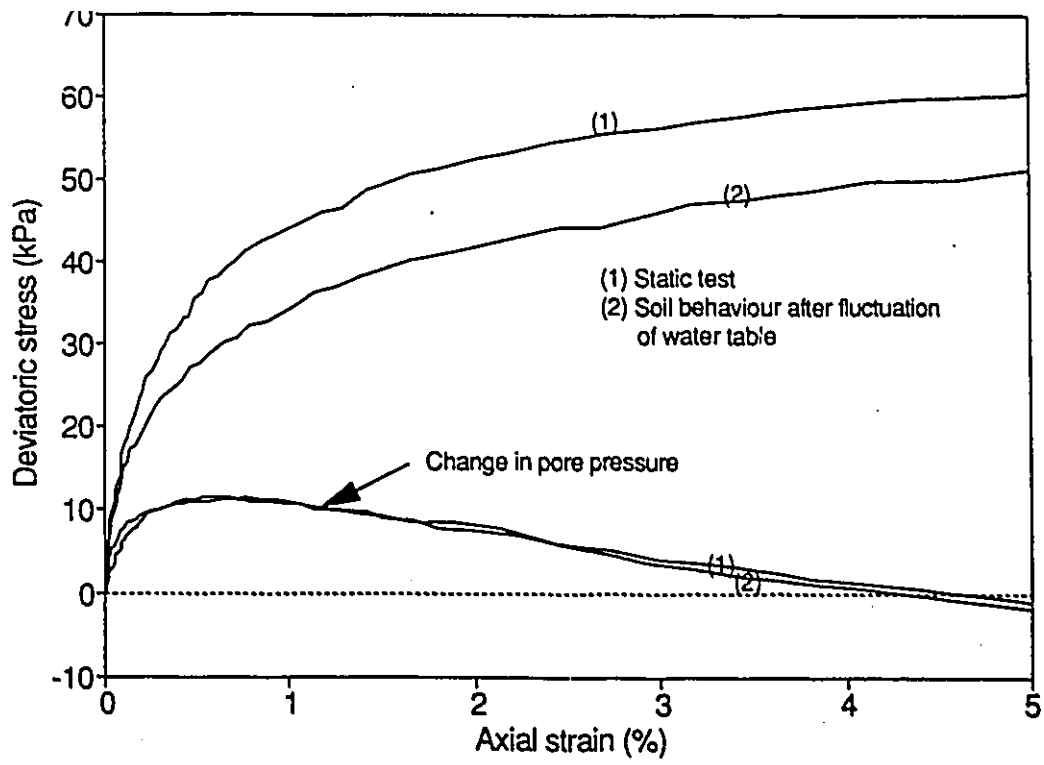


Fig. 6.6. Stress-strain, pore pressure-strain, and stress path curves for CIUC tests under monotonic load: Tests K2 and S51.

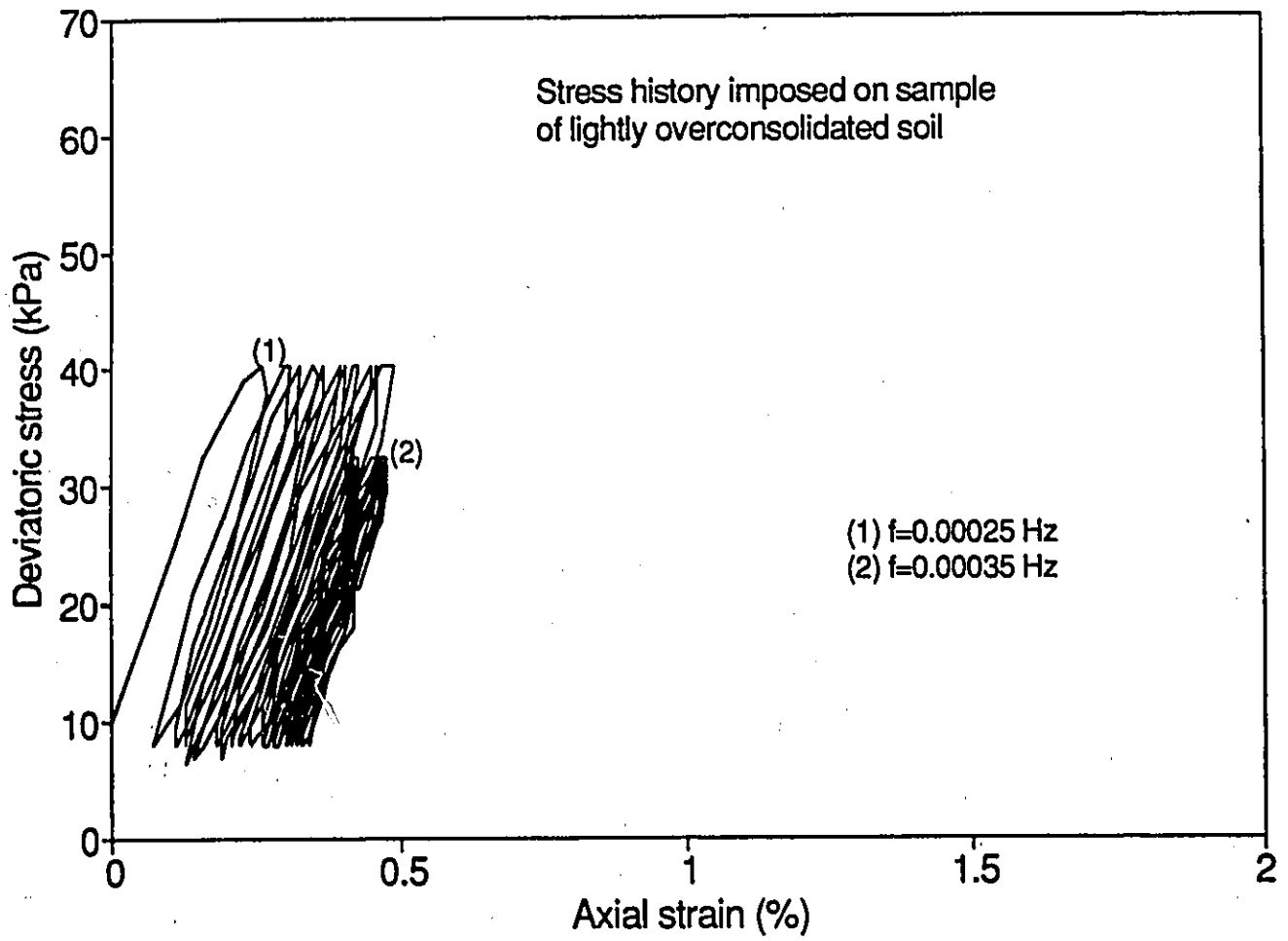


Fig. 6.7. Stress history imposed on samples C43 and C44.

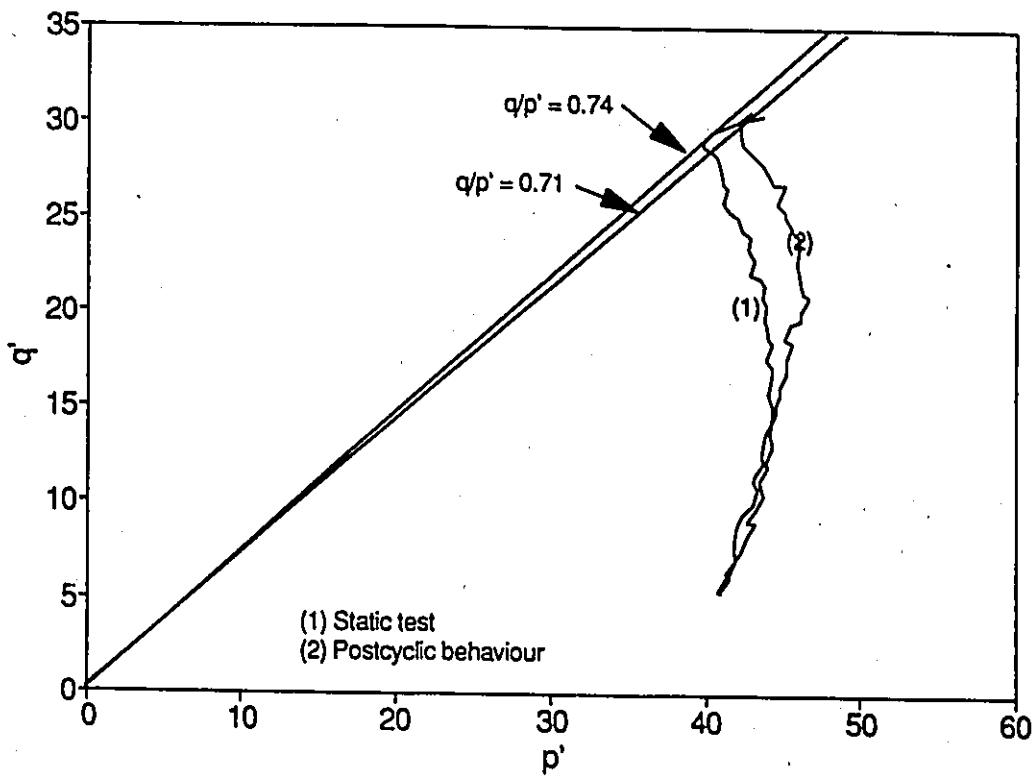
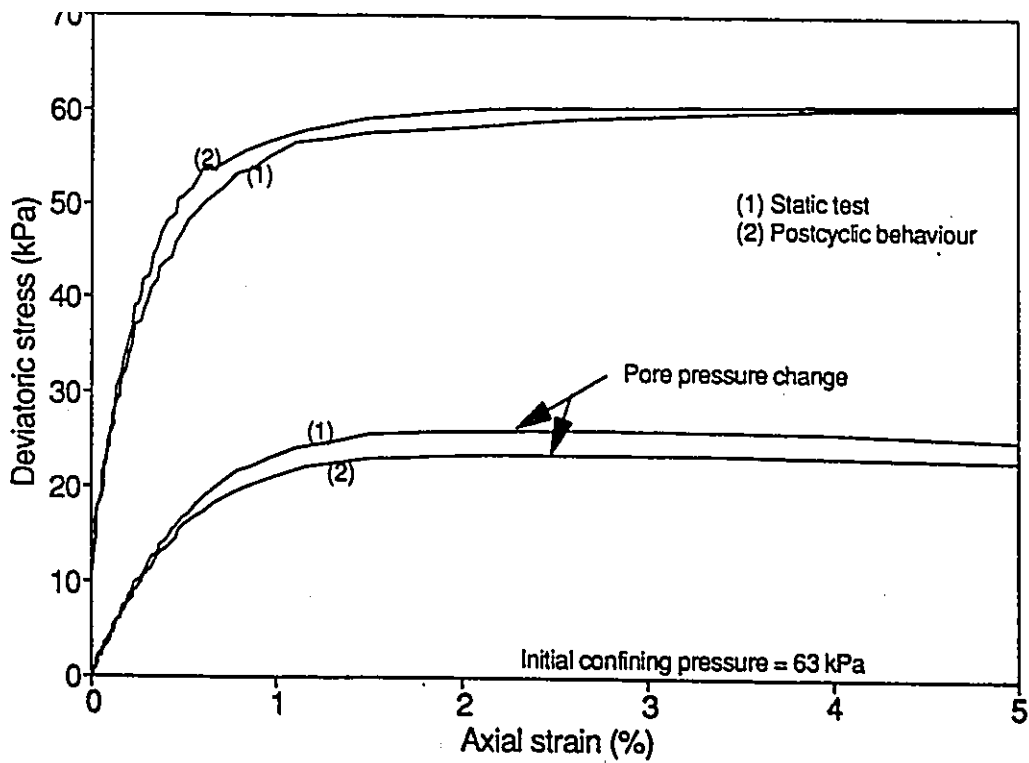


Fig. 6.8. Stress-strain, pore pressure-strain, and stress path curves for CIUC tests under monotonic load: Tests C42 and C44.

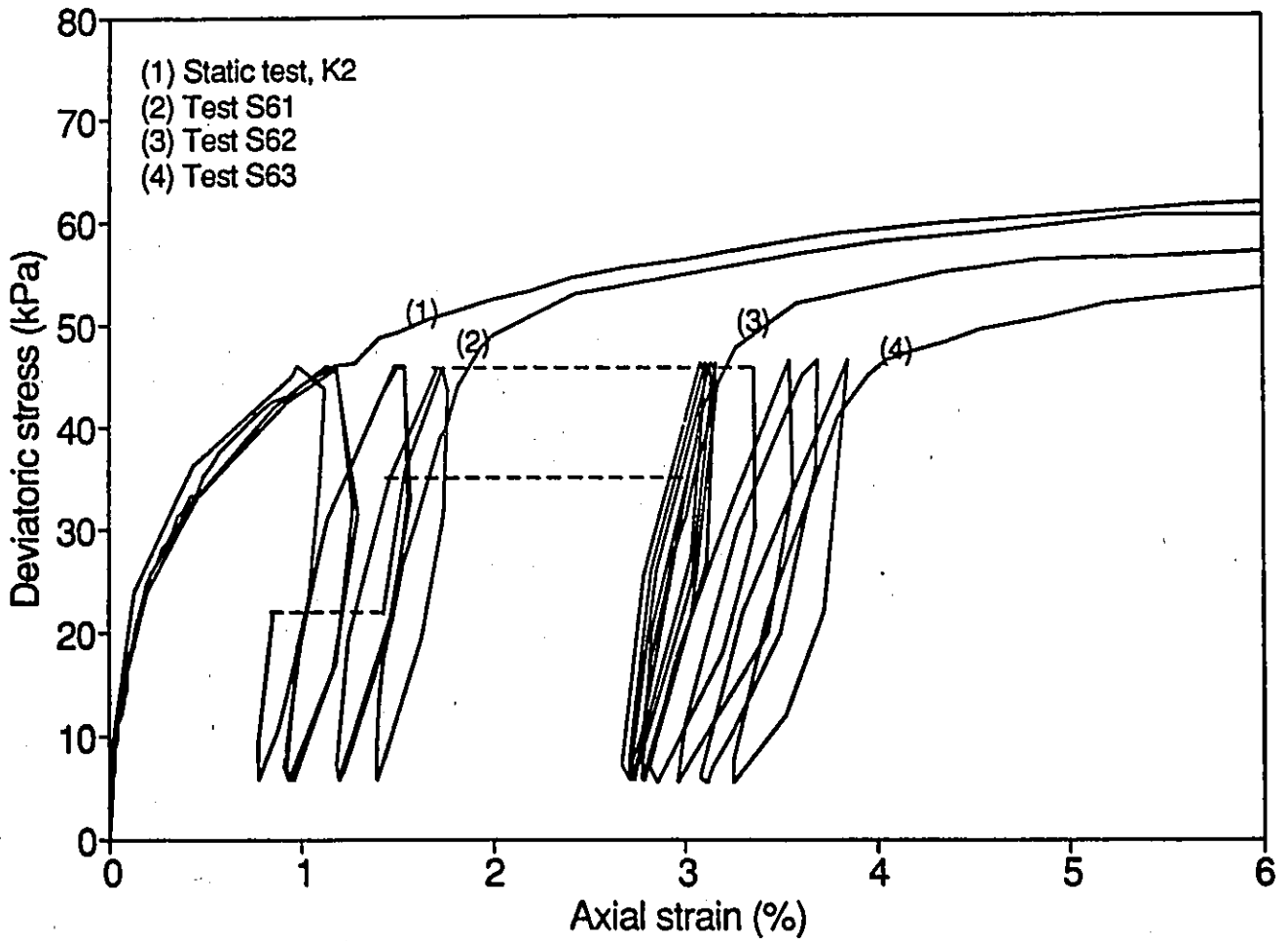


Fig. 6.9. Stress-strain curves for CIUC tests under one way repeated loading: Tests S61, S62, and S63.

CHAPTER 7

Laboratory Evaluation of K_0 for Overconsolidated Sands

7.1 Introduction

Most soil deposits are subjected to the change in geologic conditions, which are associated with sedimentation, erosional, and other processes. This change may cause an overconsolidation of the soil and makes the determination of in situ stresses difficult. However, the evaluation of the in situ stresses for these soils is necessary for variety of geotechnical problems including the problems related to deformation behaviour, excavation, foundations, and numerical analysis.

The prediction of the in situ state of stress of overconsolidated soils has been of considerable interest to soil engineers over 100 years. Tests have been conducted by a number of investigators who have employed various methods and equipment to evaluate the in situ stresses. The relationship between the vertical and horizontal effective stresses is usually expressed by the coefficient $K_0 = \sigma'_{H0} / \sigma'_{V0}$, known as the coefficient of earth pressure at rest. The evaluation of this coefficient is one of the most difficult tasks of the in situ testing. The in situ vertical effective stress can be easily estimated from a profile of effective overburden stress with depth. But the magnitude of the horizontal effective stress has remained speculative because the measurement of this stress is highly dependent on the geologic history of the soil and a reconstruction of this in laboratory is difficult. Practically, it is virtually impossible to install an earth pressure cell in situ especially for cohesionless soils, for example, without causing a densification of the sand around the cell.

Several empirical and theoretical relationships for the evaluation of K_0 for normally consolidated soils have been postulated. The most widely used relationship is a simplified version of theoretical expression (Jaky; 1948), in which $K_0 = 1 - \sin\phi'$. However, Feda (1984) raised two objections against it. But, Mayne and Kulhawy (1982) maintained its validity for cohesive soils and suggested caution only for cohesionless soils.

The determination of K_0 for overconsolidated soils is a complex problem. Using laboratory methods to predict the in situ state of stress in most natural soil deposits is impossible because they have undergone a complex stress history of loading and unloading which is difficult to reconstruct precisely. Various investigators have investigated this concept and some expressions have been proposed (e.g.; Schmidt 1966; Wroth 1975; Mayne and Kulhawy 1982). However, these expressions can not estimate K_0 exactly and still no reliable mathematical expression or laboratory method apparently exists for the evaluation of the in situ stress for these soil deposits.

This chapter presents a method for evaluation of K_0 for heavily overconsolidated sand using a stress-path triaxial apparatus. This method was proposed by Garga and Khan (1991) who applied it for overconsolidated clays. They evaluated K_0 for undisturbed samples of overconsolidated clay and examined the validity of this method by using a sample of known stress history. In this investigation, the above method is applied to samples of known stress histories of an overconsolidated sand. The effect of the change in geologic history on the estimation of K_0 by the proposed method is demonstrated and simulation of that in laboratory is undertaken by subjecting the sand samples to one and two cycles of loading at higher amplitudes of applied stresses. The rate of loading and unloading is approximately 0.05 kPa/min. This rate is slow enough to ensure full consolidation during testing. It has been found the proposed method can reproduce the imposed K_0 value.

7.2 Stress history of overconsolidated sands

A simplified stress history for a homogeneous soil deposit with horizontal ground surface is shown in Fig. 7.1. The line OA indicates the stress path due to virgin loading of the soil,

associated with sedimentation process during which the soil is normally consolidated under K_0 conditions. The stress path presented by the curve ABC indicates a reduction in the effective overburden stress due to some erosional process, excavation, etc. This reduction in overburden pressure causes an overconsolidation of the soil, in which the overconsolidated ratio ($OCR = \sigma'_{vmax}/\sigma'_v$) increases, and hence K_0 increases. If loading is reapplied to the soil due to some mechanisms such as surcharge load, the stress path will be represented by the curve CDE. This curve may be a straight line (Wroth 1975). Point E represents the in situ conditions with present stresses σ'_{110} and σ'_{v0} . The objective of the proposed method is to evaluate the in situ effective stress represented by the point E whatever is the complex stress history undergone by the soil.

7.3 The proposed method

This method was proposed by Garga and Khan (1991) who applied it for overconsolidated clay. This method is based on the concept that if an undisturbed overconsolidated soil sample is consolidated isotropically to the effective in situ vertical stress and subsequently the radial stress increased while maintaining the effective in situ vertical stress constant, the soil sample will experience significant axial strain only when the radial stress exceeds the effective in situ horizontal stress. The concept is shown in Fig. 7.2, in which the sample is first consolidated isotropically to "in situ" effective vertical stress (point F), then the effective horizontal stress is increased in drained conditions at a low rate of loading (0.05 kPa/min) while keeping the vertical stress constant. The soil sample will experience a significant axial strain only when the horizontal effective stress exceeds the effective in situ horizontal stress (point E). A typical plot $\epsilon_a - \sigma'_{11}$ plot is shown in Fig. 7.3.

7.4 Material and testing procedure

All triaxial tests described in this study were performed on crushed silica sand number 24. Particles of this sand are angular and with diameter varying between 0.1 and 1 mm. The measurement of density was not taken in consideration, and are unimportant for this investigation, since the verification of the method was carried out on soil specimens previously

subjected to known stress histories.

Drained triaxial tests were carried out on this sand under stress controlled system. The triaxial apparatus used is the one described in section 3.3. As mentioned in that section, the apparatus has the capability of applying vertical and radial stress independently to simulate different various stress paths. The stress application can be controlled by computer which is preferable for this purpose.

The preparation of the sample was undertaken by compacting a sand in different layers, each layer being 2 cm in height. Hand compaction was used to obtain overconsolidated specimen (Duncan and Seed 1986). The final dimension of the sample was 50 mm in diameter and a height to diameter ratio of two. An all-around consolidation pressure was first applied, which varied between 20 up to 250 kPa for this series of tests. This, was done to investigate the effect of confining pressure on the accuracy of the method.

Simulation of in situ stresses was undertaken by consolidating the soil sample arbitrarily to some known anisotropic stress maintaining $K_c > 1$. After full consolidation, the vertical and horizontal stresses were reduced simultaneously in drained condition to a low value of isotropic stress (generally approximately 4 kPa). Then, the sample was consolidated isotropically to the previously imposed in situ vertical stress. The test was continued fully drained by next increasing the radial effective stress while keeping the vertical effective stress constant. The rate of loading was fixed at 0.05 kPa/min which was slow enough to permit a full dissipation of excess pore pressure.

7.5 Evaluation of K_0 by the proposed method using samples of known stress histories

Normally, two different methods can be used to consolidated the soil samples to the anisotropical state in which the values of $K_c = \sigma'_h / \sigma'_v$ were greater than unity. In the first method, the soil samples are consolidated arbitrarily to some anisotropic stress state without imposing a

condition of no lateral deformation. The consolidation stresses can be applied simultaneously in horizontal and vertical directions. The final consolidation stress ratio in this case is K_c , and not K_0 .

In the second method, the soil samples are consolidated under K_0 condition to some anisotropic stress level ($K_0 > 1$). This method simulates a more realistic field stress history of an overconsolidated soil. Both these methods were applied by Garga and Khan (1991) on remoulded clay. They found that, using both these methods, the imposed in situ horizontal stress could be estimated by the proposed method accurately. Consequently, in this study only the first method was considered for verification of the technique for sands.

Soil samples were consolidated to some known anisotropic state with $K_c > 1$. After simulating a known stress history, the samples were tested to verify whether the proposed method would replicate the horizontal stress which was previously imposed.

Interpretation of test data

The sand sample was first consolidated anisotropically to an arbitrary imposed in situ stresses σ'_{HP} and σ'_{VP} . The stress path for this anisotropically consolidation is the straight line OE, as shown in Fig. 7.2. After full consolidation, both imposed in situ stresses were reduced simultaneously to some low isotropic stresses (6 kPa) with a measured negligible horizontal radial strain less than 0.05%. By consolidating the sample isotropically to the imposed in situ effective vertical stress, point F in Fig. 7.2, and continuing the test fully drained by increasing the radial stress while keeping the vertical one constant.

The results of 5 tests consolidated under a different anisotropic stresses ($K_c > 1$), are presented in Table 7.1. In these tests, each sample was consolidated anisotropically to values of K_c that varied from 1.2 to 3.6. Test plots of axial deformation and effective horizontal stress indicate that the measured horizontal stress replicated the imposed the "in situ" horizontal stress exactly, as shown in Figs 7.4(a) to (e).

7.6 Effect of the change in geologic conditions on the estimation of K_0 by the proposed method

Most soil deposits are subjected to the change in geologic conditions, which are associated with sedimentation, erosional, and other processes. This change causes an overconsolidation of the soil and makes the determination of in situ stresses difficult. The applicability of the proposed method to measure K_0 for these soil deposits is investigated. The technique used to simulate the change in geologic conditions in laboratory is by subjecting soil samples to one and two cycles of loading. The rate of loading and unloading was slow enough and around 0.05 kPa/min to ensure a full consolidation during testing. In fact, one cycle of loading represents only one series of sedimentation and erosional process. However, two cycles may represent a more complex stress history of the soil.

7.6.1 One cycle of loading:

Two drained triaxial tests R1S01 and R1S02 were carried out in which the sample was consolidated first along the stress path presented by the line OA in Fig. 7.5. Unloading was continued from point A to E. After full consolidation, the imposed in situ stresses were reduced to some isotropic low stress (6 kPa). By consolidating the sample isotropically to the imposed "in situ" effective vertical stress and by applying the proposed method, it is found that the sample experienced significant axial strain only when the horizontal stress exceeds the "in situ" horizontal stress presented by point E.

Test results

The results of tests R1S01 and R1S02 are presented in Table 7.2. Fig. 7.6 shows σ'_v versus σ'_{H1} , σ'_v versus axial strain, and σ'_{H1} versus axial strain during loading and unloading for the test R1S02. This figure indicate that, the sample was consolidated to a maximum value of $\sigma'_v=162.1$ and $\sigma'_{H1}=123.4$ kPa. During this loading stage, only an axial strain of 0.17% was developed. After that, the sample was unloaded to an effective state of stresses of $\sigma'_{vp}=38.7$ and $\sigma'_{HP}=63$ kPa.

These values are the imposed "in situ" effective stresses on the sample. At the end of unloading only 0.03% of axial strain remained in the soil sample. After complete consolidation at the imposed "in situ" stress condition, the effective stresses were reduced to some low isotropic stresses (6 kPa). By next consolidating isotropically the sample to the imposed in situ vertical effective stress ($\sigma'_{vp}=38.7$) and by applying the proposed method, the value of the effective in situ horizontal stress estimated from the proposed method was found equal to 61.5 kPa. Similar behaviour was observed on test R1S01.

The test results for both tests R1S01 and R1S02 are summarised in Table 7.2 and plotted in Fig. 7.7. These results demonstrate that the proposed technique can replicate the "in situ" stresses irrespective of the stress imposed by the initial cycle of loading.

7.6.2 Two cycles of loading:

In order to further explore the validity of the technique, two tests R2S01 and R2S02 were conducted with different previously imposed stress conditions. In test R2S01, the sample was consolidated along stress path OABCE as shown in Fig. 7.8(a). The imposed in situ effective vertical stress at point B is lower than that at point E. In the test R2S02, the sample was consolidated along stress path OABCE (Fig. 7.8(b)), where the imposed in situ effective vertical stress at point B is higher than at point E. After complete consolidation at stress state E, the imposed in situ stresses in both samples were reduced to some low isotropic stress (8 kPa). By consolidating isotropically both of the samples to the imposed in situ vertical stresses and by applying the proposed method, it is found that both samples experience axial extension strain only when the effective horizontal stress exceeds the in situ horizontal stress imposed at point E.

Test result

The results tests R2S01 and R2S02 are presented in below. Figs 7.9 and 7.10 shows σ'_v versus σ'_H , σ'_v versus axial strain, and σ'_H versus axial strain during loading and unloading for the tests R1S02 and R2S02, respectively. For the test R2S01, in the first cycle of loading, the sample was

consolidated to a maximum state of stress in which $\sigma'_v=140.3$ and $\sigma'_{11}=106.1$ kPa. During this stage, an axial strain of 0.15% was developed in the sample. After that, the sample was unloaded to the first imposed stress ($\sigma'_{vp1}=30.6$ and $\sigma'_{11p1}=51.9$ kPa). In the second cycle of loading, the sample was consolidated to a maximum value of $\sigma'_v=221$ and $\sigma'_{11}=180.1$ kPa. Due to this second cycle, the axial strain increases with σ'_v and a total axial strain of 0.2% was measured. Then, the soil sample was unloaded to a state of stress where $\sigma'_{vp2}=48.8$ and $\sigma'_{11p2}=80.5$ kPa. These values are the imposed "in situ" stresses. The summary of the test results (R2S01 and R2S02) is given in Table 7.3 and plotted in Fig. 7.11. These results again demonstrate that the proposed technique is capable of estimating K_0 of an overconsolidated soil irrespective of the previously imposed stress history.

7.7 Conclusions

The main conclusions of this chapter may be summarized as follows:

- (1) The test results of this study demonstrate that the proposed method can predict the imposed in situ stresses exactly.
- (2) The proposed method can be applied for both lightly overconsolidated soil (K_0 slightly greater than unity) and heavily overconsolidated soil.
- (3) The proposed technique is capable of estimating K_0 of an overconsolidated soil irrespective of the previously imposed stress history.

Table 7.1. Artificially prepared samples with simulated in situ stress state.

Simulated anisotropic consolidation			Evaluation by the proposed method		
Sample number	σ'_{vp} (kPa)	σ'_{hp} (kPa)	K_c	σ'_{hp} (kPa)	K_c
S01	125.6	150.8	1.20	149.1	1.19
S02	133.2	179.2	1.35	181.8	1.37
S03	84.2	137.8	1.64	135.4	1.61
S04	20.3	51.6	2.54	50.2	2.47
S05	21.4	75.8	3.54	74.7	3.49

Table 7.2. Estimation of the imposed in situ stress state for artificially prepared samples subjected to one cycle of loading.

sample number	Normally consolidated K_c loading			K_c unloading to simulate in situ condition			Proposed method	
	σ'_v (kPa)	σ'_H (kPa)	K_c	σ'_{vp} (kPa)	σ'_{HP} (kPa)	K_c	σ'_{HP} (kPa)	K_c
R1S01	133.1	91.4	0.69	21.2	36.1	1.70	37.4	1.76
R1S02	162.1	123.4	0.76	38.7	63.0	1.60	61.5	1.69

Table 7.3. Estimation of the imposed in situ stress state for artificially prepared samples subjected to two cycles of loading.

Sample Number	normally consolidated K_c loading (O-A)		K_c unloading to (B)		Normally consolidated K_c loading (B-C)		K_c unloading to simulated in situ condition (E)		Proposed method	
	σ'_v (kPa)	σ'_{H1} (kPa)	σ'_{VP1} (kPa)	σ'_{HP1} (kPa)	σ'_v (kPa)	σ'_{H1} (kPa)	σ'_{VP2} (kPa)	σ'_{HP2} (kPa)	σ'_{HP} (kPa)	K_c
R2S01	140.3	106.1	0.76	51.9	221	180.1	48.8	80.5	81.6	1.67
R2S02	153.7	112.9	0.73	60.1	207.8	139.0	36.6	71.0	71.5	1.95

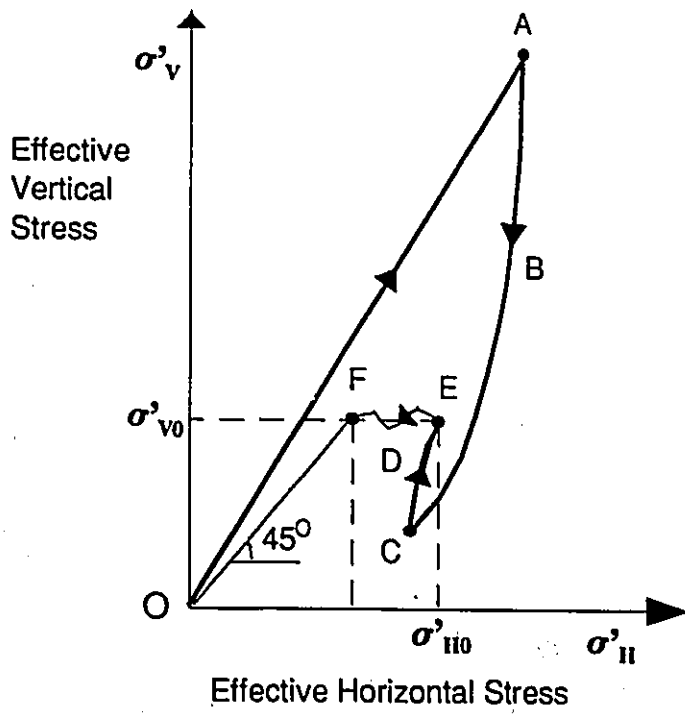


Fig. 7.1. Simplified stress history of overconsolidated soils.

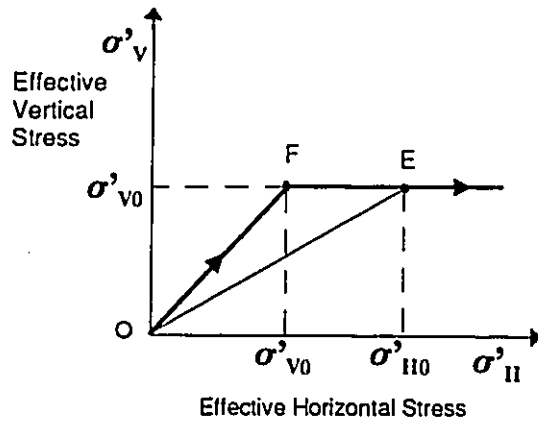


Fig. 2. The concept of Garga and Khan (1991) method.

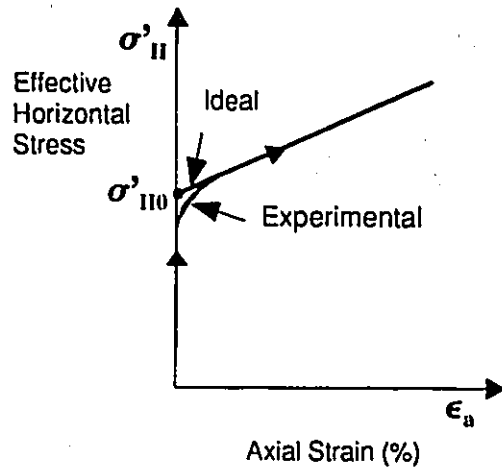


Fig. 7.3. Ideal and experimental ϵ_a - σ'_H plot (after Garga and Khan 1991).

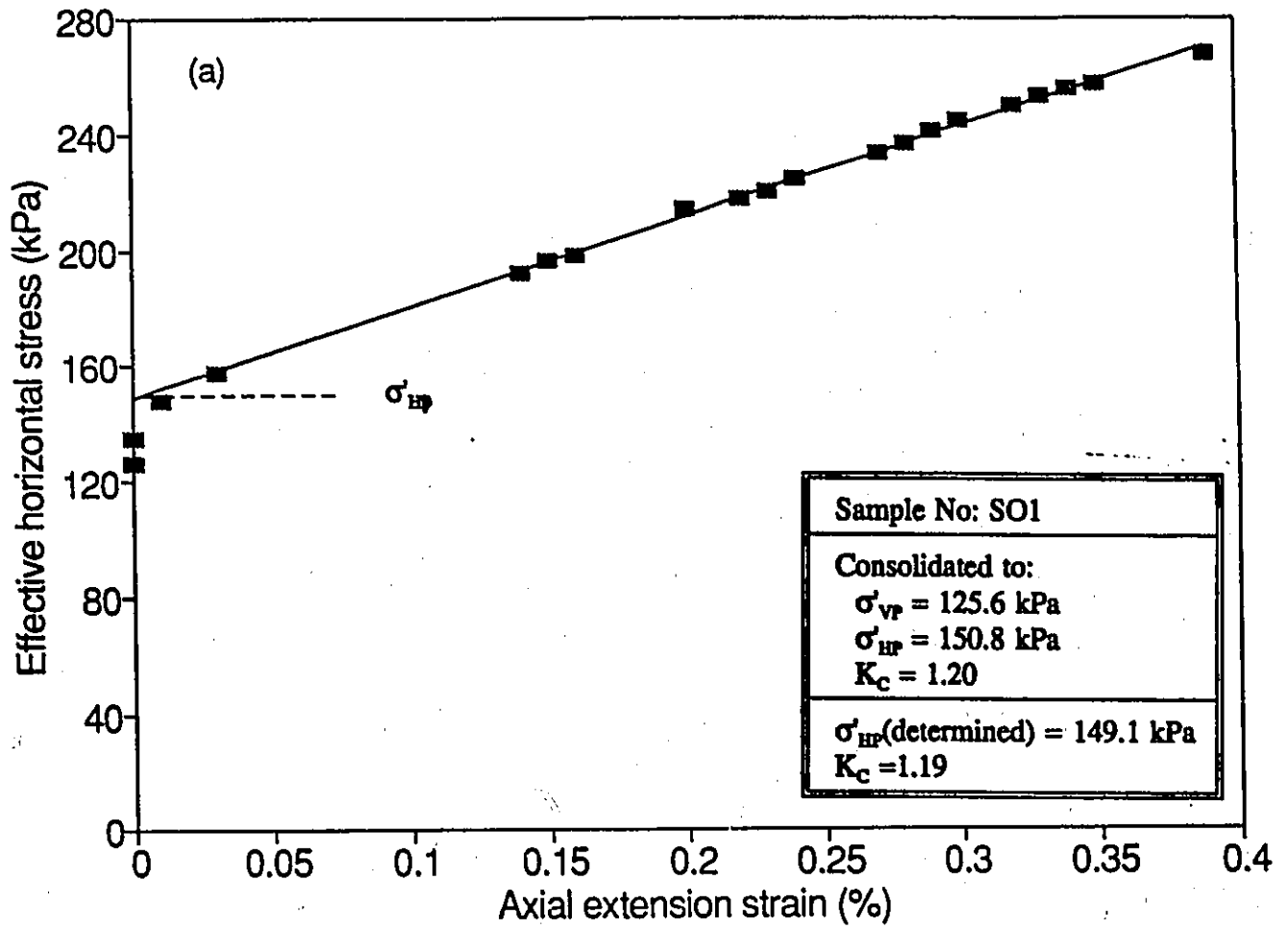


Fig. 7.4(a). K_c determination.

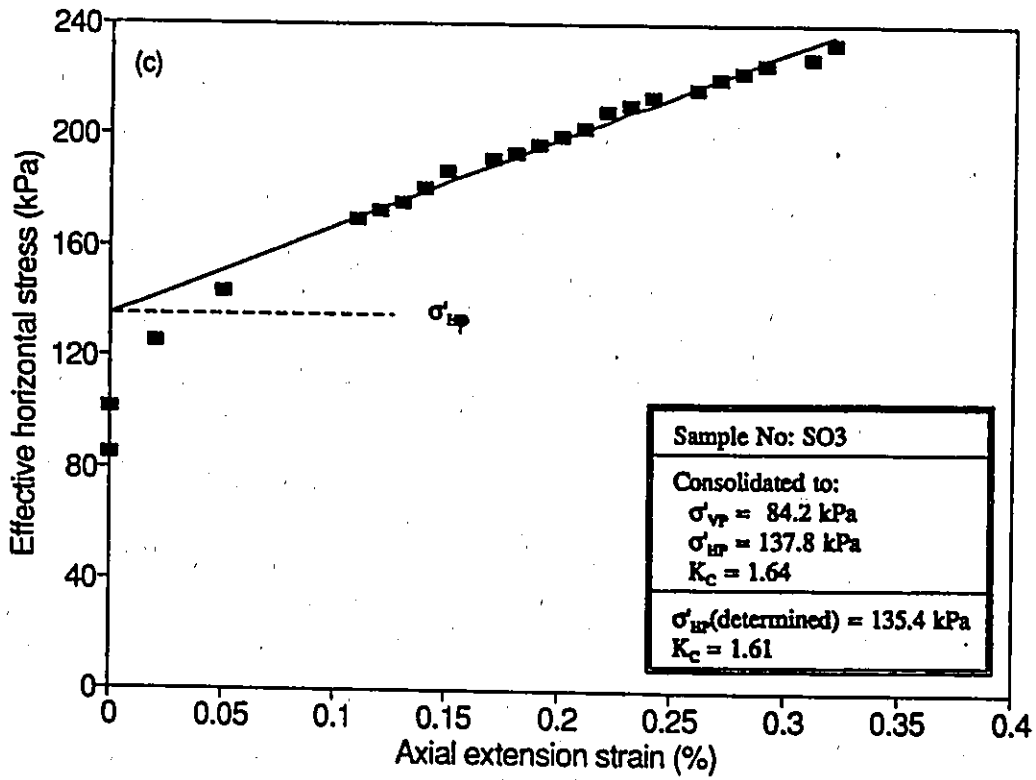
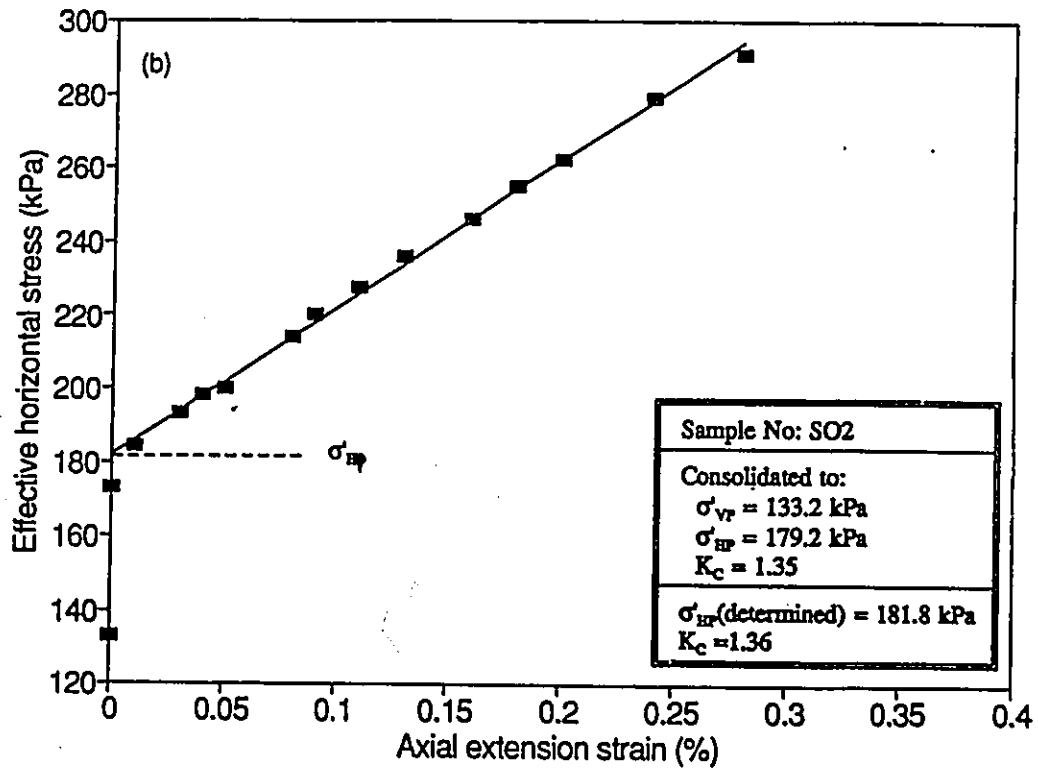


Fig. 7.4(b) and (c). K_c determination.

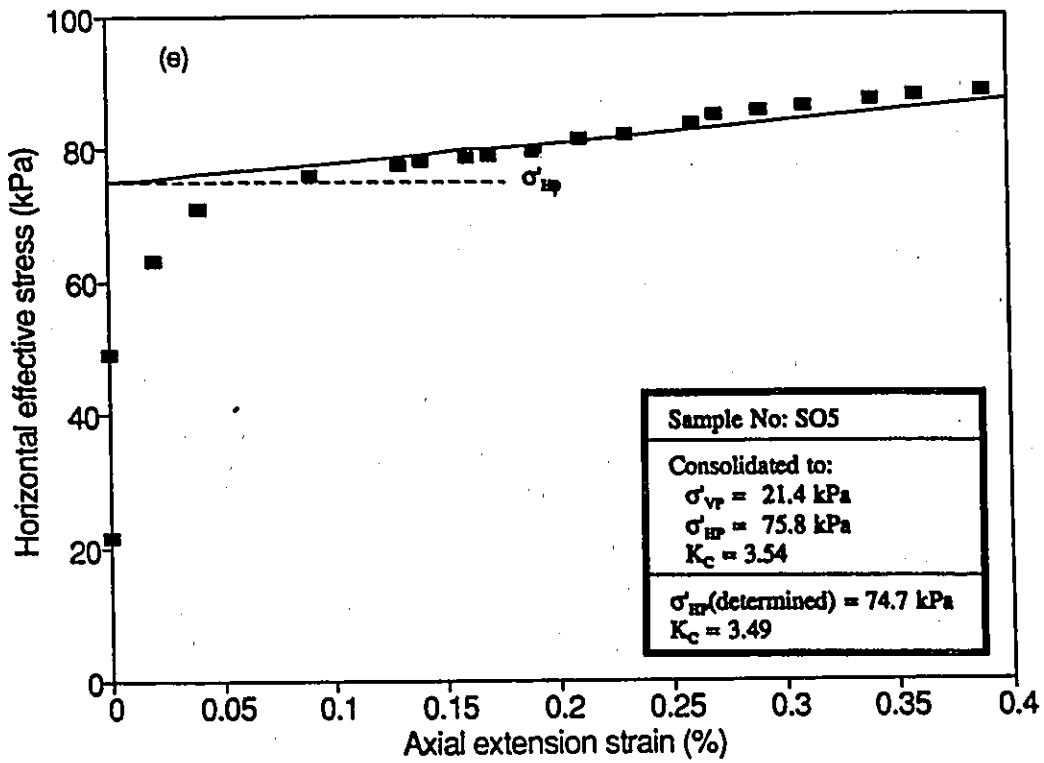
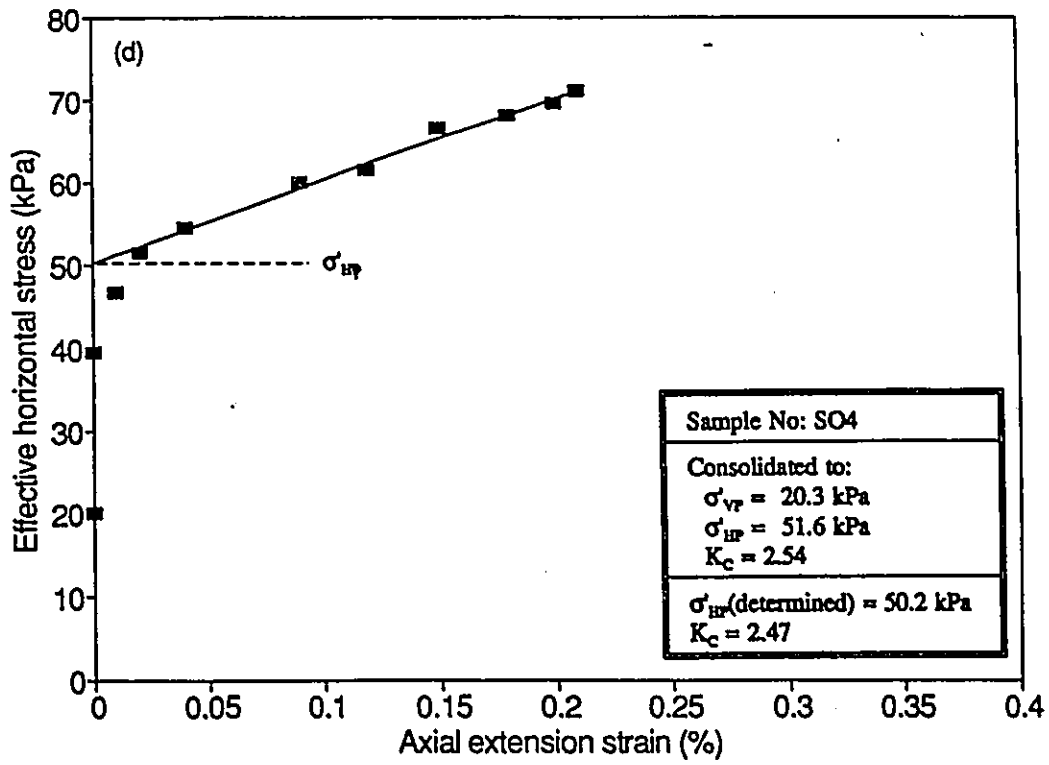


Fig. 7.4(d) and (e). K_c determination.

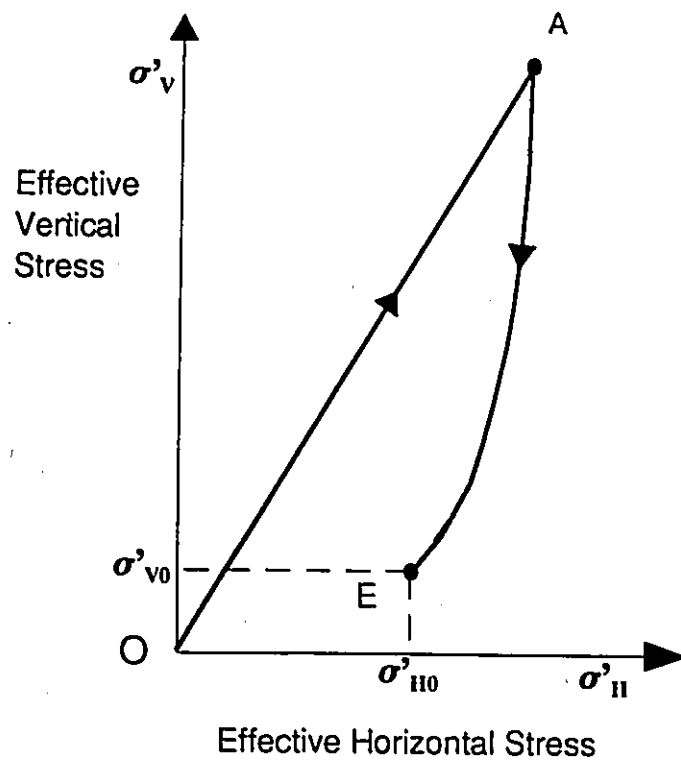


Fig. 7.5. Representation of the stress history (loading and unloading).

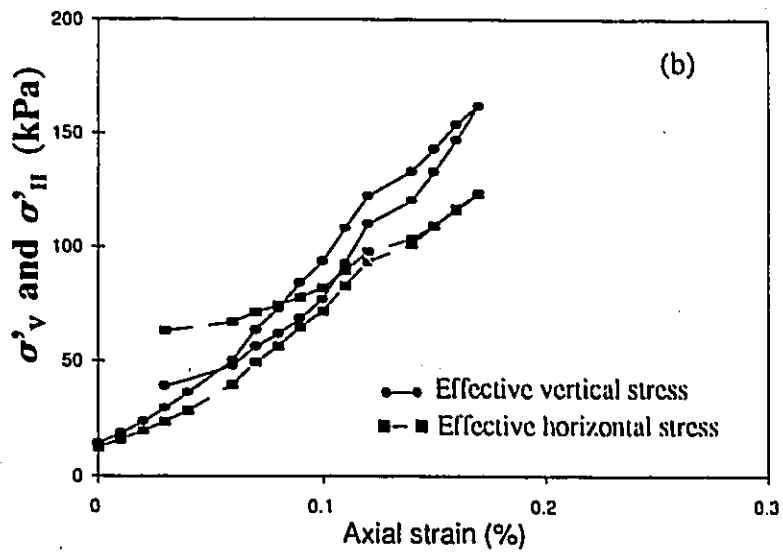
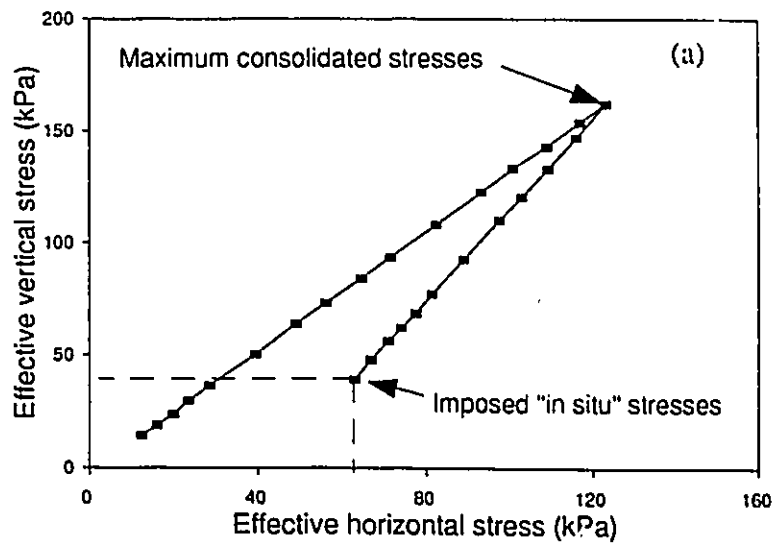


Fig. 7.6. σ'_v - σ'_H , σ'_v - ϵ_a , σ'_H - ϵ_a plots for the test R1S01.

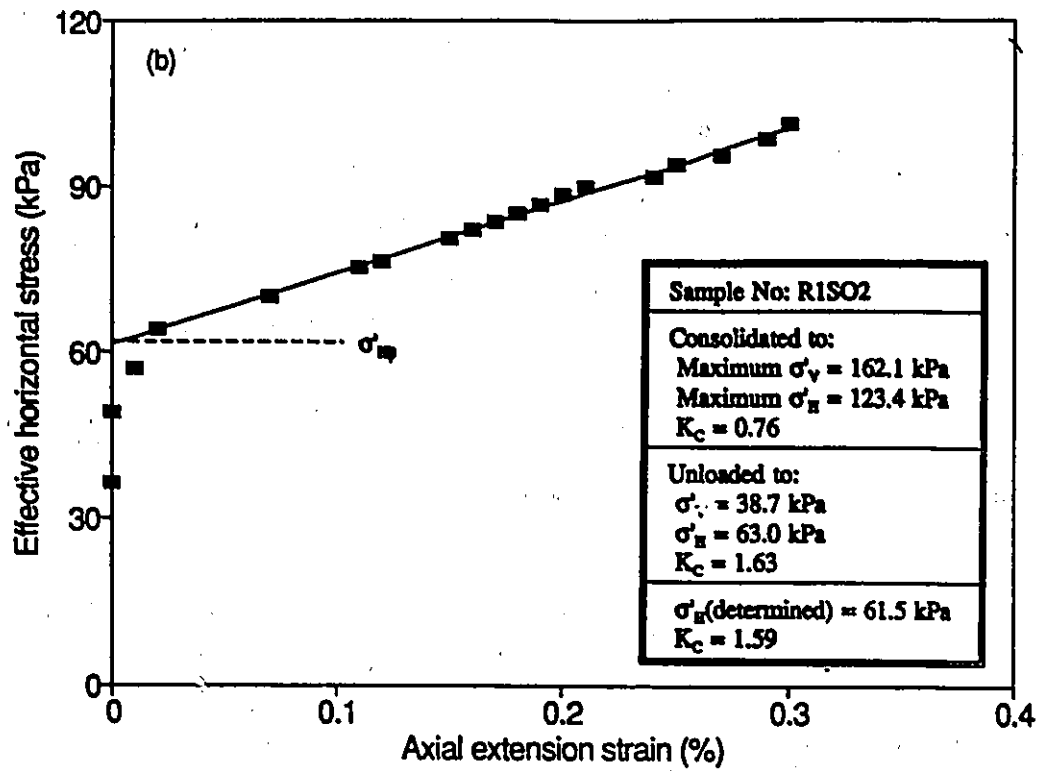
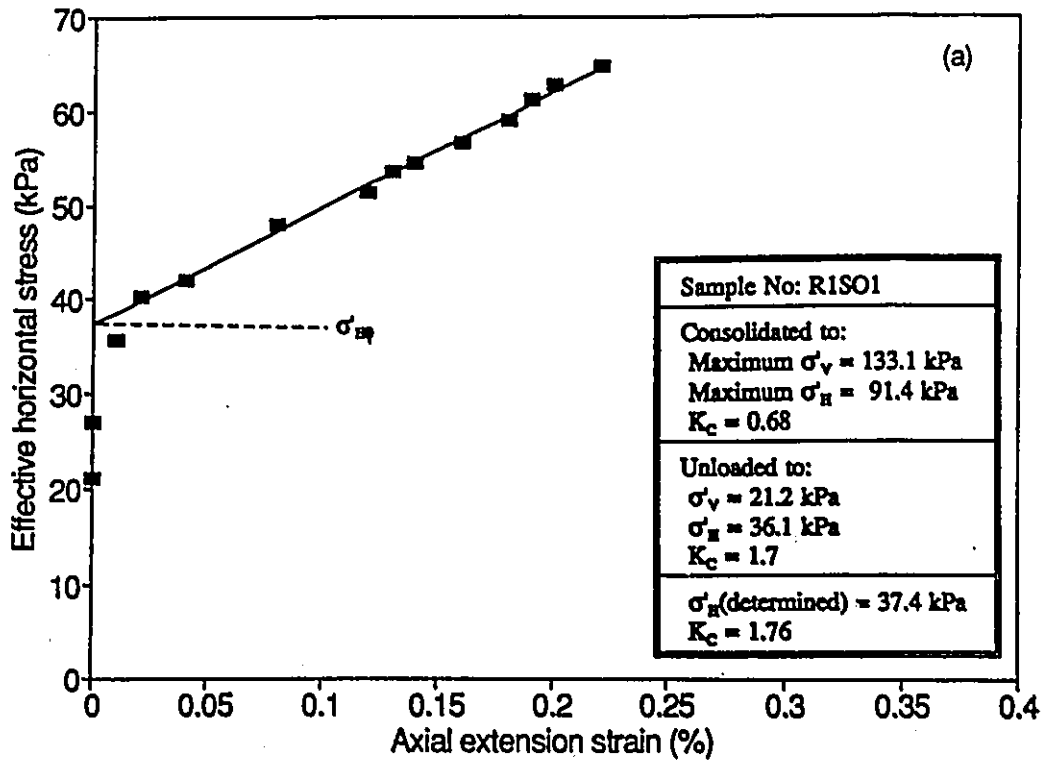


Fig. 7.7. K_c determination after loading and unloading.

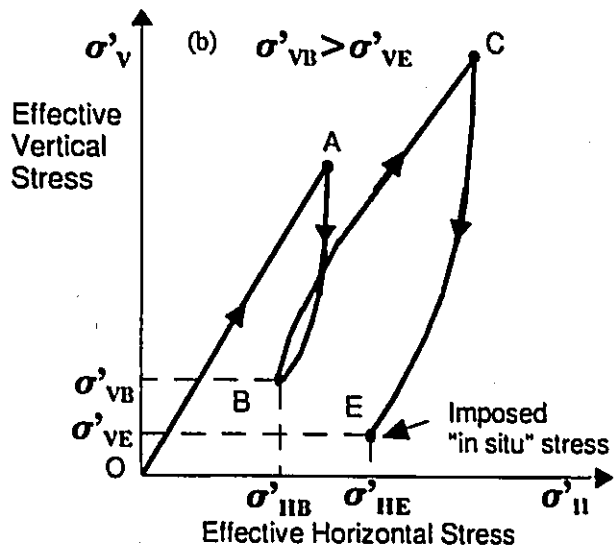
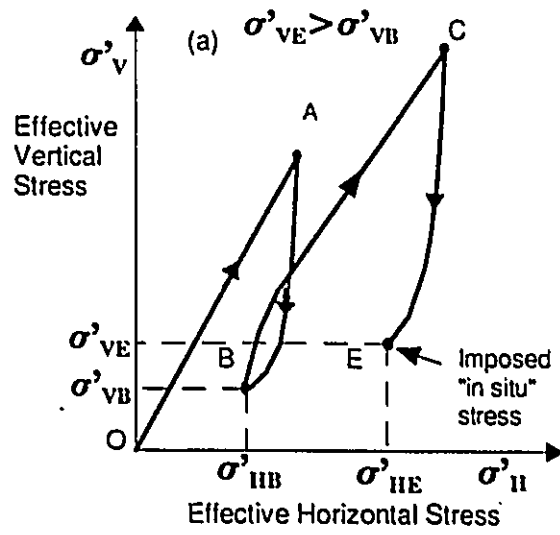


Fig. 7.8(a) and (b): Representation of the stress history (two cycles of loading) for the tests R2S01 and R2S02, respectively.

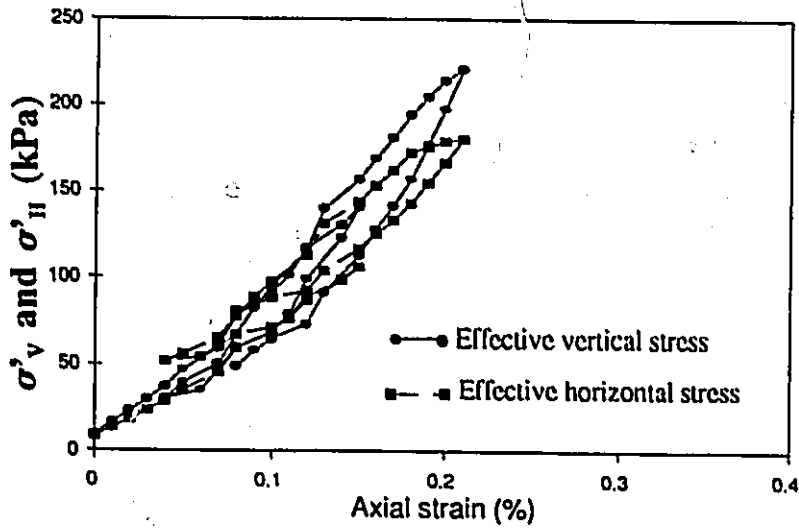
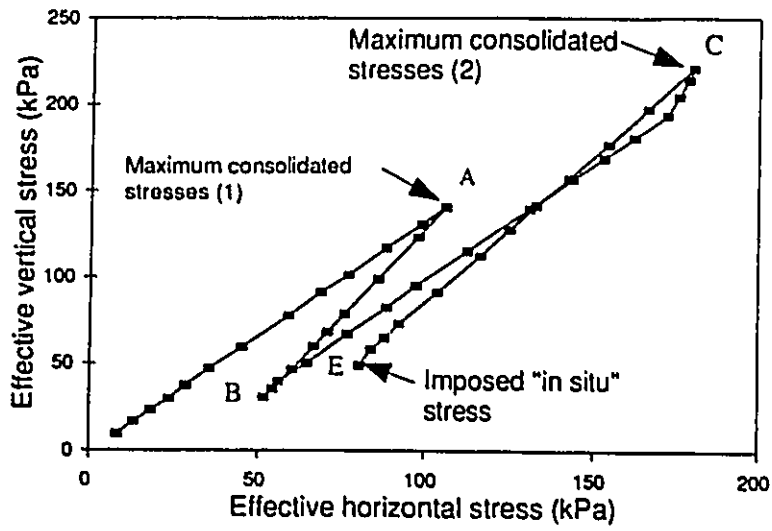


Fig. 7.9. σ'_v - σ'_H , σ'_v - ϵ_a , σ'_H - ϵ_a plots for the test R2S01.

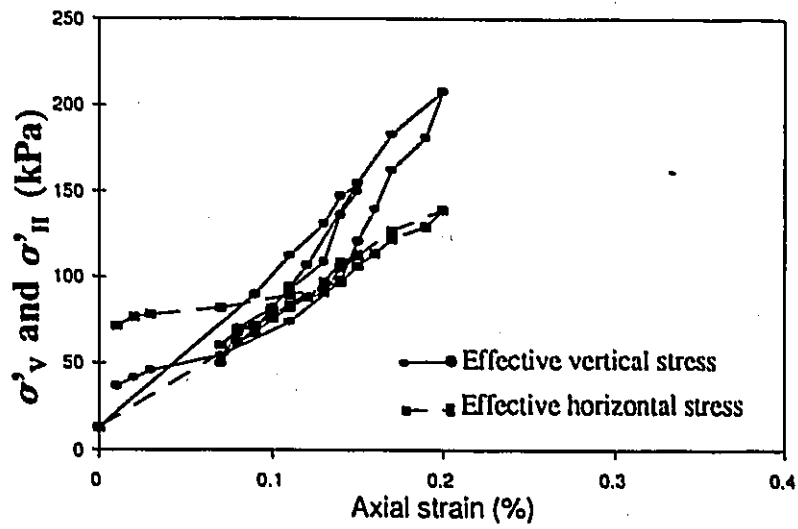
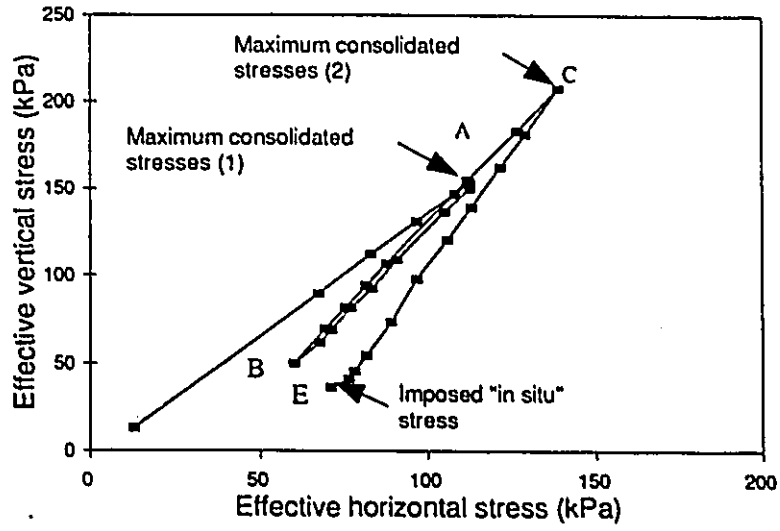


Fig. 7.10. σ'_v - σ'_H , σ'_v - ϵ_a , σ'_H - ϵ_a plots for the test R2S02.

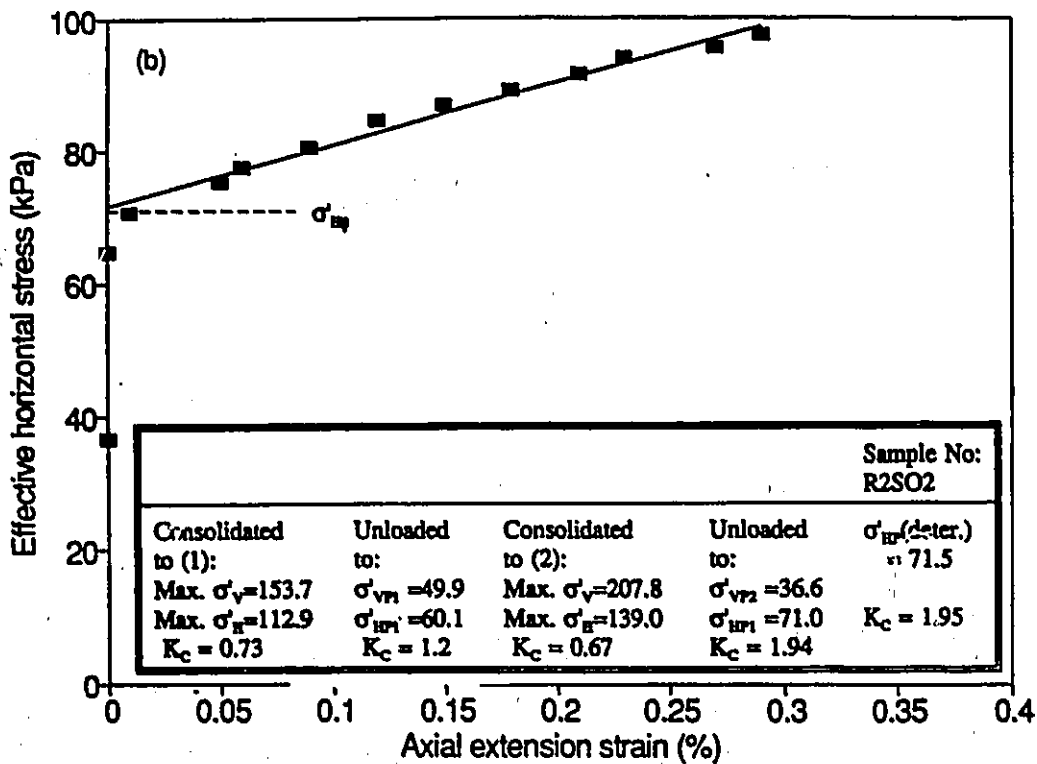
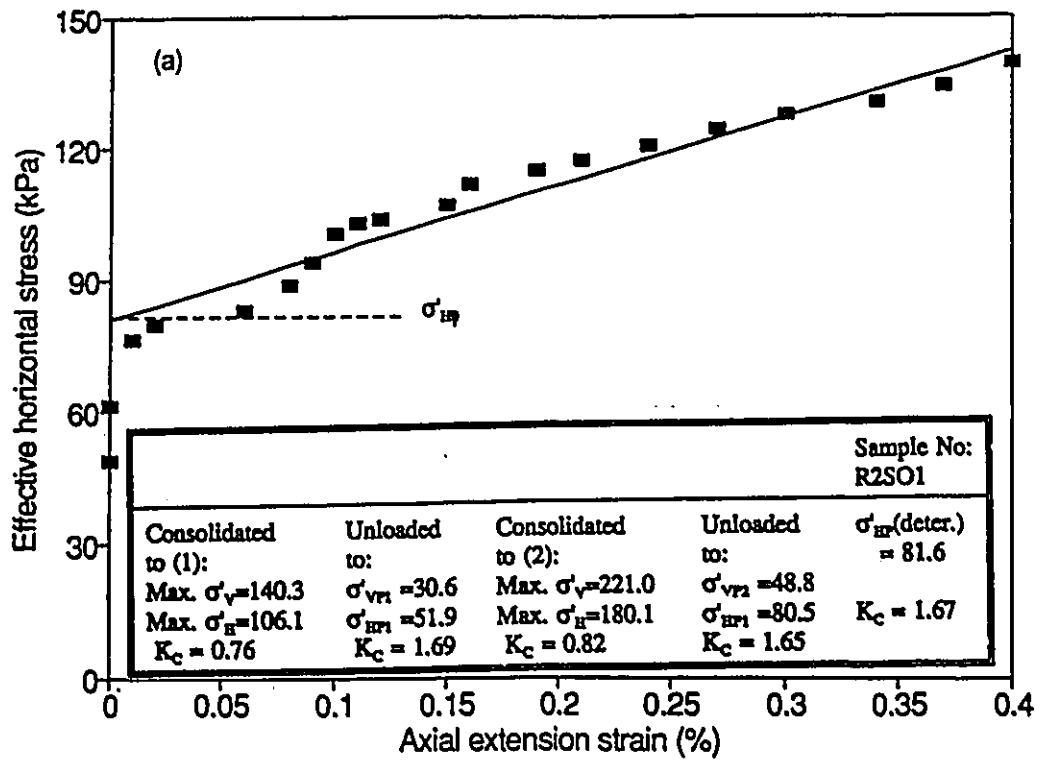


Fig. 7.11. K_C determination after two cycles of loading.

CHAPTER 8

Conclusions and Recommendations

8.1 Conclusions

The conclusions drawn from this experimental research are:

- (1) For a specific amplitude of applied stress, a CLRL was evaluated for both kaolinitic and clayey crust soils. This CLRL was approximately 70% of the original undrained shear strength for kaolinitic clay and 60% for clay crust.
- (2) The development of the axial strain under repeated loading in most of the soils is quite similar. Below the CLRL, cycling always causes a small change in axial strain before the equilibrium conditions are reached. The magnitude of this strain depend on the cyclic stress ratio used and the OCR of the material. Above the CLRL, the rate of development of axial strain increases with cycling until failure is reached.
- (3) The development of the pore pressure under repeated loading depend on the stress history of the soil:
 - For the kaolinitic clay, the behaviour of the change in pore pressure is similar to the behaviour of change in axial strain. It was observed when cycling at CSR higher than the CLRL, the soil shows a higher negative pore pressure at failure compared to the static test.

- If cycling in the clay crust is at lower levels of CSR (below CLRL), more than 90% of the total pore pressure that can develop in the soil sample will develop in this stage. The more cycles the sample is subjected to, the higher the developed pore pressure. The stress path moves beyond the monotonic loading effective stress failure envelope. Values of q/p' at failure for these samples are not equal. Cycling only above the CLRL produces the same pore pressure as the one measured in the static test. The identical failure envelope for these samples is bounded by monotonic loading effective stress failure envelope.

(4) The behaviour of kaolinitic clay under cycling (below CLRL) can be described by some empirical equations which are a function only of the amplitude of the applied stress. However, cycling only above the CLRL, the behaviour of this clay can be divided in three stages:

- Primary stage: characterized by strain and pore pressure development at a decreasing rate.
- Secondary stage: characterized by strain and pore pressure development at a constant rate.
- Tertiary stage: characterized by axial strain and pore pressure development at an accelerating rate.

(5) Cumulative axial strain measured at equilibrium conditions were generally less than 3% for kaolinitic clay and 0.7% for clay crust. These strains are less than the strains obtained at failure in the corresponding static tests.

(6) For the clay crust, the anisotropically consolidated samples are more resistant to cyclic loading than the normally consolidated samples.

- (7) Since the two clays used in this investigation have the same plasticity index and were tested under the same conditions, it is concluded that normally consolidated clays are more resistant to cyclic loading than the overconsolidated clayey soils.
- (8) Repeated loading below the CLRL causes an increase in the overconsolidation of the material. This increase in overconsolidation is related to both axial strains and pore pressure developed under cycling.
- (9) For homogeneous soils such as the kaolinitic clay used in this investigation, the CLRL varies linearly with the amplitude of applied stress. This may not be true for non-homogeneous soils.
- (10) The slow frequencies are more likely to cause higher strains than faster frequencies.
- (11) Periodic fluctuation of the water table can induce a loss in strength of the soil.
- (12) For the two clays tested, there is a decrease in undrained shear strength following repeated loading. This decrease is strain-dependent and increases with the increase in axial strain produced by cyclic loading.
- (13) The method proposed by Garga and Khan (1991) for the estimation of K_0 can be used for both overconsolidated clays and sands. The results show that the proposed method is capable of estimating K_0 for an overconsolidated soil irrespective of the previously imposed stress history.

8.2 Recommendations

It is well known that the development of the pore pressure under cycling has an important effect on the behaviour of soils. The test data presented in this thesis demonstrates that the development of the pore pressure under cycling depends on the stress history of the soil. Therefore, it is interesting to study the undrained behaviour of soils, especially for heavily overconsolidated soil.

References

- Airey, D.W., and Fahey, M. 1991. *Cyclic response of calcareous soil from the North-West Shelf of Australia*. Geotechnique 41, No.1, pp. 101-121.
- Andersen, K.H., Kleven, A., and Heien, D. 1988. *Cyclic soil data for design of gravity structures*. ASCE Journal of the Geotechnical Engineering Division, 114: 517-540.
- Andersen, K.H., Brown, S.F., Foss, I., Pool, J.H. and Rosenbrand, W.F. 1976. *Effect of cyclic loading on clay behaviour*. Design and Construction of Offshore Structures, ICE, London, pp. 5-79.
- Andersen, K.H., Hansteen, O.E., Hoeg, K. and Prevost, J.H. 1977. *Soil deformation due to cyclic loads on offshore structures*. Numerical Methods in Offshore Engineering, chapter 13, pp. 413-452, John Wiley and Sons.
- Andersen, K.H. 1976. *Behaviour of clay subjected to undrained cyclic loading*. 1st Boss Conference. 1: 392-403.
- Andersen, K.H., Pool, J.H., Brown, S.F., and Rosenbrand, W.F. 1980. *Cyclic and static laboratory tests on Drammen clay*. ASCE Journal of the Geotechnical Engineering Division, 106:499-529.
- Andraws, K.Z., and El-Sohby, M.A. 1973. *Factors affecting coefficient of earth pressure K_0* . ASCE Journal of the Geotechnical Engineering Division, 99: 527-539.
- Ansar, A.M., and Erken, A. 1989. *Undrained behaviour of clay under cyclic shear stresses*. ASCE Journal of the Geotechnical Engineering Division, 115: 968-983.
- Brooker, E.W., and Ireland, H.O. 1965. *Earth pressures at rest related to stress history*. Canadian Geotechnical Journal, Vol. 2: 1-15.
- Brown, S.F., Lashine, A.D.F., and Hyde, A.F.L. 1975. *Repeated load testing of a silty clay*. Géotechnique 25, No.1, pp. 95-114.
- Castro, G., and Christian, J.T. 1976. *Shear strength of soils and cyclic loading*. ASCE Journal of the Geotechnical Engineering Division, 102: 887-894.
- Clemence, S.P., and Pepe, F.D. 1984. *Measurement of lateral stress around multihelix anchors in sand*. ASTM, Geotechnical Testing Journal, Vol. 7: 145-152.

- Conn, G. M., and Hyde, A.F.L. 1986. *Critical level of repeated loading for a silty clay*. Proceedings, 3rd Canadian Conference on Marine Geotechnical Engineering, St. John's Nfld., Vol. 2, pp.691-705.
- Daramola, O. 1980. *On estimating K_0 for overconsolidation granular soils*. Geotechnique, **30**: 310-313.
- Deere, D.U., and Davisson, M.T. 1956. *Behaviour of grain elevator foundations subjected to cyclic loading*. 4th ICSMFE, Vol. 2, pp. 629-634.
- Diaz-Rodriguez, J.A. 1989. *Behaviour of Mexico City clay subjected to undrained repeated loading*. Canadian Geotechnical Journal, **26**: 159-162.
- Djavid, M. 1993. *Behaviour of clayey deposits under wave loading*. Proceedings, 4th Canadian Conference on Marine Geotechnical Engineering, Vol. 1, pp. 42-64.
- Duncan, J.M., and Seed, R.B. 1986. *Compaction-induced earth pressures under K_0 conditions*. ASCE Journal of the Geotechnical Engineering Division, **112**: 1-22.
- Feda, J. 1984. *K_0 -Coefficient of sand in triaxial apparatus*. ASCE Journal of the Geotechnical Engineering Division, **110**: 519-524.
- France, J.W. and Sangrey, D.A. 1977. *Effects of drainage in repeated loading*. ASCE Journal of the Geotechnical Engineering Division, **103**: 769-785.
- Garga, V.K., and Khan, M.A. 1991. *Laboratory evaluation of K_0 for overconsolidated clays*. Canadian Geotechnical Journal, **28**: 650-659.
- Ghaly, A., and Hanna, A. 1991a. *Experimental and theoretical studies on installation torque of screw anchors*. Canadian Geotechnical Journal, **28**: 353-364.
- Handy, R.L. 1983. *Discussion of " K_0 -OCR relationship in soil," by P.W. Mayne and F.H. Kulhawy*, ASCE Journal of the Geotechnical Engineering, **109**: 862-863.
- Hanna, A., and Ghaly, A. 1992. *Effects of K_0 and overconsolidation on uplift capacity*. ASCE Journal of the Geotechnical Engineering, **118**: 1449-1469.
- Herrmann, H.G. and Houston, W.N. 1978. *Behaviour of seafloor soils subjected to cyclic loading*. Proceedings, 10th Offshore Technology Conference at Houston, Texas, pp. 1797-1808.
- Houston, W.N. and Herrmann, H.G. 1980. *Undrained cyclic strength of marine soils*. ASCE Journal of the Geotechnical Engineering Division, **106**: 691-712.

- Hyde, A.F.L. and Brown, S.F. 1976. *The plastic deformation of a silty clay under creep and repeated loading*. Géotechnique, 26: 173-184.
- Hyodo, M., Hyde, A.F.L., and Konami, T. 1993. *Monotonic and cyclic triaxial behaviour of carbonate sand as a seafloor sediment*. 4th Canadian Conference on Marine Geotechnical Engineering, vol.2, pp. 478-492.
- Jaky, J. 1948. *Pressure in soils*. Proceedings, 2nd International Conference on Soil Mechanics and Foundation Engineering, Rotterdam, Vol. 1, pp. 103-107.
- Khan, M.A. and Garga, V.K. 1991. *Undrained shear strength of a clay crust using field vane*. 44th Canadian Geotechnical Conference, Calgary, Alberta, Vol. 1, Paper 3.
- Kjellman, W. 1936. Report on an apparatus for consummate investigation of the mechanical properties of soils. Proceedings, 1st International Conference on Soil Mechanics and Foundation Engineering, Cambridge, Mass., Vol. 2, pp. 16-20.
- Konard, J.M. and Wagg, B.T. 1993. *Undrained cyclic loading of anisotropically consolidated clayey silts*. ASCE Journal of the Geotechnical Engineering, 119: 929-947.
- Koutsoftas, D.C. 1978. *Effect of cyclic loads on undrained strength of two marine clays*. ASCE Journal of Geotechnical Engineering, 104: 609-620.
- Larew, H.G., and Leonards, G.A. 1962. *A repeated load strength criterion*. Highway Research Board, Proceeding 41, pp. 529-556.
- Lee, K.L. 1979. *Cyclic strength of a sensitive clay of eastern Canada*. Canadian Geotechnical Journal, 16: 163-176.
- Lee, K.L., and Focht, J.A. 1976. *Strength of clay subjected to cyclic loading*. Marine Geotechnology, 1: 165-185.
- Lefebvre, G., LeBoeuf, D., and Demers, B., 1989. *Stability threshold for cyclic loading of saturated clay*. Canadian Geotechnical Journal, 26: 122-131.
- Lefebvre, G., and LeBoeuf, D. 1987. *Rate effects and cyclic loading of sensitive clays*. ASCE Journal of Geotechnical Engineering, 113: 476-489.
- Lefebvre, G., and Poulin, C. 1979. *A new method of sampling in sensitive clay*. Canadian Geotechnical Journal, 16: 226-233.
- Lo, K.Y. 1961. *Stress-strain relationship and pore water pressure characteristics of a normally consolidated clay*. 5th ICSMFE, Paris, Vol.1, pp. 219-224.

- Marchetti, S. 1985. *On the field determination of K_0 in sand*. 11th Int. Conf. on Soil Mech. and Found. Engrg., A.A. Balkema, Rotterdam, the Netherlands, Vol. 5, pp. 2667-2672.
- Matsui, T. and Abe, N. 1981. *Behaviour of clay on cyclic stress-strain history*. 10th ICSMFE, Vol. 3, pp. 261-264.
- Matsui, T., Ohara, H., and Ito, T. 1980. *Cyclic stress-strain history and shear characteristics of clay*. ASCE Journal of the Geotechnical Engineering Division, **106**: 1101-1120.
- Mayne, P.W., and Kulhawy, F.H. 1982. *K_0 -OCR relationships in soil*. ASCE Journal of the Geotechnical Engineering Division, **108**: 851-872.
- Mitchell, R.J., and King, R.D. 1977. *Cyclic loading of an Ottawa area Champlain Sea clay*. Canadian Geotechnical Journal, **14**: 52-63.
- Monismith, C.L., Ogawa, N., and Freeme, C.R. 1975. *Permanent deformation characteristics of subgrade soils in repeated loading*. Transportation Research Record **537**: 1-17.
- Procter, D.C. and Khaffaf, J.H. 1984. *Cyclic triaxial tests on remoulded clays*. ASCE Journal of Geotechnical Engineering, **110**: 1431-1445.
- Raymond, G.P., Gaskin, P.N., and Addo-Abedi, F.Y. 1979. *Repeated compressive loading of Leda clay*. Canadian Geotechnical Journal, **16**: 1-10.
- Sangrey, D.A., Henkel, D.J., and Esrig, M.I. 1969. *The effective stress response of a saturated clay soil to repeated loading*. Canadian Geotechnical Journal, **6**: 241-252.
- Sangrey, D.A., Polard, W.S., and Egan, J.A. 1978. *Errors associated with rate of undrained cyclic testing of clay soils*. Dynamics Geotechnical Testing, ASTM, STP 654, pp. 280-294.
- Schmidt, B. 1983. *Discussion of " K_0 -OCR relationship in soils," by P.W. Mayne and F.K. Kulhawy*, ASCE journal of the Geotechnical Engineering, **109**: 866-867.
- Schmidh, B. 1966. *Discussion of "Earth pressure at rest related to stress history," by E. W. Brooker and H.O. Ireland*, Canadian Geotechnical Journal, **3**: 148-161.
- Seed, H.B. and Chan, C.K. 1961. *Effect of duration of stress application on soil deformation under repeated loading*. International Conference on Soil Mechanics and Foundation Engineering, Proceedings, pp. 341-345.
- Seed, H.B. and Chan, C.K. 1966. *Clay strength under earthquake loading conditions*. ASCE J. Soil Mech. Found. Div., **92**: 105-123.

- Takahashi, M., Hight, D.W. and Vaughan, P.R. 1980. *Effective stress changes observed during undrained cyclic triaxial tests on clay*. Proc. Int. Sympos. on soils under Cyclic and Transient loading, Swansea, (eds. Pande, G.N. and Zienkiewicz, O.C.), A.A. Balkema, Rotterdam, Vol. 1, pp. 201-209.
- Taylor, P.W. and Bacchus, D.R. 1969. *Dynamic cyclic strain tests on a clay*. 7th ICSMFE, Mexico, Vol. 1, pp. 401-409.
- Thiers, G.R., and Seed, H.B. 1968. *Cyclic stress-strain characteristics of clays*. ASCE Journal of the Geotechnical Engineering, **94**: 555-569.
- Wilson, N.E., and Greenwood, J.R. 1974. *Pore pressures and strains after repeated loading and saturated clay*. Canadian Geotechnical Journal, **11**: 269-277.
- Wood, D.M. 1982. *Laboratory investigations of the behaviour of soils under cyclic loading: a review*. Soil mechanics-transient and cyclic loads (eds G.N. Pande and O.C. Zienkiewicz), pp. 513-582. New York:Wiley.
- Wroth, C.P. 1975. *In situ measurements on initial stresses and deformations characteristics*. In Situ Measurements of Soil Properties, Vol. 2, ASCE, New York, N.Y., pp. 181-230.
- Wroth, C.P. and Loudon, P.A. 1967. *The correlation of strains within a family of triaxial tests on overconsolidated samples of kaolin*. Proc. Geot. Conf., Oslo, Vol. 1, pp. 159-163.
- Zergoun, M. 1991. *Effective stress response of clay to undrained cyclic loading*. Unpublished thesis (Ph.D), The university of British Columbia, Vancouver, Canada.